ornl

OAK
RIDGE
NATIONAL
LABORATORY

UNION
CARBIDE

ORNL-5826

MARTIN MARIETTA ENERGY SYSTEMS LIBRARIES

3 4456 0382923 0

Condensation of Ammonia on the Outside of Smooth and Fluted Tubes at Various Tube Positions

N. Domingo

OAK RIDGE NATIONAL LABORATORY
CENTRAL RESEARCH LIBRARY
CIRCULATION SECTION
4500N ROOM 175
LIBRARY LOAN COPY
DO NOT TRANSFER TO ANOTHER PERSON
If you wish someone else to see this report, send in name with report and the library will arrange a loan.
UCN-7969 (3 9-77)

OPERATED BY
UNION CARBIDE CORPORATION
FOR THE UNITED STATES
DEPARTMENT OF ENERGY

Printed in the United States of America. Available from
National Technical Information Service
U.S. Department of Commerce
5285 Port Royal Road, Springfield, Virginia 22161
NTIS price codes—Printed Copy: A06 Microfiche A01

This report was prepared as an account of work sponsored by an agency of the United States Government. Neither the United States Government nor any agency thereof, nor any of their employees, makes any warranty, express or implied, or assumes any legal liability or responsibility for the accuracy, completeness, or usefulness of any information, apparatus, product, or process disclosed, or represents that its use would not infringe privately owned rights. Reference herein to any specific commercial product, process, or service by trade name, trademark, manufacturer, or otherwise, does not necessarily constitute or imply its endorsement, recommendation, or favoring by the United States Government or any agency thereof. The views and opinions of authors expressed herein do not necessarily state or reflect those of the United States Government or any agency thereof.

CONTENTS

	Page
LIST OF FIGURES	v
LIST OF TABLES	vii
LIST OF SYMBOLS	ix
ACKNOWLEDGMENTS	xiii
ABSTRACT	1
1. INTRODUCTION	1
2. DESCRIPTION OF EQUIPMENT	3
2.1 Equipment Modifications	3
2.2 General Flow Description	6
2.3 Condenser Tube and Installation	10
2.4 Test Tubes	11
3. PROCEDURES AND INSTRUMENTATION	16
3.1 Steady-State Operation	16
3.2 Instrumentation	17
4. ANALYSIS	19
4.1 Overall Condensing Coefficients	19
4.2 Individual Heat Transfer Coefficients	20
4.3 Evaluation of Water-Side Coefficients by the Wilson-Plot Method	22
5. RESULTS AND DISCUSSION	24
5.1 Smooth Tube A	34
5.1.1 Horizontal test results	34
5.1.2 Inclined test results	36
5.2 Finned Tube V	39
5.3 Vertical Single-Fluted Tubes L and T	40
5.4 Vertical Double-Fluted Tubes H* and L*	43
5.4.1 Tube H* test results	43
5.4.2 Tube L* test results	45
6. CONCLUSIONS	47
REFERENCES	49
APPENDIX A. SAMPLES OF DATA REDUCTION	51
APPENDIX B. DROPWISE CONDENSATION ON SMOOTH TUBE A	63
APPENDIX C. WILSON-PLOT RESULTS	67
APPENDIX D. EXPERIMENTAL DATA	77
APPENDIX E. SI CONVERSION FACTORS	103

MARTIN MARIETTA ENERGY SYSTEMS LIBRARIES

3 4456 0382923 0

LIST OF FIGURES

Figure		Page
1	Schematic diagram of experimental apparatus	4
2	Overall view of OTEC test loop	5
3	View of condenser test section with emphasis on modifications	7
4	Close-up view of condenser test section	8
5	Details of condenser test section	9
6	Photographs of tube samples	13
7	Photograph of Tube V	14
8	Horizontal smooth-tube condensation data for ammonia (nondimensional form)	24
9	Wilson-plot results for smooth Tube A condensing at various angles (0 to 90°) — h* vs Q/A	25
10	Wilson-plot results for smooth Tube A condensing at various angles (0 to 90°) — Q vs ΔT*	25
11	Comparison of Wilson-plot results for smooth Tube A and finned Tube V — h* vs Q/A	26
12	Comparison of Wilson-plot results for smooth Tube A and finned Tube V — Q vs ΔT*	27
13	Wilson-plot results for vertical single-fluted Tubes L and T and other previously tested tubes — h* vs Q/A	28
14	Wilson-plot results for vertical single-fluted Tubes L and T and other previously tested tubes — Q vs ΔT*	28
15	Overall heat transfer performance of double-fluted Tubes H and H* with water flowing through an annulus at 3.5×10^{-4} m³/s (5.5 gpm)	29
16	Overall heat transfer performance of double-fluted Tubes H and H* with water flowing inside tube (no rod) at 3.4×10^{-4} m³/s (5.4 gpm)	29
17	Overall heat transfer performance of double-fluted Tube H* at various water flow rates (rod installed on water side)	30
18	Overall heat transfer performance of double-fluted Tube H* at various water flow rates (no rod on water side)	30
19	Overall heat transfer performance of Tubes A, L, and L* with water flowing through an annulus at 3.4×10^{-4} m³/s (5.4 gpm)	31

Figure		Page
20	Overall heat transfer performance of Tubes A, L, and L* with water flowing through an annulus at 6.2 x 10^{-4} m^3/s (9.8 gpm)	31
21	Overall heat transfer performance of double-fluted Tube L* at various water flow rates (rod installed on water side)	32
22	Overall heat transfer performance of double-fluted Tube L* at various water flow rates (no rod on water side)	32
23	Tube-wall cross section for Tubes E and L	41
A.1	Wilson plot for ammonia (R-717) condensing outside fluted Tube L — runs R-717-L to R-717-L	58
B.1	Dropwise condensation of ammonia outside horizontal Tube A	64

LIST OF TABLES

Table		Page
1	Characteristics of tubes	12
2	Parameter ranges for condensing tests	33
A.1	Sample of experimental data — ammonia (R-717) condensing on Tube L	52
A.2	Sample information for the Wilson plot — ammonia (R-717) condensing on Tube L	56
C.1	Summary of experimental conditions and results from Wilson plots for ammonia condensing on vertical Tube A	68
C.2	Summary of experimental conditions and results from Wilson plots for ammonia condensing on horizontal Tube A	69
C.3	Summary of experimental conditions and results from Wilson plots for ammonia condensing on Tube A (30° from the horizontal)	70
C.4	Summary of experimental conditions and results from Wilson plots for ammonia condensing on Tube A (60° from the horizontal)	71
C.5	Summary of experimental conditions and results from Wilson plots for ammonia condensing on vertical Tube E	72
C.6	Summary of experimental conditions and results from Wilson plots for ammonia condensing on vertical Tube L	73
C.7	Summary of experimental conditions and results from Wilson plots for ammonia condensing on vertical Tube T	74
C.8	Summary of experimental conditions and results from Wilson plots for ammonia condensing on horizontal Tube V	75
D.1	Experimental data for ammonia condensing on Tube A (vertical)	78
D.2	Experimental data for ammonia condensing on Tube A (horizontal)	82
D.3	Experimental data for ammonia condensing on Tube A (30° from the horizontal)	83
D.4	Experimental data for ammonia condensing on Tube A (60° from the horizontal)	84
D.5	Experimental data for ammonia condensing on Tube E (vertical)	85
D.6	Experimental data for ammonia condensing on Tube H (vertical)	88
D.7	Experimental data for ammonia condensing on Tube H (vertical, no rod on water side)	90

Table		Page
D.8	Experimental data for ammonia condensing on Tube H* (vertical)	92
D.9	Experimental data for ammonia condensing on Tube H* (vertical, no rod on water side)	93
D.10	Experimental data for ammonia condensing on Tube L (vertical)	95
D.11	Experimental data for ammonia condensing on Tube L* (vertical)	96
D.12	Experimental data for ammonia condensing on Tube L* (vertical, no rod on water side)	98
D.13	Experimental data for ammonia condensing on Tube T (vertical)	99
D.14	Experimental data for ammonia condensing on Tube V (horizontal)	101

LIST OF SYMBOLS

a_0	y-intercept on the Wilson plot representing composite resistance of the condensing film and wall
a_1	slope of the line on the Wilson plot
A	heat transfer surface area of test tube
c_p	specific heat
D	tube diameter
F	volume flow rate
g	local gravitational acceleration
g_0	conversion factor, 4.17×10^8 $lb_m \cdot ft/lb_f \cdot h^2$
H	standard nondimensional heat transfer coefficient (average or mean)
h	average or mean individual heat transfer coefficient
h_{fg}	latent heat of vaporization
h_v	condensing heat transfer coefficient on vapor side
h*	composite condensing heat transfer coefficient (including both wall and condensing film)
k	thermal conductivity
l	tube length
ln	log mean
$\dot{m}$	mass flow rate
P	pressure
Q	heat load
Q/A	heat flux
r	radius
R	resistance to heat flow
Re	Reynolds number

T	temperature
ΔT	temperature difference
$\overline{\Delta T}$	overall temperature difference between ammonia condensing vapor and coolant
ΔT^*	composite temperature difference including both condensing film and wall
U	overall condensing heat transfer coefficient
v	water velocity

Greek Symbols

Γ	mass flow rate per unit length of tube
α	angle of inclination of condenser test section
Δ	finite difference
μ	absolute viscosity
ρ	mass density
$\sum$	summation

Subscripts

avg	average
c	condensate
cs	cross section
f	film
fi	inside fouling
fo	outside fouling
h	hydraulic
i	inside
in	inlet
o	outside

out	outlet
r	rod
sat	saturation
v	vapor; condensing side
w	water; water side
wall	wall; surface

ACKNOWLEDGMENTS

This investigation was performed at the Oak Ridge National Laboratory (ORNL) operated by the Union Carbide Corporation for the Department of Energy (DOE). The study was part of the general program on Ocean Thermal Energy Conversion performed by the Engineering Technology Division, ORNL, for the DOE Division of Central Solar Technology, Ocean Systems Branch.

The author appreciates the assistance of many ORNL staff members and is particularly grateful for the contributions of the following people: H. W. Hoffman, section head, Engineering Technology Division; J. W. Michel, program manager, Energy Division; and R. W. Murphy, project engineer, Engineering Technology Division; for their helpful suggestions throughout the program; C. V Hardin, engineering technologist, for operation of the test equipment and collection and organization of the report data; and the members of the Engineering Technology Division Publications Office and Word Processing Center for assistance in organizing the material and typing the manuscript.

CONDENSATION OF AMMONIA ON THE OUTSIDE OF SMOOTH AND FLUTED TUBES AT VARIOUS TUBE POSITIONS

N. Domingo

ABSTRACT

Experiments were conducted to determine the heat transfer performance obtained for ammonia condensing on the outside of six tubes of four distinct types: (1) a smooth tube, (2) two single-fluted tubes, (3) two double-fluted tubes, and (4) an external-finned tube. All tubes tested were 2.54 cm (1.0 in.) in nominal diameter and 1.22 m (4.0 ft) in length. Condensing heat transfer coefficients are reported as composite coefficients (including the resistances of both condensing film and tube wall) for (1) a smooth tube condensing in the horizontal position and at various tilt angles, (2) two single-fluted tubes condensing in the vertical position, and (3) a finned tube condensing in the horizontal position. Overall heat transfer data are given for both double-fluted tubes. Data show that for a given heat flux, a horizontal smooth tube can increase composite coefficients by up to 2.1 times the vertical smooth-tube values. For a single-fluted tube, composite coefficients increased by up to 5.2 times the corresponding vertical smooth-tube values. However, on a horizontal position, the finned tube gave the lowest performance of any other tube tested in this study. Finally, for one double-fluted tube, inside fluting increased the overall heat transfer coefficient by as much as 25% more than that for a tube with identical external flutes and a smooth inside surface.

---

1. INTRODUCTION

The heat exchangers of an ocean thermal energy conversion (OTEC) closed-cycle power system are large and constitute a major part of the total-system capital costs. Therefore, improvements in heat exchanger thermal performance can clearly result in substantial cost reduction and will favorably affect the overall feasibility of developing the ocean thermal energy resource. The essential problem is the design of a unit that will yield acceptably high heat transfer under low-temperature potential and minimal power loss.

One approach to lowering the cost of the heat exchangers is to reduce their size by using enhanced heat transfer surfaces to increase heat transfer coefficients. Earlier studies at the Oak Ridge National Laboratory

(ORNL) by Combs[1,2] investigated the heat transfer performance for ammonia condensing on the outside of vertical and inclined tubes with enhanced (fluted) outside surfaces. Although the magnitude of enhancements varied with tube geometry, tube inclination, and heat flux, condensing heat transfer coefficients for vertical fluted tubes showed improvement factors of up to 7.2 times vertical smooth-tube values.

This report presents additional experimental data for ammonia condensing on a variety of vertical fluted tubes. The study also includes data for condensation on a smooth tube in the horizontal position and at various tilt angles and on a horizontal external-finned tube.

Background material for this study was given in a previous report,[1] with detailed descriptions of the equipment, procedures, and instrumentation, all of which remained the same throughout this study. Therefore, only brief descriptions are provided herein.

2. DESCRIPTION OF EQUIPMENT

The ORNL test loop in this study is shown schematically in Fig. 1 and is presented in an overall view in Fig. 2. The equipment is basically as described in earlier studies.[1,2] Major components of the loop include the (1) boiler, (2) entrainment separator, (3) condenser test section, and (4) condenser water-storage tank and pump. A detailed description of each component was presented in Ref. 1 and therefore will not be repeated in this report. Prior to this series of experiments significant design modifications were made to the loop and condenser test section to accommodate all of the condenser orientations that would be encountered in satisfying the test requirements of this study. A summary of these modifications, with a brief description of the loop's general flow and condenser tube installation, is given in succeeding sections of this report.

2.1 Equipment Modifications

In initial studies,[1] the condenser test section was installed in the vertical position to obtain ammonia condensation data on the outside of vertical smooth and fluted tubes. Later, for another study,[2] the test section was rigidly installed 30° from the vertical to determine the effect of inclination on the condensing performance for both a smooth and a fluted tube.

To obviate the difficulties encountered in this study by repeated loop design modifications with each change in condenser tilt position, several provisions were incorporated into the existing loop, making the condenser test section adaptable to any angle of inclination, including horizontal and vertical positions. These provisions included the installation of the following:

1. flexible 2.54-cm (1-in.) nominal diam corrugated stainless steel hoses between the entrainment separator and condenser vapor inlet, and between the condenser outlet and condensate measuring station (Fig. 1);
2. flexible 3.18-cm-ID (1.25-in.) rubber hoses for the water inlet and outlet lines to and from the condenser, respectively;

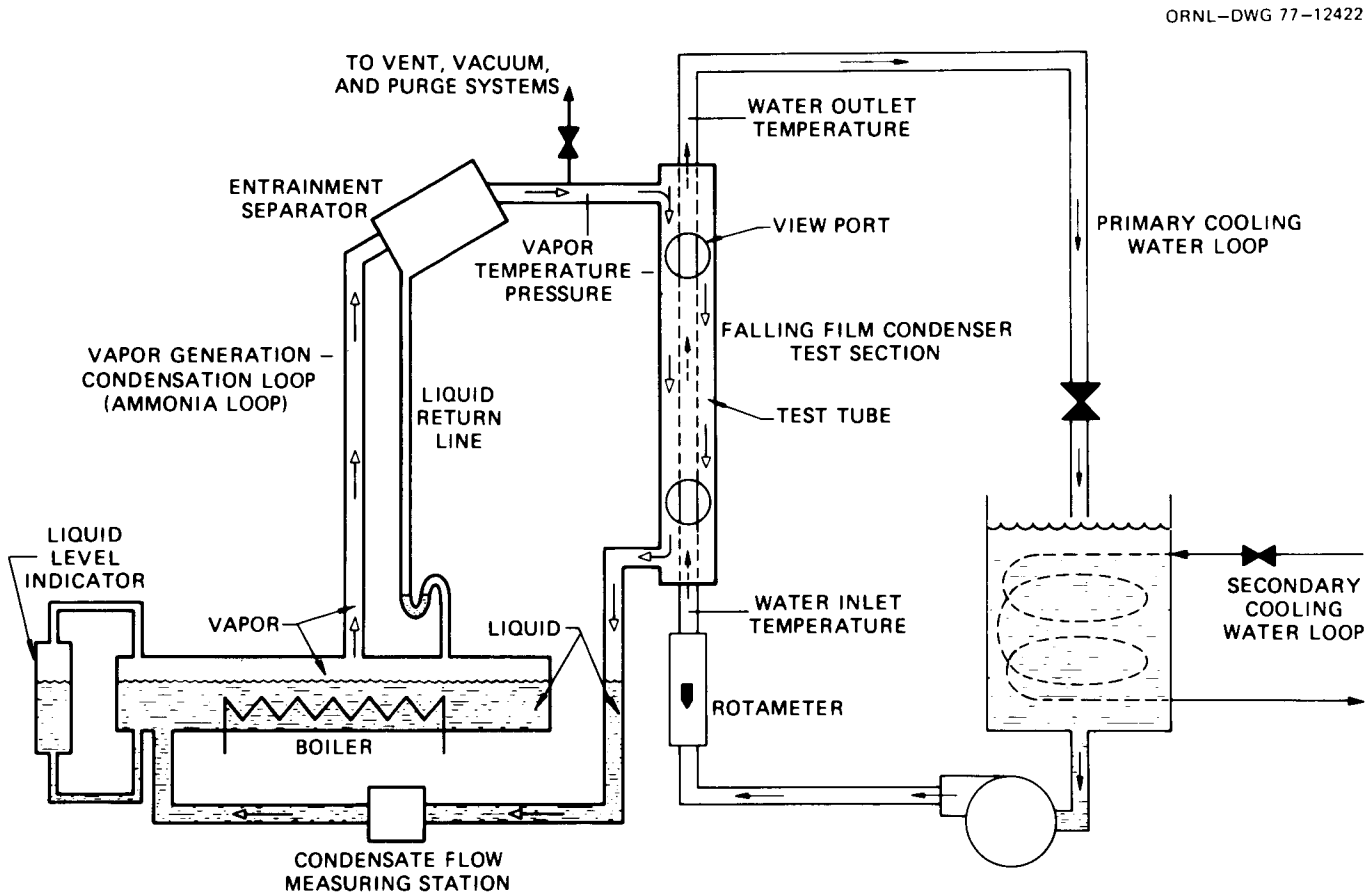

Fig. 1. Schematic diagram of experimental apparatus.

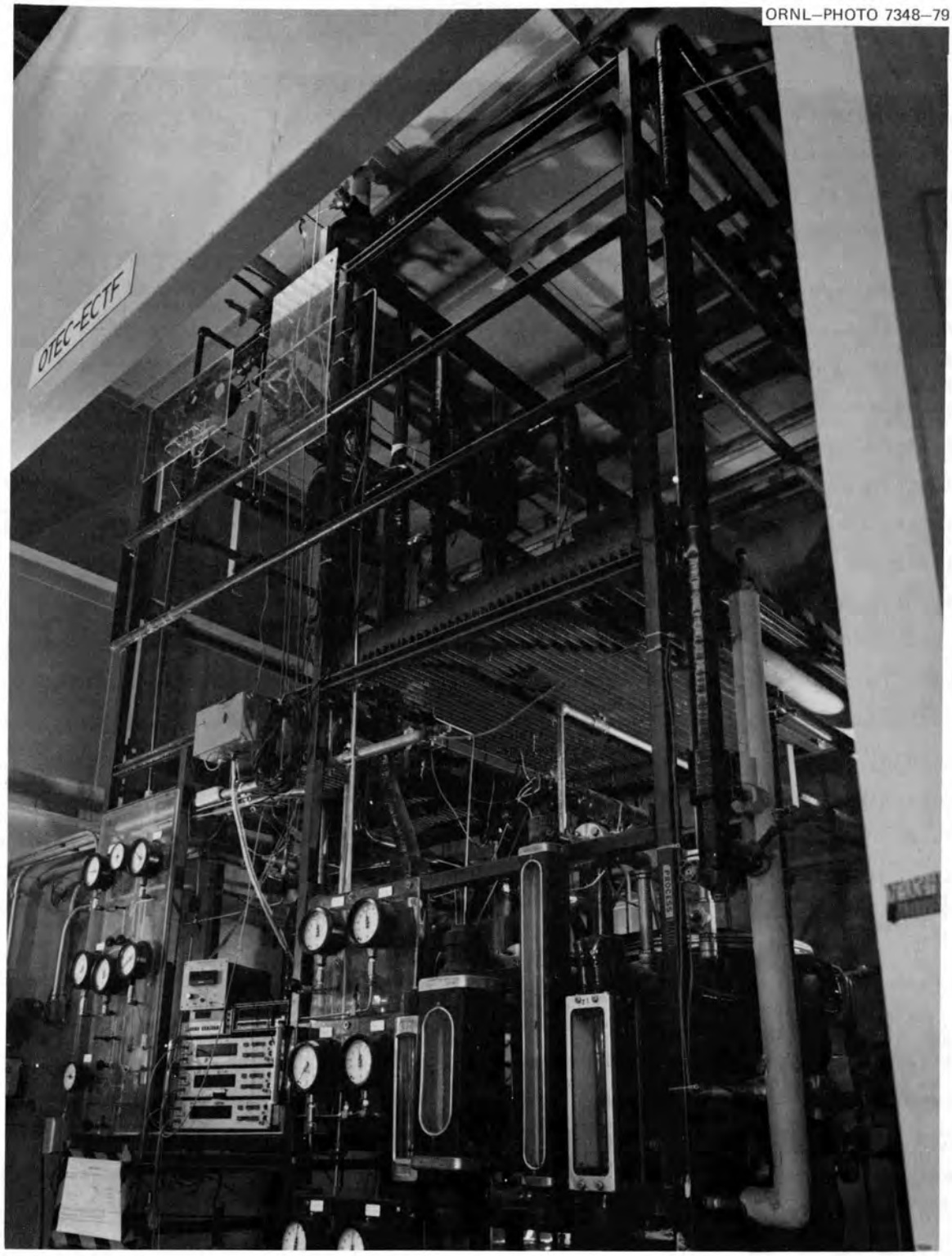

Fig. 2. Overall view of OTEC test loop.

3. stainless steel quick-connect fittings at the condenser vapor inlet and condensate outlet, which provided swivel movement at both of these ends;
4. a metal frame that supported the test section and was allowed to pivot at one end; and
5. a hoist for raising or lowering the frame and test section assembly to the desired angle of inclination.

Figures 3 and 4 are photographs of the condenser test section after these modifications to the loop were made.

As reported in Refs. 1 and 2, the test section was a single-tube condenser made of stainless steel and was designed to accommodate tubes 2.54 cm (1 in.) in nominal diameter and 1.2 m (4 ft) in length. Two view ports were used in the test section to permit visual and photographic observation of the condensing tube's surface (Fig. 4). In addition to these equipment changes, two other features were added to the condenser test section itself. A 1.3-m-long (47-in.), 7.6-cm-diam (3-in.) stainless steel trough was installed inside the condenser and placed below the test tube to collect the condensate attributed only to the condensing tube's surface. The bottom head of the condenser test section (Fig. 5) was modified by welding a 7.6-cm (3-in.) extension to the existing shell-drain separator cup. Both of these features were necessary to increase the accuracy of the condensate flow measurements during horizontal and inclined condenser tests.

2.2 General Flow Description

Flow directions are indicated by arrows in the simplified schematic diagram (Fig. 1). The system (designed for a maximum heat load of 5 kW) consisted of three circuits: working fluid, primary cooling, and secondary cooling loops. The working fluid loop was designed for ammonia with maximum operating pressure and temperature set at 1724 kPa (250 psia) and 316 K (110°F). The system was manually controlled, and the heat load was set by the power output to the boiler.

The working fluid was vaporized in the boiler and passed through an entrainment separator before entering the condenser test section. The

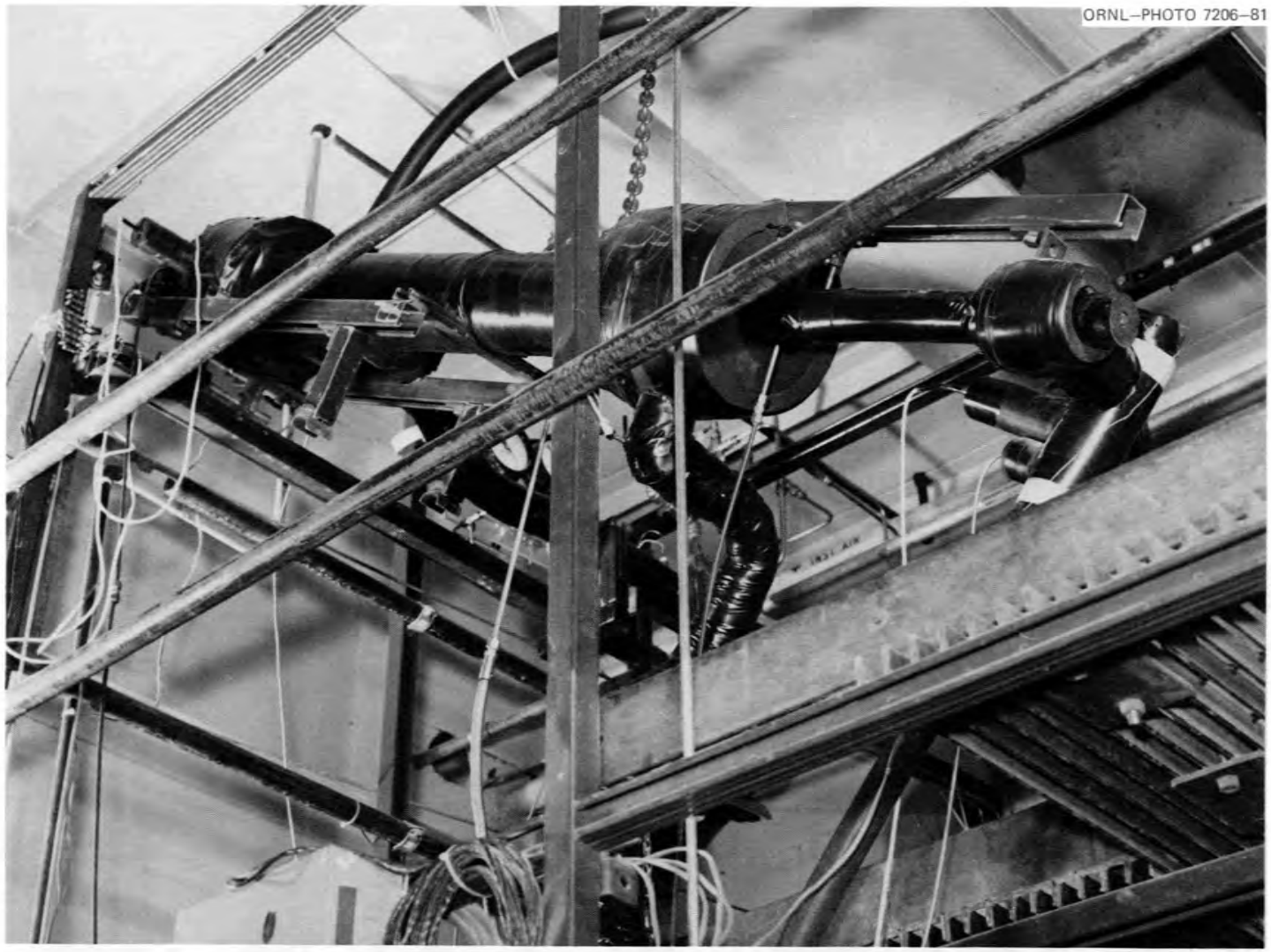

Fig. 3. View of condenser test section with emphasis on modifications.

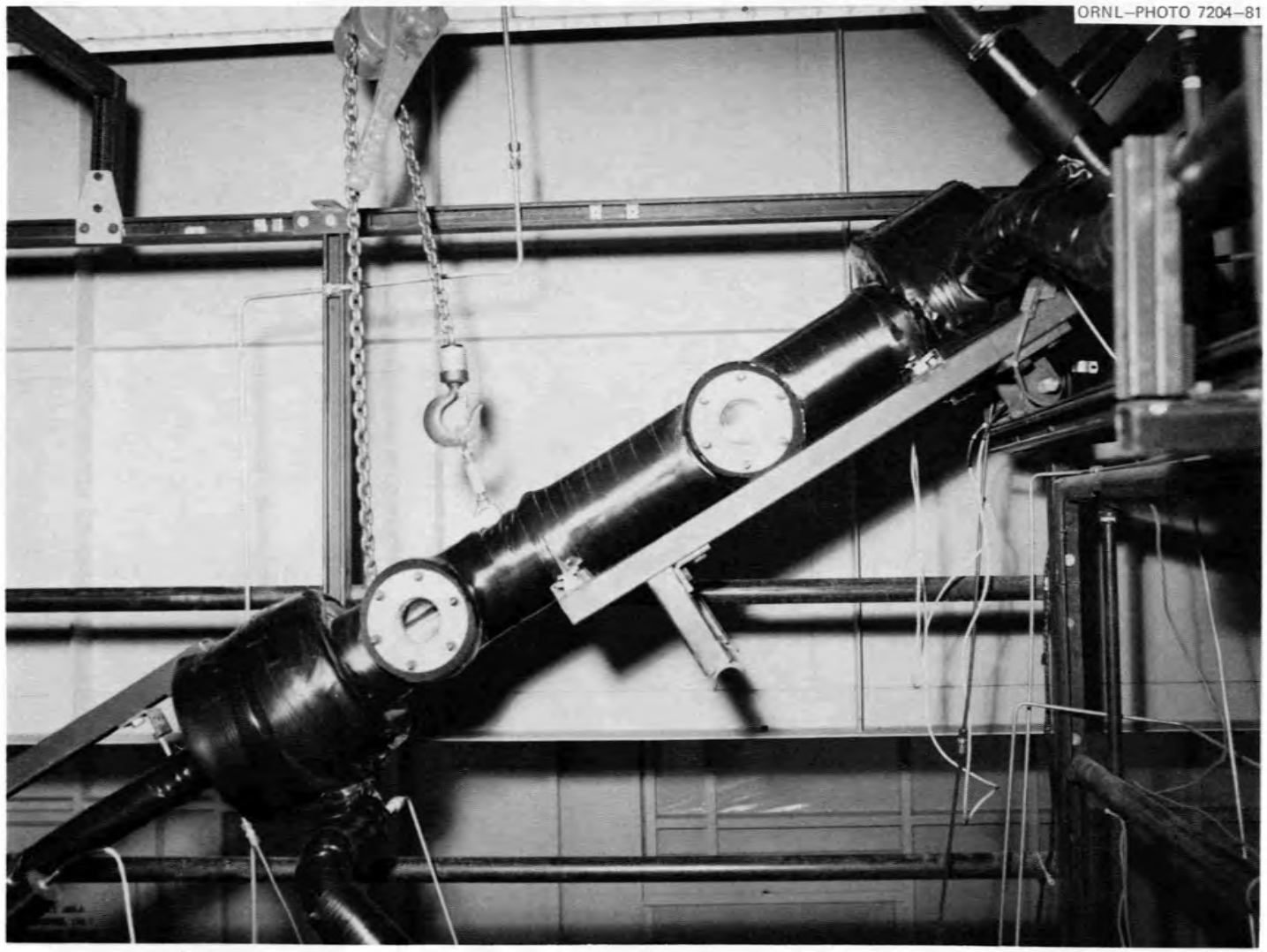

Fig. 4. Close-up view of condenser test section.

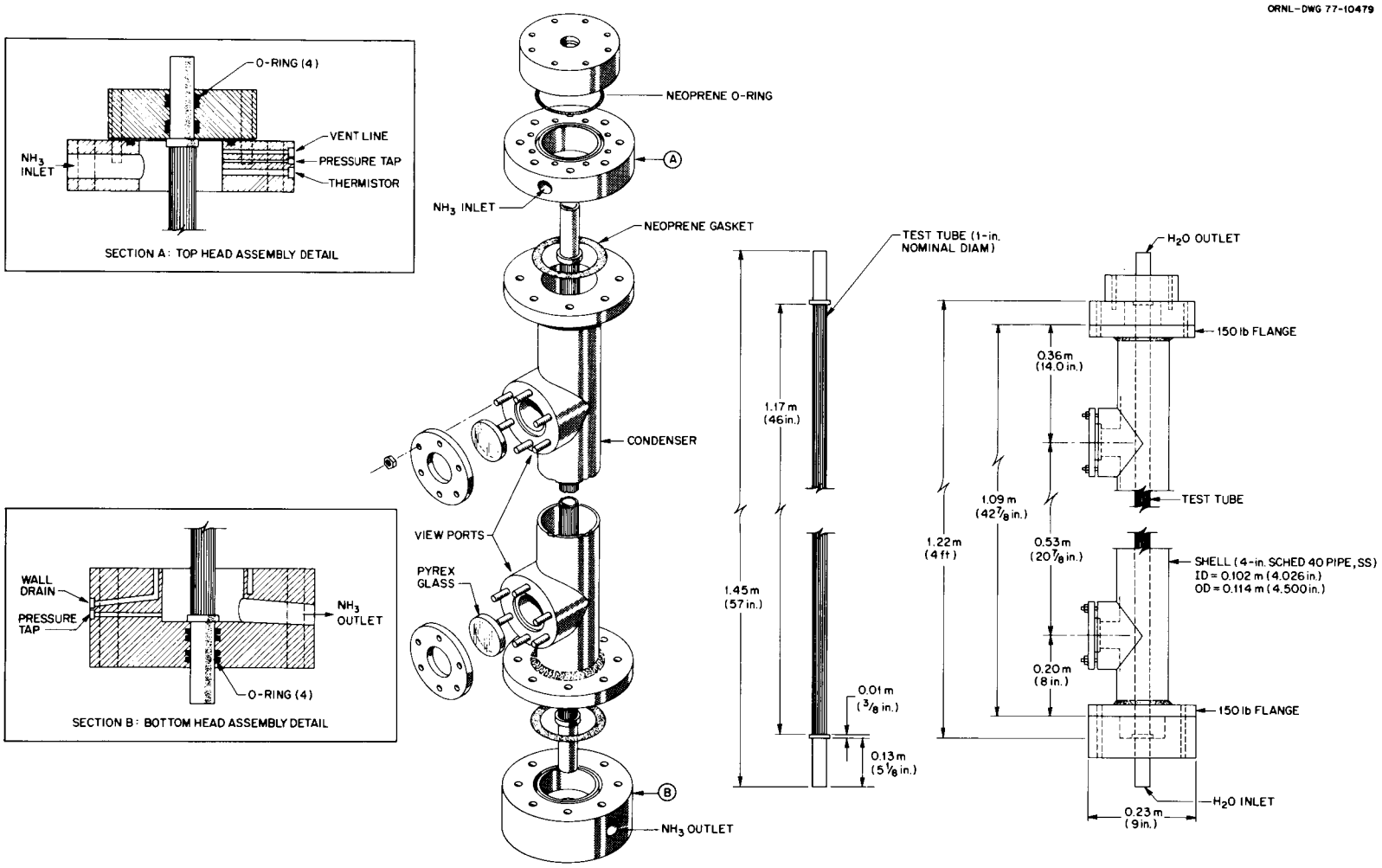

Fig. 5. Details of condenser test section.

vapor entered at the top of the condenser, and the liquid collected in the entrainment separator returned to the boiler. Vapor condensed on the outer surface of the test tube in the test section, exited as a nearly saturated liquid at the condenser bottom, and passed through a condensate measuring station before returning to the bottom of the boiler to complete the closed loop. A pump was not needed for ammonia circulation because the liquid head in the test section side of the loop furnished the driving force required for flow through the condensate measuring station.

In the primary cooling loop, demineralized water was circulated by a small centrifugal pump from a storage tank upward through the condenser test section and back to the storage tank. The primary coolant flow was measured by rotameters upstream of the test section and was controlled by a manually operated valve located downstream.

The secondary cooling loop removed the heat load from the system by transferring the heat from the primary cooling water to the plant process water that circulated through a cooling coil in the storage tank. The secondary coolant flow rates were regulated by manually operated valves and were measured by rotameters located upstream of the cooling coil. Plant process water-line pressure furnished adequate circulation through the secondary cooling loop.

2.3 Condenser Tube and Installation

Because the heads on the condenser test section (Fig. 5) were designed to seal around a smooth 2.54-cm-OD (1-in.) tube, other candidate test tubes were prepared for testing by welding a 2.54-cm-OD, 13.34-cm-long (5.25-in.) sleeve to each end of a 1.17-m (46-in.) length of tube. During installation, the upper section of the top head was removed, and the test tube was inserted downward into the shell until the bottom sleeve slid through the four O-ring seals in the bottom head. The upper section of the top head was then slipped over the top sleeve and bolted to the lower section to complete the shell-side sealing operation. Then, inlet and outlet cooling water connections were made to the protruding sleeves at the bottom and top heads, respectively.

A 1.27-cm-OD (0.5-in.) stainless steel rod was installed through the center of the condenser section (inside the test tube) to decrease the hydraulic diameter and to increase the water velocity for a given primary cooling volume flow and thus improve the accuracy of the Wilson-plot technique[3] used to interpret the experimental data.

2.4 Test Tubes

The condensing heat transfer performance of seven tubes (designated A, E, F, F-1, F-7, G, and H) of four distinct types (smooth, single-fluted, skirted, and double-fluted) has been previously reported.[1,2] In this study, performance data for five additional tubes (H*, L, L*, T, and V), with horizontal and inclined condensation data for smooth Tube A, are presented. Vertical condensation data for the previously tested Tubes A, E, and H are also reported and form the basis for comparison with the other tubes examined.

Pertinent characteristics of the tubes are given in Table 1. Enlarged photographs of sample tube sections are shown in Figs. 6 and 7. Tubes were formed of aluminum, except for types T and V, which were made of carbon steel and stainless steel, respectively. Tube A had a smooth inside and outside surface. Tube H* had 34 internal and 36 external flutes (similar to Tube H in Ref. 2). Tube L* had 90 internal and 60 external flutes. Tube L had a smooth inside surface and 60 external flutes (externally identical to Tube L*). Tube T (similar to Tube E in Ref. 1) had a smooth inside surface and 60 external squared flutes. Tube V had a smooth inside surface but featured external fins.

Tube A was a standard commercial smooth tube.[1,2] Tube H*, like the earlier Tube H, was designed, supplied, and also tested by Carnegie-Mellon University (CMU);[4] these tubes have been used in the fabrication of two CMU heat exchangers recently tested at Argonne National Laboratory (ANL).[5,6] Tubes L and L* were experimental tubes designed by ORNL and custom-made by Precision Extrusion, Incorporated. Tube T was custom-made by Grob, Incorporated. Tube V was designed and supplied by the Trent Tube Division of Colt Industries, using their newly developed alloy "Seacure."

Table 1. Characteristics of tubes

[Nominal 2.54-cm (1-in.) OD, 1.22 m (4 ft) long]

Tube	Description	Material	Surface area [m² (ft²)]		Number of flutes	
			Inside	Outside	External	Internal
A	Smooth	Aluminum 6061	0.085 (0.911)	0.097 (1.047)	0	0
E[a]	Single-fluted	Aluminum 6061	0.081 (0.873)	0.149 (1.605)	60	0
H	Double-fluted	Aluminum 6061	0.085 (0.918)[b]	0.164 (1.760)	45	34
H*	Double-fluted	Aluminum 6061	0.085 (0.918)[b]	0.150 (1.617)	36	34
L	Single-fluted	Aluminum 6061	0.081 (0.863)	0.140 (1.504)	60	0
L*	Double-fluted	Aluminum 6061	0.106 (1.140)	0.140 (1.504)	60	90
T	Single-fluted	Carbon steel 1010	0.081 (0.863)	0.149 (1.605)	60	0
V[c]	Finned	Stainless steel	0.045 (0.480)	0.182 (1.961)	*d*	0

[a]Similar to Tube L, but with squared instead of rounded flutes. Also identical to Tube T, except for material.

[b]Area based on a diameter-to-midpoint on inside flutes.

[c]Areas based on a 67.63-cm (2.22-ft) condensing length.

[d]Twenty-six fins per inch, ~3.05 mm (0.012 in.) thick.

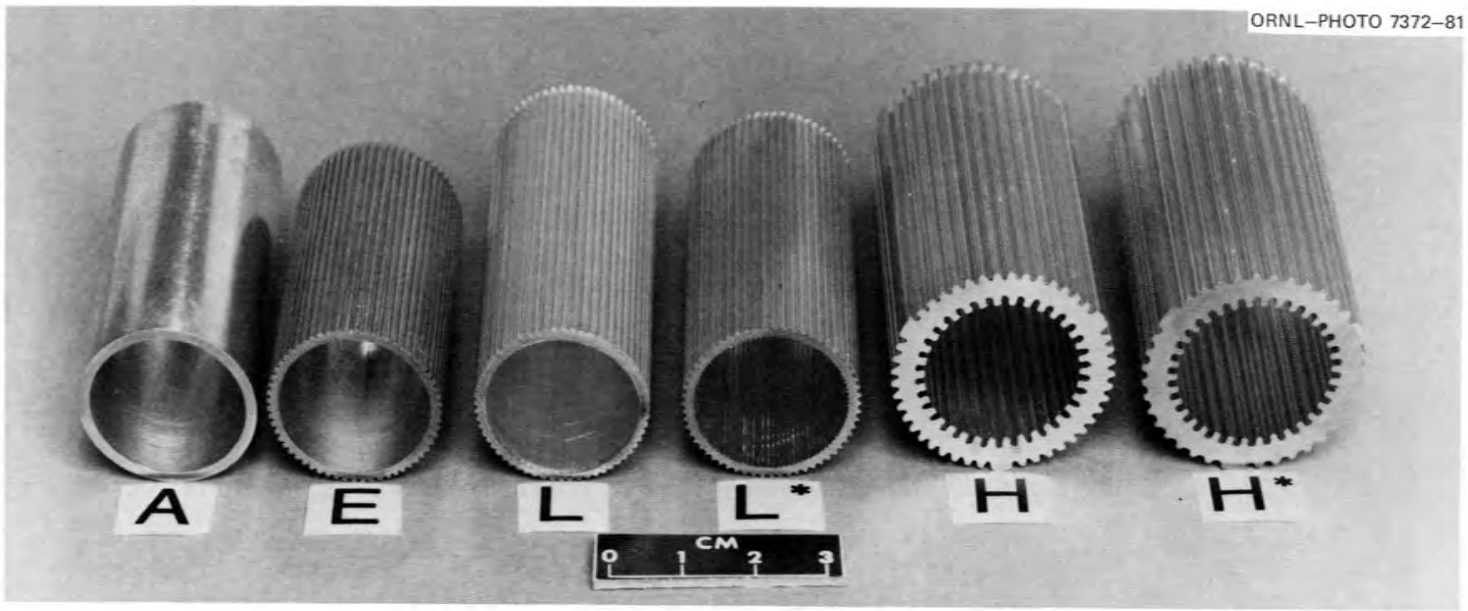

Fig. 6. Photographs of tube samples.

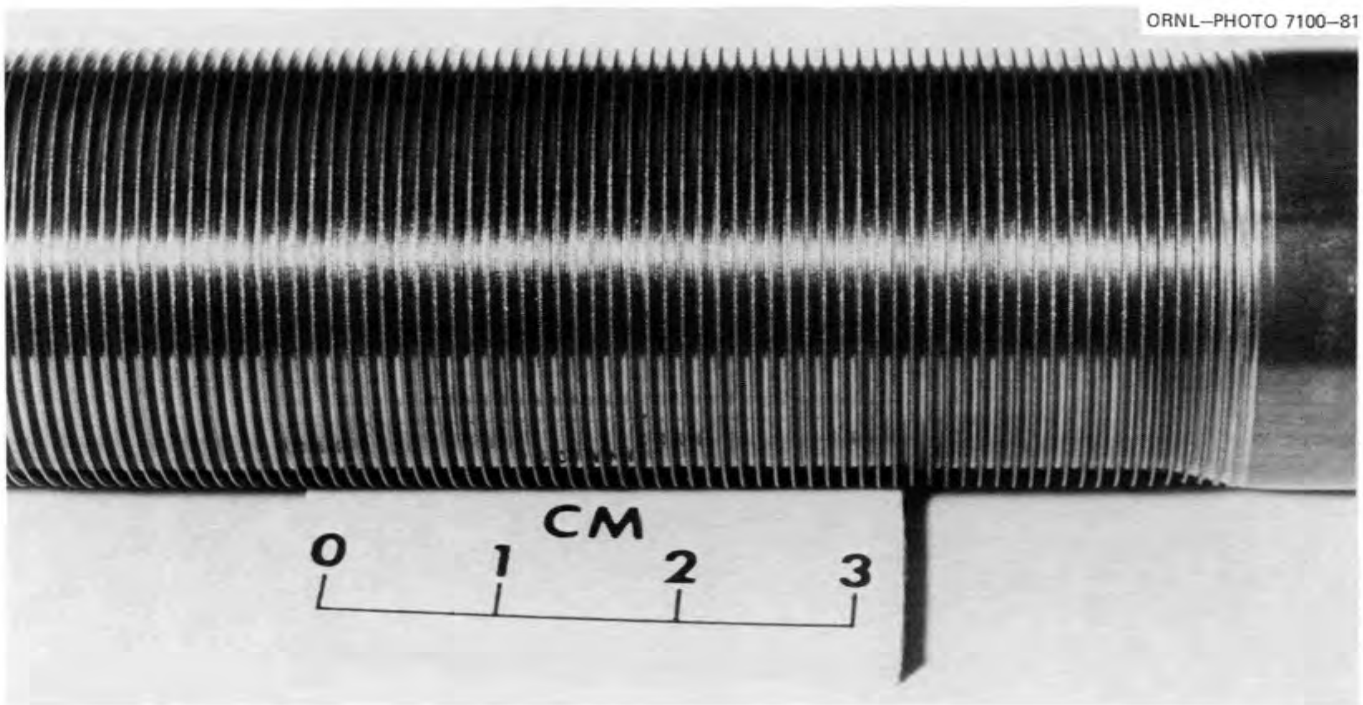

Fig. 7. Photograph of Tube V.

The external perimeter of most tubes was measured as the length of thin tape forced to conform closely and completely around the tube's outside surface. Measurements were also made from enlarged photographic cross sections of available tube samples. The surface area of smooth Tube A was based on a 1.22-m (48-in.) length — the total length available within the test section (Fig. 5). However, the areas of the enhanced tubes, except for Tube V, were based on a 1.17-m (46-in.) effective length to account for the 1.27-m (0.5-in.) adapter sleeve and installation clearance on each end of the enhanced tubes. The area of Tube V was based on a 67.63-cm (2.22-ft) effective length — the total available finned length supplied by the manufacturer; the tube was prepared by welding a longer stainless steel adapter sleeve and insulating the excess length within the test section.

3. PROCEDURES AND INSTRUMENTATION

The objective of this study was the determination of composite heat transfer coefficients for ammonia condensing on the outside surface of horizontal, inclined, and vertical tubes. To apply the Wilson-plot technique to the condensation process, heat rates and temperature differences were calculated from data taken during steady-state operations. (See Appendix A for sample calculations.) Accurate temperature measurements were critical to evaluation of condenser performance; measurement of temperature differences as small as 0.11 K (0.2°F) to within ±0.02 K (0.04°F) was sometimes necessary. Further, very small condensate flows [as low as 6.31×10^{-7} m^3/s (0.01 gpm)] had to be measured accurately for good interpretation of the experimental data.

Because the details of the operating procedures and instrumentation were given in a previous report,[1] only a brief summary will be presented in the following sections.

3.1 Steady-State Operation

The heat rate to the boiler was controlled by a stack of six Variacs. Each Variac regulated the voltage to two tubular heaters, and any combination of the six Variacs could be used to obtain desired experimental heat rates. After the heat rate to the boiler was set, the primary cooling flow rate was adjusted by the valve downstream of the test section. Because the inlet temperature of the secondary cooling water was fixed by the plant process water conditions, the flow rate of the secondary cooling water was used to control the temperature of the primary cooling water. This in turn controlled the vapor temperature in the test section. Temperatures and pressures throughout the system were monitored to determine when a steady-state condition was reached; steady state existed when no significant change in temperature [±0.06 to 0.11 K (±0.1 to 0.2°F)] occurred throughout the system over a 5- to 10-min span.

Once a steady state was achieved, the experimental data were recorded. The recorded information included (1) vapor temperature and pressure in both the condenser and boiler, (2) flow rate and temperature

of the condensate, (3) inlet and outlet temperatures and flow rates of the primary and secondary coolants, and (4) voltage and current to each pair of heater rods. These data were then used to calculate heat transfer rates and temperature differences in the system and to check pressure-temperature values against saturation data in the literature. (See Appendix A for examples.)

After all data were recorded for a given steady-state condition, the flow rate of the primary cooling water was changed, and the flow rate of the secondary cooling water was adjusted until the system reached a new steady state. When this steady state was reached, the experimental data were again recorded. This same procedure was followed until data were collected for five to six primary coolant flow rates at the same boiler heat rate. In the experiments, the primary coolant flow rates ranged from 0.19 to 2.15×10^{-3} m^3/s (3.0 to 34.0 gpm). The heat rate to the boiler was then changed, and the entire procedure was repeated at the new heat rate.

3.2 Instrumentation

The power input to the boiler was monitored by voltage and current measurements for each pair of tubular heaters. The pressures in the boiler and condenser were measured with gages (U.S. gage, dial No. 33006) capable of spanning the range of 0 to 2.07×10^3 kPa (0 to 300 psig). The ammonia loop was also equipped with a compound gage for reading both low and subatmospheric pressures.

The system was equipped with Chromel-Alumel thermocouples to obtain temperatures used for monitoring loop operation. Two multipoint recorders were available to obtain a permanent record of temperature measurements. Thermocouples were located (1) in the liquid and vapor of the boiler, (2) in the vapor feed to the test section, (3) in the inlet and outlet of both cooling water loops, (4) near the condensate measuring station, and (5) on each heater. The recorded thermocouple data were used in deciding when the system reached a steady state.

Thermistors (Thermometrics, part No. S-10-4 wire) and quartz thermometers (Hewlett-Packard, model 2801 A) were installed in the water inlet and outlet lines of the condenser and in the ammonia vapor feed line to

the test section. A quartz thermometer was also located near the condensate measuring station. All thermistors were wired to a switch box that permitted individual resistance readout on a digital multimeter (Data Precision, model 3500). The information from the thermistors and quartz thermometers was used for data reduction because of the greater accuracy attributed to these instruments. The three sets of temperature measuring instruments were checked against each other to increase confidence in their measurements.

The condensate flow in the ammonia loop could be measured by two instruments: (1) an integral orifice meter and (2) a turbine flow transducer. These two instruments were arranged in parallel, with piping permitting the flow to pass through either device. During this investigation, the turbine flow transducer (Flow Technology, model FTM-NX3-LJS) equipped with a range-extending amplifier (Flow Technology, model LFA-300AX) was used to facilitate operation because the integral orifice meter would have required frequent changes in orifice plates to accommodate various flow ranges. Because of the range-extending amplifier, the full range of interest, 0.63 to 12.6 x 10^{-6} m^3/s (0.01 to 0.2 gpm) was covered with only one instrument. Earlier work[1,2] had shown that measured values from the two instruments agreed to within a few percent.

The primary cooling water flow was measured by one of two rotameters in parallel upstream of the test section. The rotameters were capable of covering the operating range of 0.19 to 2.15 x 10^{-3} m^3/s (3.0 to 34.0 gpm). The larger rotameter was used to measure primary coolant flows greater than 0.63 x 10^{-3} m^3/s (10 gpm), while the small rotameter measured primary coolant flows below 0.63 x 10^{-3} m^3/s (10 gpm). The information from these two rotameters was utilized in the data reduction (see Appendix A).

The secondary cooling water was measured by a small rotameter upstream of the cooling coil. The rotameter was used for monitoring secondary coolant flows that ranged from 0 to 0.25 x 10^{-3} m^3/s (0 to 4.0 gpm).

4. ANALYSIS

4.1 Overall Condensing Coefficients

The overall heat transfer conductance (coefficient) in the condenser is given by:

$$U = \frac{Q}{A_o \overline{\Delta T}} , \tag{4.1}$$

where

$\overline{\Delta T}$ = overall temperature difference between the condensing ammonia vapor and the primary cooling water,

A_o = total outside heat transfer surface area of the tube,

Q = condenser heat rate.

The arithmetic mean difference can be used for $\overline{\Delta T}$ because in most cases the temperature difference across the water was relatively small. Therefore:

$$\overline{\Delta T} = T_v - (T_{w,in} + T_{w,out})/2 , \tag{4.2}$$

where T_v is the vapor temperature and the second term on the right is the average of the inlet water temperature $T_{w,in}$ and the outlet water temperature $T_{w,out}$.

Three independent ways to determine the heat rate Q of the condenser test section are from (1) the ammonia side of the condenser, (2) the primary cooling water passing through the condenser, and (3) the secondary cooling water passing through a coil located within the primary cooling water storage tank. For this study, the first method was found to be the most accurate and was used exclusively in all calculations in this report, but other methods agreed well. The condenser heat transfer rate may be determined according to the relation*

$$Q = \dot{m}_c h_{fg} , \tag{4.3}$$

---

*Condensate subcooling is disregarded; contribution to the heat transfer rate Q is less than 0.1%.

where $\dot{m}_c$ is the condensate mass flow rate and h_{fg} is the latent heat of the condensing fluid. In this analysis, all physical property data for ammonia (R-717) are taken from American Society of Heating, Refrigeration, and Air Conditioning Engineers handbooks.[7-9]

The overall heat transfer coefficient, based on the total tube outside-surface area, can be calculated from Eq. (4.1), using Eq. (4.2) to calculate $\overline{\Delta T}$ and Eq. (4.3) to calculate Q.

4.2 Individual Heat Transfer Coefficients

The overall resistance to heat flow ($\Sigma R = 1/U$) is equal to the sum of the individual resistances; therefore:

$$\frac{1}{U} = R_v + R_{wall} + R_w + R_{fo} + R_{fi} , \tag{4.4}$$

where

R_v = resistance on the vapor (condensing) side,
R_{wall} = resistance of the wall,
R_w = resistance of the water side,
R_{fo} and R_{fi} = any fouling resistance on the outside and inside surfaces of the tube, respectively.

If fouling is neglected and individual heat transfer coefficients h are introduced, the overall coefficient based on outside-surface area A_o becomes:

$$\frac{1}{U} = \frac{1}{h_v} + R_{wall} + \frac{A_o}{A_i h_w} , \tag{4.5}$$

where

h_v = condensing ammonia film coefficient,
h_w = water-side coefficient,
A_o and A_i = total outside and inside surface areas of the tube, respectively.

For a smooth tube, the wall resistance based on the outside tube area is given by:

$$R_{wall} = r_o \ln (r_o/r_i)k \ , \tag{4.6}$$

where

k = tube wall thermal conductivity,
r_o = outside radius,
r_i = inside radius of the tube.

However, the wall resistance for the more complicated wall geometry and heat distribution of enhanced tubes is very difficult to estimate. To compare performances of smooth and enhanced tubes, a combined resistance (or inverse conductance) lumping the tube's condensing side and wall resistances was defined. This "composite" resistance $1/h^*$ can be represented as:

$$\frac{1}{h^*} = \frac{1}{h_v} + R_{wall} \ . \tag{4.7}$$

The substitution of Eq. (4.7) into Eq. (4.5) and rearrangement in a composite coefficient h^* form gives:

$$h^* = 1\Big/\left(\frac{1}{U} - \frac{A_o}{A_i h_w}\right) . \tag{4.8}$$

Similarly, a corresponding composite temperature difference can be defined as:

$$\Delta T^* = \frac{Q}{h^* A_o} \ ; \tag{4.9}$$

this describes the temperature difference between condensing ammonia vapor and the inside tube wall.

Composite quantities are derived by elimination of the water-side coefficient contribution to overall resistance. The next step in the analysis is evaluation of the water-side coefficients.

4.3 Evaluation of Water-Side Coefficients by the Wilson-Plot Method

A technique introduced by Wilson[3] in 1915 was used for determining water-side coefficients in this study. This technique is a graphic method of interpreting overall coefficients so that individual condensing-side coefficients can be evaluated. The following treatment presents this method and describes its application to the data in this study.

Neglecting the effects of changes in water temperature, the water-side resistance $1/h_W$ for turbulent flow[10-12] as a function of water velocity v may be approximated by:

$$\frac{1}{h_w} \propto \frac{1}{v^{0.8}} ; \tag{4.10}$$

therefore, Eq. (4.5) can be rewritten as:

$$\frac{1}{U} = \frac{1}{h_v} + R_{wall} + a_1 v^{-0.8} . \tag{4.11}$$

If, following Wilson, the sum of the first two resistances $1/h_v + R_{wall}$ is taken as approximately constant, Eq. (4.11) becomes:

$$\frac{1}{U} = a_0 + a_1 v^{-0.8} . \tag{4.12}$$

In this form, a plot of 1/U vs $v^{-0.8}$ in rectangular coordinates should give a straight line from which the constants a_0 (intercept) and a_1 (slope) can be determined. Because a_0 is the sum of the first two resistances (vapor side plus wall) in Eq. (4.11), substitution and rearrangement of Eq. (4.7) yields:

$$h^* = 1/a_0 , \tag{4.13}$$

which is the parameter of interest in this analysis.

For the experimental data points used in construction of the Wilson plot, a constant heat load and condensate flow rate were maintained, while water-side velocities were varied. Because properties for

ammonia did not vary significantly over the small range of temperatures covered in this study, no appreciable error was introduced by assuming the sum of the vapor side and tube wall resistances $1/h^* + R_{wall}$ to be essentially constant.

5. RESULTS AND DISCUSSION

Ammonia condensation tests in this study were divided into the following four test categories: (1) smooth Tube A in the horizontal position and at various tilt angles, (2) external-finned Tube V in the horizontal position, (3) single-fluted Tubes L and T in the vertical position, and (4) double-fluted Tubes H* and L*, also in the vertical position.

Heat transfer results from this study are presented in Figs. 8 through 22. Except for the double-fluted tubes, all experimental data are presented in two dimensional forms. The first dimensional form (Figs. 9, 11, and 13) presents a composite condensing film coefficient h* vs heat flux Q/A. Condensing-side coefficients are reported as composite coefficients (combining vapor-side resistance and wall resistance) because of the difficulty in describing wall resistance for the complex geometry of enhanced tubes. Augmentation arising from the surface area increase in enhanced tubes is accounted for by use of the total outside condensing

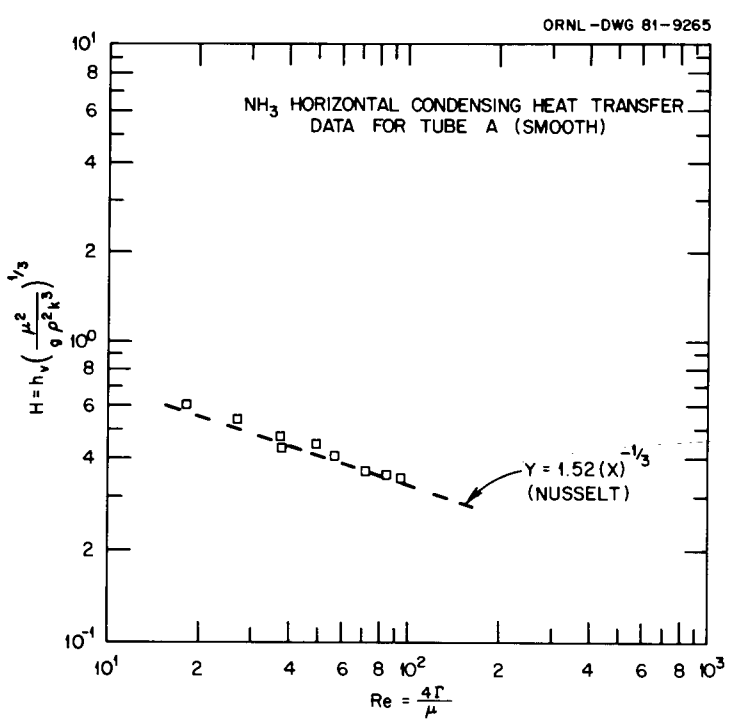

Fig. 8. Horizontal smooth-tube condensation data for ammonia (nondimensional form).

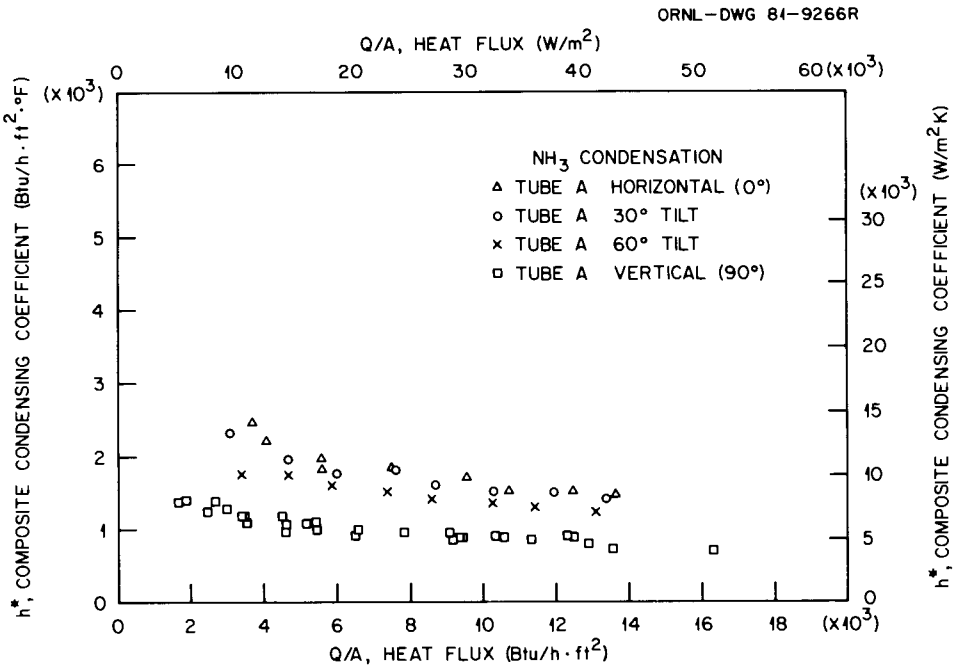

Fig. 9. Wilson-plot results for smooth Tube A condensing at various angles (0 to 90°) – h* vs Q/A.

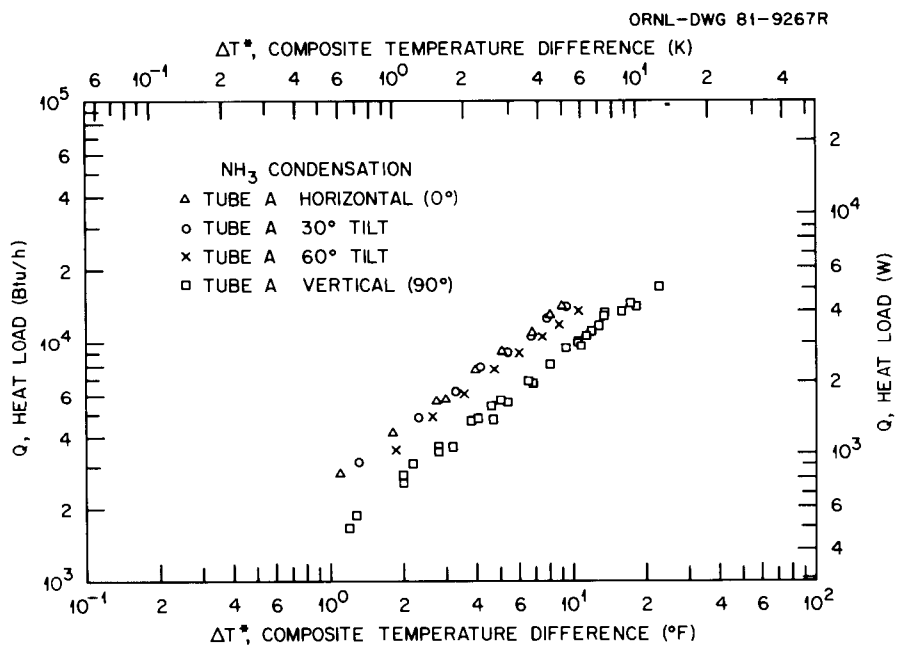

Fig. 10. Wilson-plot results for smooth Tube A condensing at various angles (0 to 90°) – Q vs ΔT*.

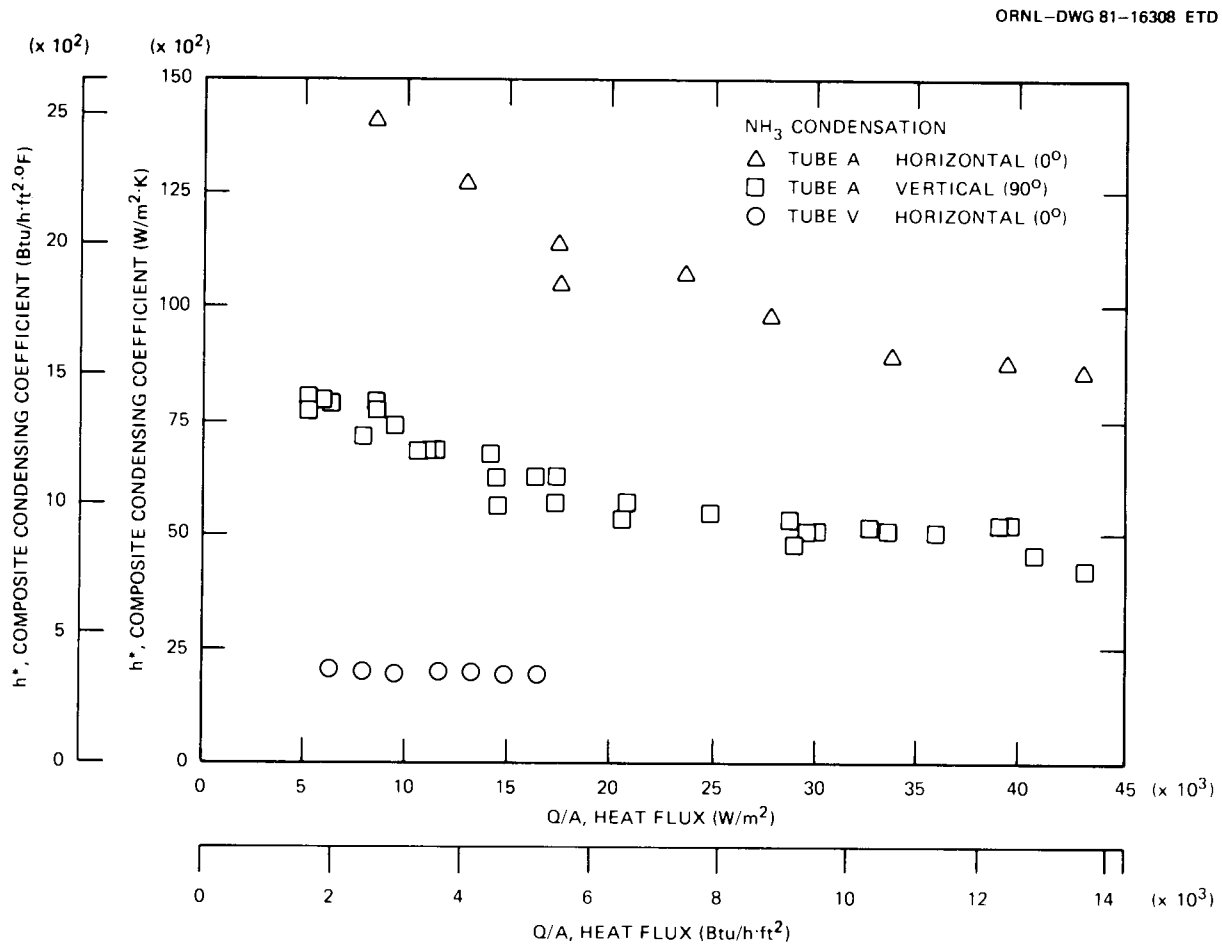

Fig. 11. Comparison of Wilson-plot results for smooth Tube A and finned Tube V – h* vs Q/A.

area for each tube (Table 1) in expressing h* and Q/A. The second dimensional form, heat load Q vs composite condensing temperature ΔT* (difference between the vapor temperature and inside wall temperature of the tube), shows the effect of the increased area of the enhanced tubes. For the double-fluted tubes, only overall heat transfer results (Figs. 15 through 22) are plotted in the form of heat load vs overall temperature difference. For these tubes, the use of the Wilson-plot method in determining condensing-side coefficients gave uncertain results, a phenomenon that will be discussed in a later section.

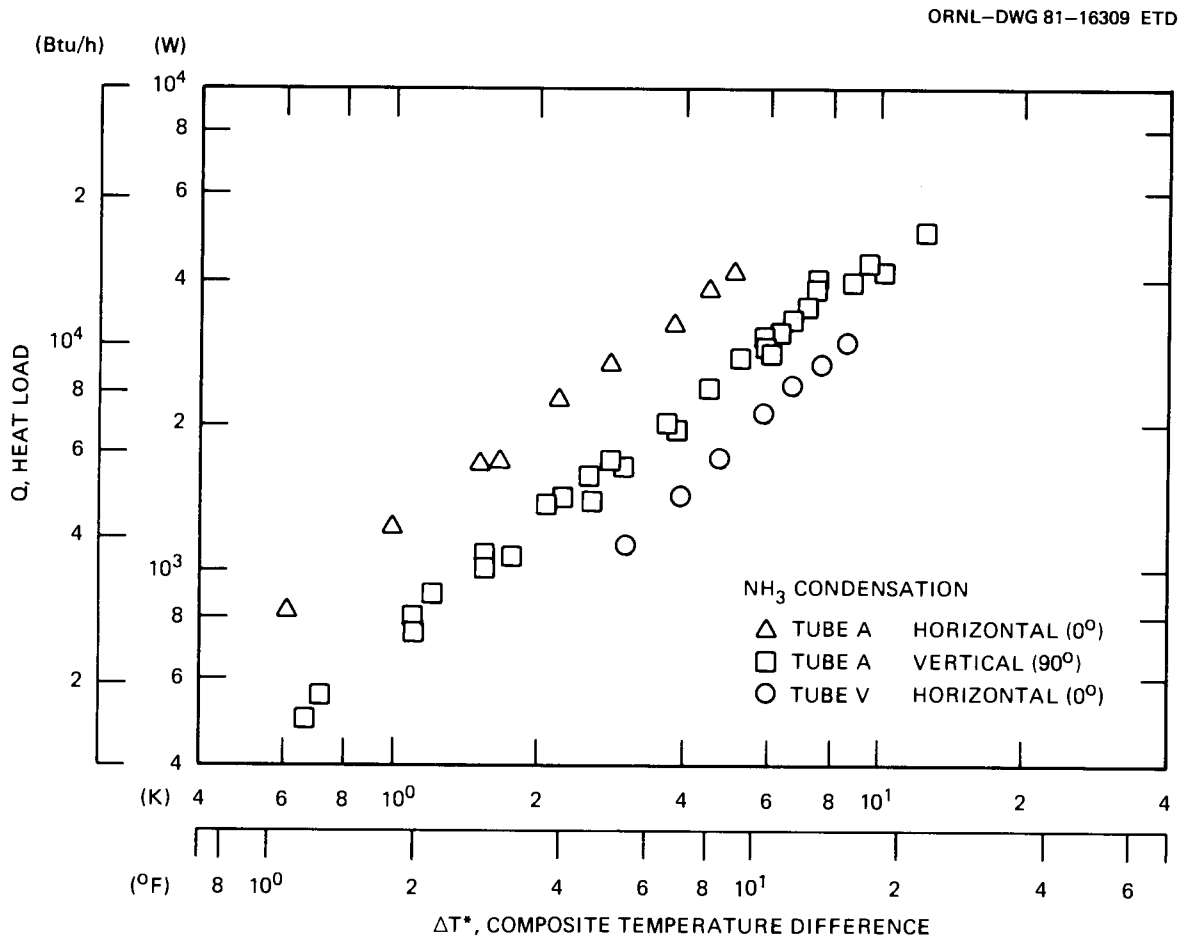

Fig. 12. Comparison of Wilson-plot results for smooth Tube A and finned Tube V – Q vs ΔT*.

Experimental data are documented in Appendix D (Tables D.1 through D.14), where the data are tabulated along with the overall condensing heat transfer coefficients and heat balance checks for the condenser test section. Tables D.1 and D.5 and Tables D.6 and D.7 are taken from Refs. 1 and 2, respectively.

Wilson-plot results for the applicable test tubes are tabulated in Appendix C, where Tables C.1 and C.5 are also taken from Ref. 1. A sample Wilson-plot is shown in Appendix A with associated calculations.

Parameter ranges for the experiments were as presented in Table 2.

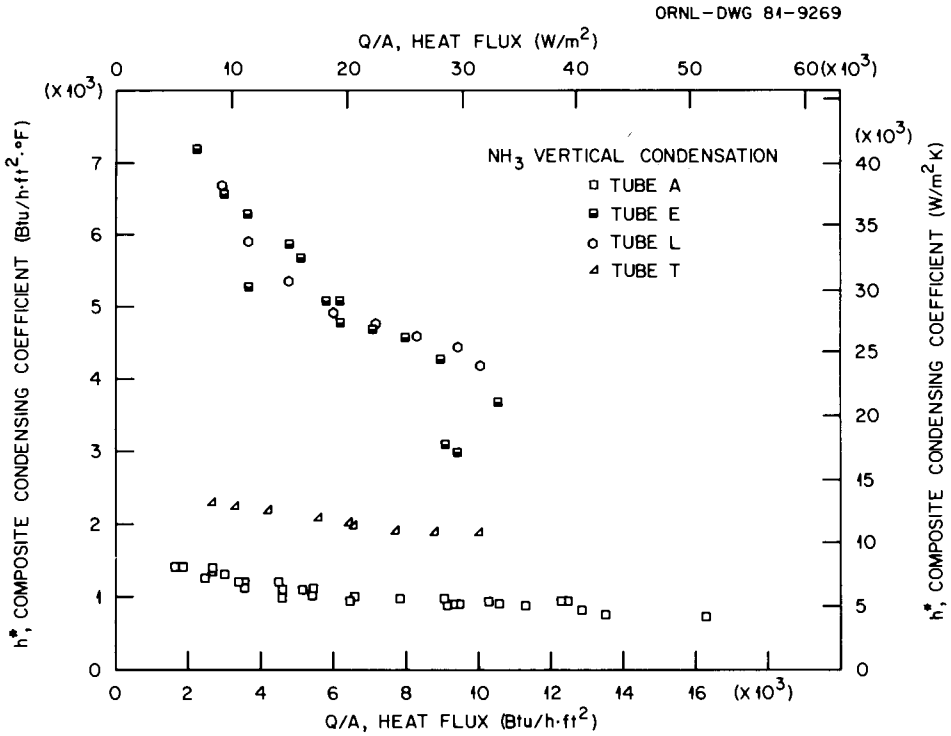

Fig. 13. Wilson-plot results for vertical single-fluted Tubes L and T and other previously tested tubes — h* vs Q/A.

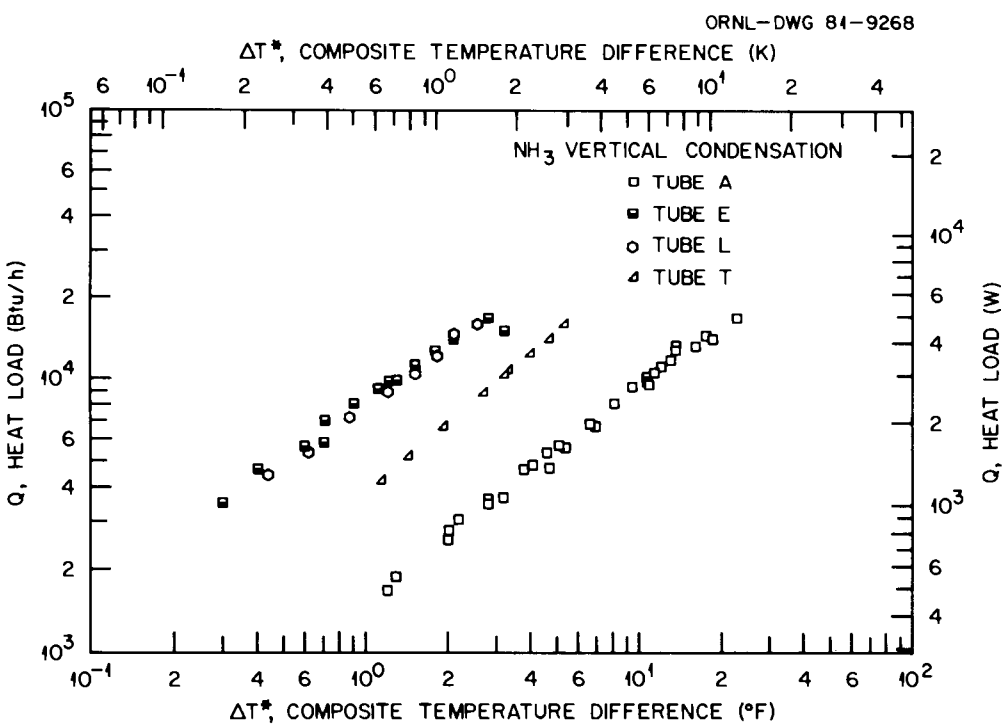

Fig. 14. Wilson-plot results for vertical single-fluted Tubes L and T and other previously tested tubes — Q vs ΔT*.

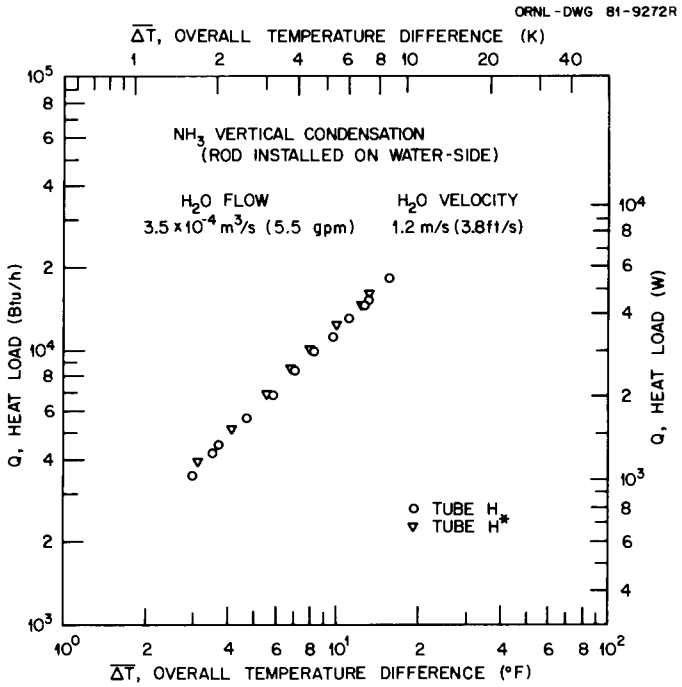

Fig. 15. Overall heat transfer performance of double-fluted Tubes H and H* with water flowing through an annulus at 3.5 x 10^{-4} m^3/s (5.5 gpm).

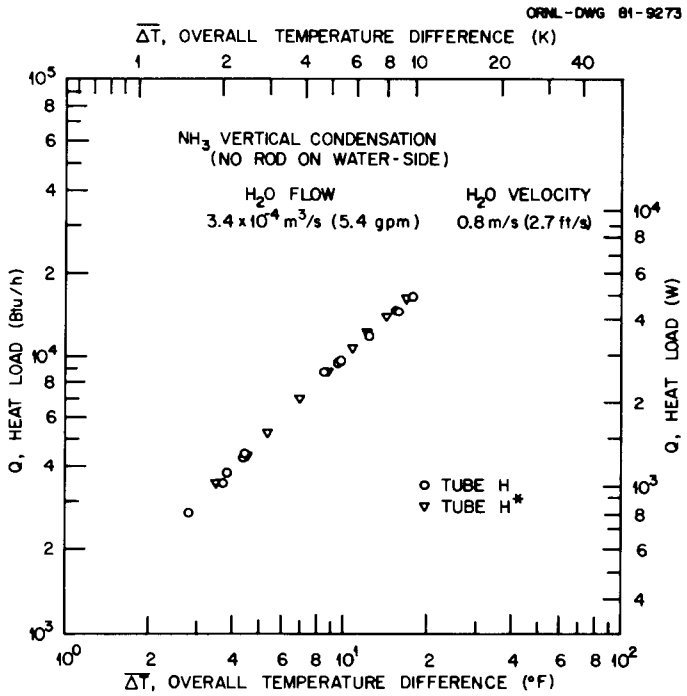

Fig. 16. Overall heat transfer performance of double-fluted Tubes H and H* with water flowing inside tube (no rod) at 3.4 x 10^{-4} m^3/s (5.4 gpm).

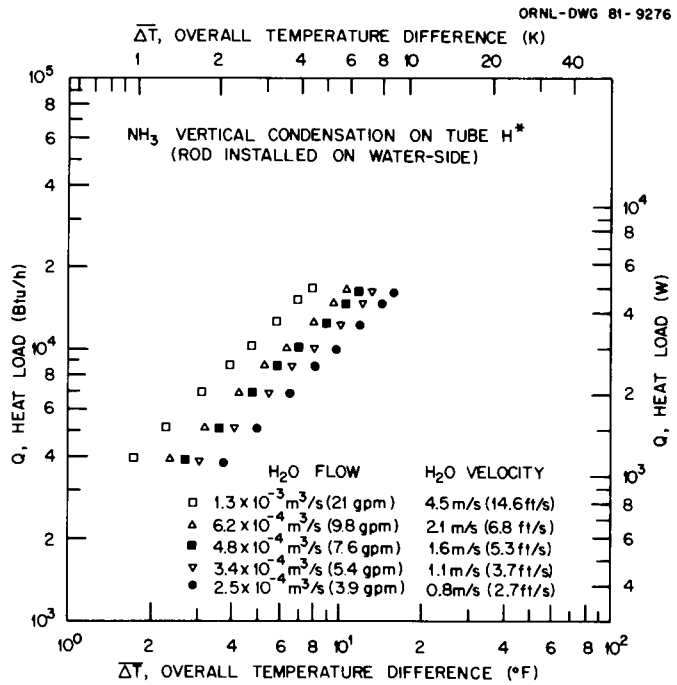

Fig. 17. Overall heat transfer performance of double-fluted Tube H* at various water flow rates (rod installed on water side).

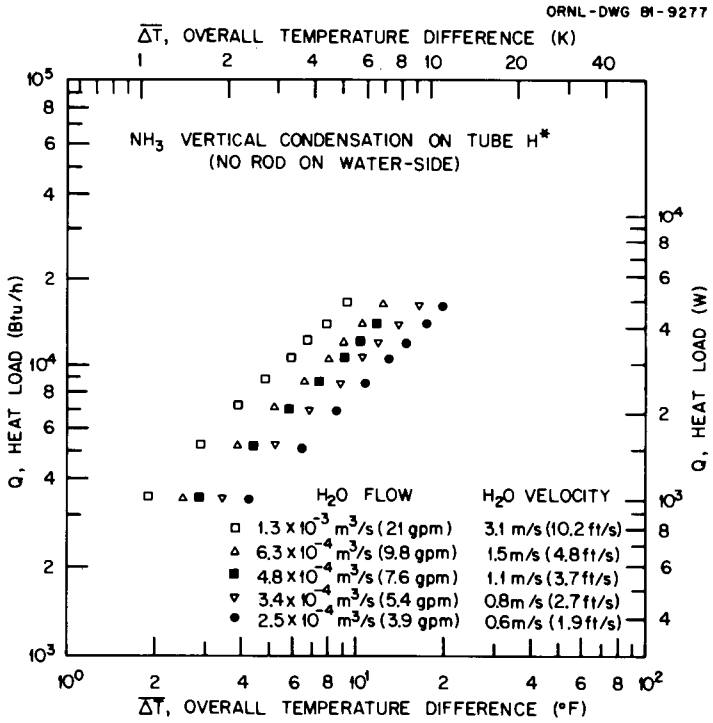

Fig. 18. Overall heat transfer performance of double-fluted Tube H* at various water flow rates (no rod on water side).

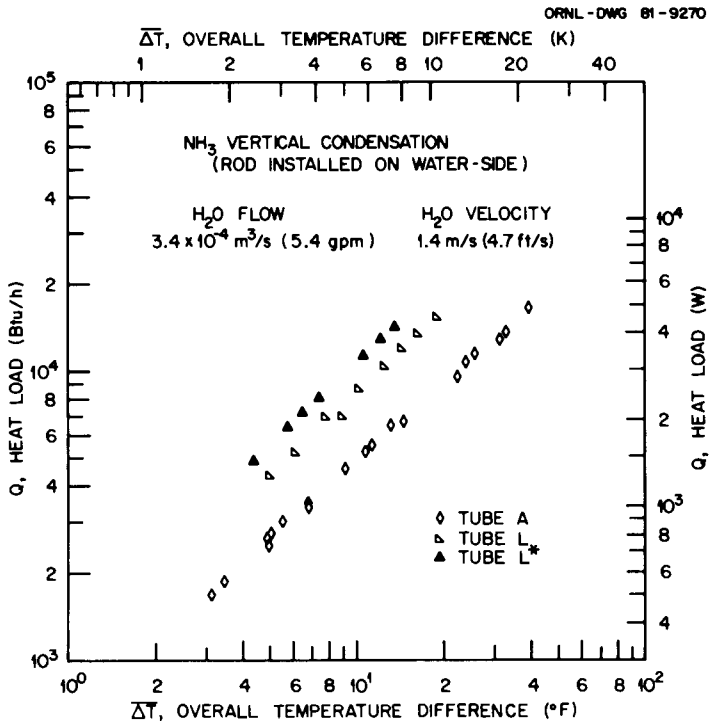

Fig. 19. Overall heat transfer performance of Tubes A, L, and L* with water flowing through an annulus at 3.4 x 10^{-4} m^3/s (5.4 gpm).

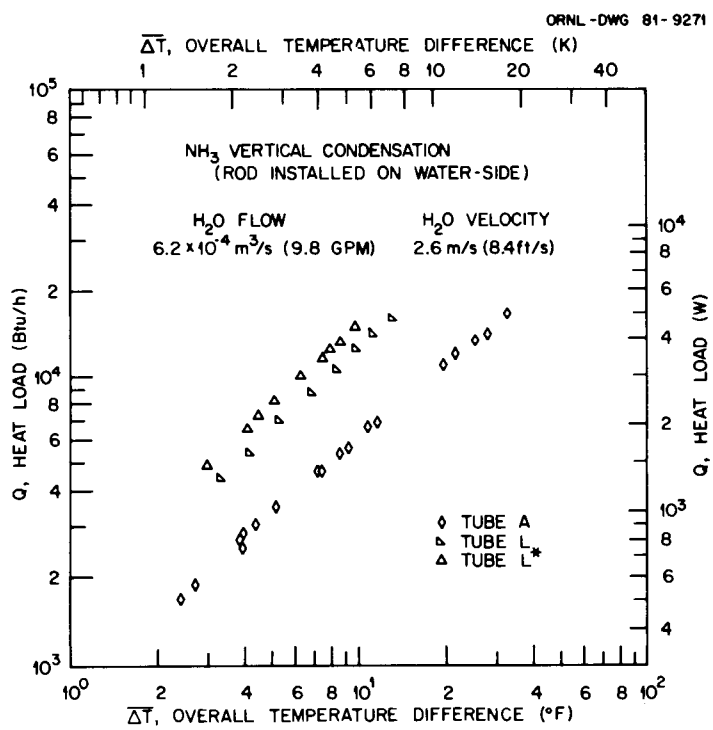

Fig. 20. Overall heat transfer performance of Tubes A, L, and L* with water flowing through an annulus at 6.2 x 10^{-4} m^3/s (9.8 gpm).

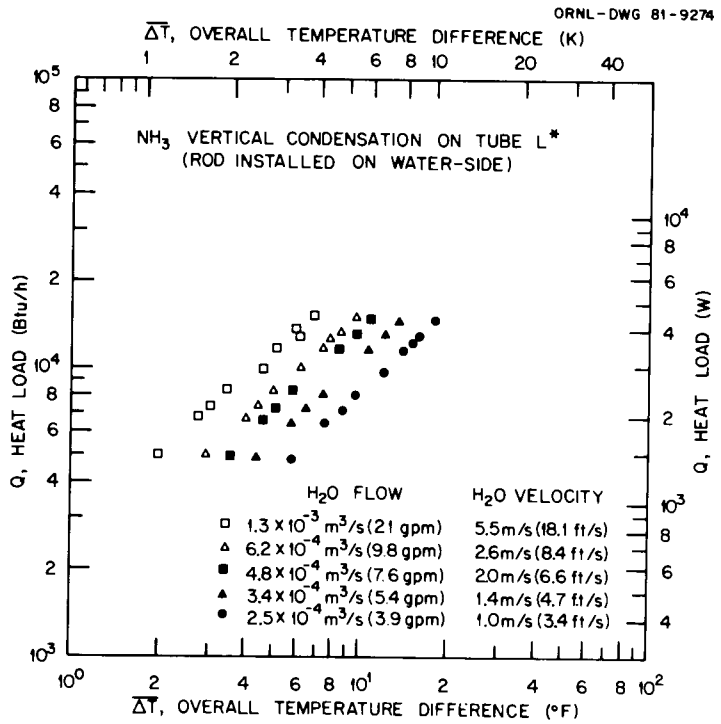

Fig. 21. Overall heat transfer performance of double-fluted Tube L* at various water flow rates (rod installed on water side).

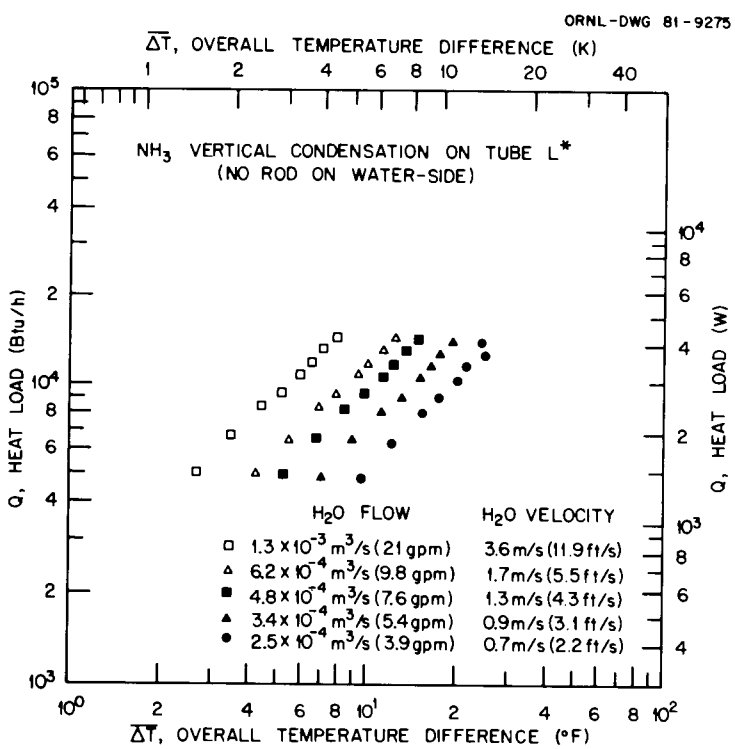

Fig. 22. Overall heat transfer performance of double-fluted Tube L* at various water flow rates (no rod on water side).

Table 2. Parameter ranges for condensing tests

Parameter	Test tube					
	A[a]	L	L*[b]	H*[b]	T	V
Condensing temperature, K (°F)	302–315 (85–108)	299–310 (78–99)	299–315 (78–108)	298–311 (77–101)	300–311 (80–100)	301–313 (82–104)
Condensing pressure, MPa (psia)	1.15–1.65 (167–240)	1.02–1.45 (148–210)	1.02–1.65 (148–240)	1.01–1.49 (146–216)	1.05–1.48 (153–214)	1.1–1.56 (160–227)
Composite condensing temperature difference, K (°F)	0.6–5.9 (1.1–10.6)	0.3–1.4 (0.5–2.5)			0.7–2.9 (1.2–5.3)	3.1–8.7 (5.5–15.7)
Heat load, W (Btu/h)	820–4,190 (2,800–14,300)	1,320–4,690 (4,500–16,000)	1,470–4,400 (5,000–15,000)	970–4,830 (3,300–16,500)	1,250–4,690 (4,300–16,000)	1,150–2,930 (3,900–10,000)
Heat flux, W/m² (Btu/h·ft²)	8,500–42,900 (2,700–13,600)	9,500–33,700 (3,000–10,700)	10,400–31,500 (3,300–10,000)	6,600–32,200 (2,100–10,200)	8,500–31,500 (2,700–10,000)	6,300–16,400 (2,000–5,200)
Overall heat transfer coefficient, W/m²·K (Btu/h·ft²·°F)	2,700–8,800 (471–1,548)	2,500–11,000 (435–1,930)	1,900–11,500 (330–2,010)	2,800–9,500 (496–1,677)	2,100–7,000 (378–1,229)	870–1,670 (153–276)
Composite condensing heat transfer coefficient, W/m²·K (Btu/h·ft²·°F)	7,000–14,100 (1,235–2,477)	23,900–38,200 (4,203–6,729)			10,700–13,100 (1,881–2,307)	1,900–2,000 (332–358)

[a]Parameter ranges include horizontal, 30°, and 60° tilt tests with Tube A.

[b]Composite condensing heat transfer coefficients and temperature differences are not presented because of uncertainties in the Wilson-plot results.

5.1 Smooth Tube A

Experiments were run to determine the effect of tilt angle α on the condensing heat transfer performance of a smooth tube. A series of tests was conducted for ammonia condensing on the outside of Tube A with the condenser test section arranged in a horizontal position ($\alpha = 0^\circ$) and at 30° and 60° from the horizontal plane.

During the early part of this test series, unexpected dropwise condensation was observed on the outer surface of Tube A; this was apparently initiated by impurities introduced at the time of a gasket failure (see Appendix B). As a result, much higher composite coefficients were observed than any obtained in earlier ammonia condensation work.[1,2] The cause of this phenomenon was corrected, however, by flushing, evacuating, and recharging the system with ammonia and replacing the test tube with one of similar design. Subsequent observations of the condensing film through existing view ports showed proper film cohesiveness throughout this study.

In this study, confidence in the accuracy of the experimental data is justified for the following reasons: (1) after correcting earlier difficulties encountered with the presence of dropwise condensation, shakedown test results for Tube A in the vertical position were found to agree very well with those obtained from previous Tube A vertical-condensation tests;[1] (2) as reported in the next section, experimental data for horizontal Tube A were found to agree well with analytical predictions suggested by Nusselt;[13,14] and (3) refinements made prior to operation of the test loop aided in increasing the accuracy of condensate flow measurements and allowed for the visual and photographic observation of the condensing surface.

5.1.1 Horizontal test results

Figure 8 shows horizontal condensation results for Tube A in nondimensional form. The ordinate is the standard nondimensional heat transfer

coefficient (averaged over the length of the tube):

$$H = h_v \left(\frac{\mu^2}{g\rho^2 k^3}\right)^{1/3} . \tag{5.1}$$

In this case, the wall resistance has been eliminated from the composite coefficient h* by the use of Eq. (4.7). The abscissa is the liquid film Reynolds number:

$$Re = 4\Gamma/\mu , \tag{5.2}$$

where for a horizontal tube, Γ is the condensate flow rate at the bottom of the tube per unit length of tube. Fluid properties k, ρ, and μ have been evaluated at the equivalent film temperature T_f as suggested by McAdams.[13] The method for obtaining the equivalent film temperature is illustrated in Appendix A under "Nondimensional Quantities."

Experimental data for ammonia condensing on Tube A are plotted (Fig. 8) and compared with the line representing the well-known analytical correlation by Nusselt.[13,14] As illustrated, the position of the data is in the region of the Nusselt prediction, with a $\pm 6\%$ maximum scatter between calculated and predicted values. In general, the smooth tube data are in good agreement with predictions using the Nusselt relation. Such a comparison indicates the confidence level characteristic of the present data.

Figures 9 and 10 present data in dimensional form for Tube A condensing at $\alpha = 0°$, $30°$, $60°$, and $90°$. Ammonia heat transfer data for Tube A condensing at $\alpha = 90°$ are taken from Ref. 1 and are plotted in Figs. 9 and 10 for baseline comparison with the data at other tube angles tested in this study. Only horizontal condensation results are discussed in this section; inclined test results will be discussed in the next section.

As expected from theory, results in Fig. 9 (plotted as composite coefficient vs heat flux) show the excellent performance of Tube A in the horizontal configuration, as compared with earlier tests in the vertical position. As indicated (Fig. 9), composite condensing coefficients ranged between 8,500 $W/m^2 \cdot K$ (1,497 $Btu/h \cdot ft^2 \cdot {}^oF$) and 14,000 $W/m^2 \cdot K$ (2,466 $Btu/h \cdot ft^2 \cdot {}^oF$) for horizontal condensation, as compared with 4,200 $W/m^2 \cdot K$

(740 Btu/h·ft²·°F) and 6,530 W/m²·K (1,150 Btu/h·ft²·°F) for vertical condensation at similar heat fluxes. At a low heat flux, 11,668 W/m² (3,700 Btu/h·ft²), the composite coefficient for horizontal Tube A increased by up to 2.1 times the vertical Tube A value. Even at the higher fluxes (~43,000 W/m²), the horizontal composite coefficients were twice the comparable vertical tube values.

In Fig. 10, the horizontal condensation data for Tube A (plotted in heat load vs composite condensing temperature difference form) similarly illustrates its superiority when compared with previous vertical test results. For a given condensing temperature difference, the horizontal Tube A accommodated a heat load of up to 1.6 times the vertical Tube A value. For example, at a composite condensing temperature difference of 5.7 K (8.0°F), horizontal Tube A accommodated a heat load of 3,809 W (13,000 Btu/h) while in the vertical mode, only 2,344 W (8,000 Btu/h) was obtained, thus providing a heat load ratio of 1.6. In fact, over the range of condensing temperature differences indicated in Fig. 10, the heat load ratios between the horizontal and vertical results were ~1.6.

5.1.2 Inclined test results

Previous ammonia condensation data taken at ORNL for an inclined smooth tube[2] indicated that considerable heat transfer enhancement could be achieved by simply inclining the test tube 30° from the vertical (corresponding to $\alpha = 60°$ in this report).

As reported in Ref. 2, "for the smooth Tube A, the heat transfer performance of the inclined tube was significantly greater than that of the vertical tube (approximately doubled over the full heat flux test range)."

In an effort to verify and extend earlier inclined test results, a series of tests was performed on an identical smooth tube oriented 30° and 60° from the horizontal position. Unexpectedly, test results at a 60° tilt disagreed with previously published data. The earlier condensing heat transfer coefficients were up to 230% higher than those obtained in this study. Although the cause for such discrepancy is still not certain, a possible explanation may be that dropwise condensation may have occurred without the experimenter's knowledge during the earlier inclined tube tests, in a manner somewhat similar to the dropwise condensation

phenomenon observed during the earlier part of this study (see Appendix B). For reasons noted earlier, we believe that the inclined test data presented herein are more accurate than those previously published in Ref. 2.

As shown in Figs. 9 and 10, an increase in tilt angle from the horizontal decreases in some degree the condensing-side performance of smooth Tube A. Conversely, these figures indicate an increase in condensing performance as the tilt angle is decreased from the vertical to the horizontal position. This effect is clearly shown in Fig. 9, where at $\alpha = 60^\circ$, composite condensing coefficients for Tube A increased by up to 1.5 times vertical Tube A values over the range of heat flux tested. From Fig. 9, at a low heat flux of 10,595 W/m^2 (3,360 $Btu/h \cdot ft^2$), the smooth-tube composite coefficient at $\alpha = 60^\circ$ was 9,937 $W/m^2 \cdot K$ (1,750 $Btu/h \cdot ft^2 \cdot {}^\circ F$), compared with 6,757 $W/m^2 \cdot K$ (1,190 $Btu/h \cdot ft^2 \cdot {}^\circ F$) for the vertical orientation, thus providing a 50% increase in coefficient. In addition, a similar observation made in Fig. 10 shows that for a given composite condensing temperature difference, Tube A at $\alpha = 60^\circ$ can accommodate a heat load of up to 1.4 times the vertical Tube A value. Alternatively, for a given heat load, the vertical Tube A required a condensing temperature difference of up to 1.6 times the 60° tube angle value.

As illustrated in Figs. 9 and 10, for a 30° angle, the condensing-side performance of Tube A appears to approach that obtained for the horizontal position, particularly at the higher heat loads and/or fluxes.

Further, unlike the experimental curve for $\alpha = 60^\circ$, composite coefficients for $\alpha = 30^\circ$ (Fig. 9) appear to decrease more rapidly with increasing heat flux. Figure 9 indicates that the resulting composite coefficients at $\alpha = 30^\circ$ increased by 14 to 29% more than the data at $\alpha = 60^\circ$ for the high and low heat fluxes, respectively.

The effect of tube tilt on the condensing heat transfer coefficient is attributed to the character of the condensate film, which is dependent on the angle of inclination of the tube and the heat transfer rate. From observations made through existing view ports, ammonia condensate on a horizontal smooth tube appeared to accumulate in the form of drops at various points on the underside of the tube. The liquid was retained until the weight of the condensate was sufficient to overcome surface tension

forces. Subsequently, the condensate dripped from the tube as droplets rather than in a continuous film. This condensate drainage results in decreasing the "effective thickness" (resistance) of the condensate film, thus providing increased condensing-side coefficients at a given heat flux. At the higher heat fluxes, however, the condensate film is somewhat thicker, thus lowering the condensing heat transfer coefficient. Apparently, for small tube angles ($<30^\circ$), the condensate flow seems to drain (or drip) somewhat similarly to the horizontal mode along most of the length of the tube. This mechanism may account for the fact that in Figs. 9 and 10 the condensing performance at $\alpha = 30^\circ$ approaches that of the horizontal position. However, as the tilt angle increases toward a vertical position, the amount of condensate remaining on the tube surface increases to the point where nearly all of the condensate leaves at the lower end of the tube. The result is a greater "effective" film thickness that contributes to a lower condensing-side heat transfer coefficient.

From a heat exchanger economics point of view, it is obvious from Figs. 9 and 10 that only a small inclination ($\sim 30^\circ$) of Tube A from the vertical will give better condensing performance than for the vertical position. From the viewpoint of heat transfer, however, the maximum condensing performance is achieved at the horizontal position, for the range of heat loads investigated.

Conclusions from Figs. 8 through 10 include:

1. Experimental data for ammonia condensing on the outside of a horizontal smooth tube (Tube A) were found to agree well with analytical predictions following Nusselt.[13,14]

2. For Tube A, the maximum condensing performance was achieved at the horizontal tube position. For a given heat flux, horizontal Tube A achieved composite condensing coefficients of up to 2.1 times vertical smooth tube values. For a given composite condensing temperature difference, horizontal Tube A accommodated heat loads up to 1.6 times vertical smooth tube values. Note that these levels of improvement are not, however, expected to be sustained with large horizontal tube bundles because of the effects of accumulated condensate drainage through the bundle.

3. When judged on a heat load vs composite condensing temperature difference, the condensing performance for Tube A oriented 30° from the horizontal was similar to that obtained for the horizontal position.

4. The condensing performance for Tube A tilted 60° from the horizontal was lower than that obtained at a 30° tilt. For a given heat flux with smooth Tube A tilted 60° from the horizontal, composite condensing coefficients of up to 1.5 times vertical Tube A values were achieved. For a given composite condensing temperature difference, Tube A at a 60°-tilt accommodated a heat load up to 1.4 times vertical Tube A value. For a given heat load, vertical Tube A required a composite condensing temperature difference of up to 1.6 times the 60°-tilt Tube A value.

5.2 Finned Tube V

Condensation tests on the external-finned Tube V were conducted with the tube oriented in the horizontal position. Wilson-plot results for Tube V are presented in Figs. 11 and 12 with horizontal and vertical smooth-tube data, which serve as the basis for comparison. As illustrated in these figures, the performance for Tube V fell far below that for either the horizontal or vertical smooth tube. For a given heat flux, composite condensing coefficients for Tube V (Fig. 11) were 86% below those for horizontal Tube A and 70% below those for vertical Tube A. Similarly, for a given composite temperature difference (Fig. 12), Tube V accommodated only 40 and 65% of the heat load yielded by the horizontal and vertical Tube A, respectively.

One possible explanation for the poor performance encountered with Tube V may be that its fin-to-fin spacing or drainage channel size [0.069 cm (0.027 in.)] appeared (visually) to severely restrict the flow of condensate when operating on a horizontal position, thus seriously limiting the advantage offered by the fins. Also, because stainless steel has relatively low thermal conductivity (43.75 W/m·K for Tube V vs 211 W/m·K for the aluminum Tube A) the added wall resistance would further decrease the composite condensing heat transfer coefficients.

The main conclusion drawn from Figs. 11 and 12 is that in the horizontal position, external-finned Tube V gave the lowest condensing performance of any tube discussed in this report.

5.3 Vertical Single-Fluted Tubes L and T

Wilson-plot results for single-fluted Tubes L and T are presented in Figs. 13 and 14, with previous data for smooth Tube A and single-fluted Tube E taken from Ref. 1. Plots (Figs. 13 and 14) show the condensing data in two dimensional forms: (1) on composite condensing coefficient h* vs heat flux Q/A basis and (2) on heat load Q vs composite temperature difference ΔT* basis. As indicated earlier, the composite condensing coefficient h* includes both the vapor side plus wall resistance. Similarly, the composite temperature difference ΔT* is defined as the difference between the vapor temperature and the inside tube-wall temperature.

When the condensing-side heat transfer coefficient is very large (low resistance to heat flow) as a result of external enhancement, the water-side coefficient and tube-wall thermal conductance will tend to become more dominant (a larger fraction of the total overall resistance) in determining heat flow. In general, for ammonia, which exhibits superior heat transfer characteristics, condensing-side coefficients are quite large, particularly for fluted tubes. Therefore, composite condensing coefficients become quite sensitive to changes in tube-wall thermal conductance and water-side coefficients, especially at low water velocities (low water-side coefficients). In this study, water-side coefficients were intentionally increased by using a 0.5-in.-diam rod inside the tube to decrease the hydraulic diameter and increase the water velocity, thus improving the accuracy of the composite coefficients obtained by the Wilson-plot method.

In Fig. 13, composite coefficients for Tube T lie above those for smooth Tube A, but far below those for fluted Tube E. In addition, coefficients for Tube T decrease slightly with increasing heat flux. Note that Tube T is geometrically identical to the aluminum Tube E, but made of carbon steel (Table 1). Figures 13 and 14 indicate that the wall resistance of Tube T adversely affects the overall heat transfer performance. The wall conductivity for Tube T (47.6 W/m·K) is about 77% lower than that for Tube E (211 W/m·K); hence, the wall resistance for Tube T is increased by a factor of 4 over that of Tube E. The large decrease in performance can be qualitatively accounted for by the difference in tube material thermal conductivity.

As shown in Fig. 13, at a low heat flux of 9,145 W/m² (2,900 Btu/h·ft²), the composite condensing coefficient for Tube T was increased by as much as 1.8 times the smooth Tube A value but was only about 35% of the Tube E value. Similarly, from Fig. 14, at a low condensing temperature difference of 0.7 K (1.2°F), Tube T accommodated a heat load of 2.6 times the smooth tube value but only 44% of the Tube E value. Alternatively, for a given heat load the maximum condensing temperature difference ratio (Tube A to Tube T) was 3.7 at the highest heat load [4,688 W (16,000 Btu/h)]. However, for the same heat load (~16,000 Btu/h), Tube T required a condensing temperature difference of up to 2.1 times the fluted Tube E value.

In Figs. 13 and 14, Tubes L and E appear to have approximately the same condensing performance; but, unlike Tube T, the coefficients for Tubes L and E decrease quite rapidly with increasing heat flux (Fig. 13). As indicated in Table 1, Tubes L and E are both made of aluminum and have 60 external flutes; however, where Tube E has square-shaped flutes, Tube L features rounded external flutes and greater rill cross section (Fig. 23). Previous work at ORNL with ammonia[1] had suggested condensing-side coefficients for external enhanced tubes to be dependent on the shape of the

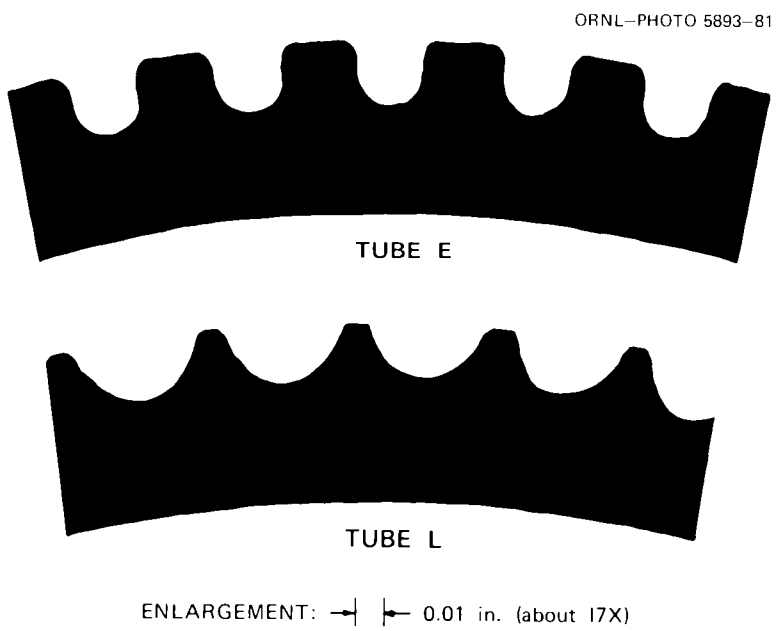

Fig. 23. Tube-wall cross section for Tubes E and L.

flute as well as the size and number of flutes. In this study, no appreciable effect in condensing performance is indicated between Tubes L and E, as a result of different flute shape. Also, while Tube L had somewhat less (~6%) condensing area (Table 1) than Tube E, any area effect was essentially accounted for in Fig. 13 by use of coordinates based on the total condensing area for each tube.

As shown in Fig. 13, for a given heat flux the maximum composite heat transfer coefficient achieved with Tube L was 5.2 times the smooth Tube A value, occurring at the lowest test heat flux of 9,145 W/m^2 (2,900 $Btu/h \cdot ft^2$). This represents the maximum enhancement ratio achieved for any of the single-fluted tubes discussed in this report. The corresponding minimum composite coefficient for Tube L was 4.5 times the smooth tube value at the highest test heat flux of 3,153 W/m^2 (10,000 $Btu/h \cdot ft^2$).

A similar analysis of the data in Fig. 14 shows that for a given condensing temperature difference, the maximum heat load achieved with Tube L was 5.4 times the smooth tube value, occurring at the lowest condensing temperature difference [0.7 K (1.2°F)]. The corresponding minimum heat-load ratio was 4.7 at the highest condensing temperature difference [1.4 K (2.6°F)].

Also, from Fig. 14, for a given heat load the maximum condensing temperature difference ratio (Tube A to Tube L) was 8.2 at the lowest heat load [1,289 W (4,400 Btu/h)]. The corresponding minimum condensing temperature difference ratio was 7.7 at the highest heat load [4,688 W (16,000 Btu/h)].

Conclusions from Figs. 13 and 14 include:

1. The best external fluted tube tested (Tube L) can increase composite condensing heat transfer coefficients for ammonia condensing at a given heat flux by up to 5.2 times vertical smooth-tube values.

2. Such an enhancement cannot be accounted for by the increased area of the fluted tube but may be attributed to surface tension effects as described by Gregorig.[15]

3. Tube L can increase heat load capability to 5.4 times the smooth vertical tube value for ammonia condensing at a given temperature difference; conversely, for a given heat load, a smooth tube can require a condensing temperature difference of up to 8.2 times that for Tube L.

4. No appreciable difference in condensing performance was found between the aluminum Tube L, which utilizes 60 rounded external flutes, and previously tested aluminum single-fluted Tube E, which features 60 square-shaped external flutes.

5. The increased wall thermal resistance of carbon-steel fluted Tube T severely decreased composite condensing heat transfer coefficients over those for the geometrically identical aluminum fluted Tube E.

6. At the lower heat fluxes, composite condensing coefficients for fluted Tube T were increased by up to 1.8 times the smooth tube values but were only 35% of fluted Tube E values.

5.4 Vertical Double-Fluted Tubes H* and L*

As previously mentioned, the Wilson-plot method for determining condensing-side heat transfer coefficients was somewhat uncertain when applied to double-fluted Tubes H* and L*. A possible explanation is that water-side coefficients for an inside fluted tube, unlike those for a smooth inside tube wall, are not the simple function of water velocity assumed for the Wilson plot. More specifically, because the Wilson-plot method is based on a 0.8 power dependence of the water-side coefficient on flow rate, such an assumption may not necessarily apply to the water-side characteristics of these tubes. As a result, some appreciable error is introduced when the method is used to determine composite condensing performance of double-fluted tubes. Consequently, a degree of uncertainty is introduced when comparisons of Wilson-plot results are made between double-fluted tubes and the other tubes tested.

To provide a more reliable basis for comparison, only overall heat transfer data (collected as a prerequisite to the Wilson-plot method) are presented for Tubes H* and L* on a heat load Q vs overall temperature difference $\overline{\Delta T}$ basis. In this form, the uncertainty introduced by the application of the Wilson-plot technique to these tubes is avoided.

5.4.1 Tube H* test results

In a previous study,[2] overall heat transfer data were reported for double-fluted Tube H. Tube H*, also designed by CMU,[4] was internally

identical to Tube H but featured 36 external flutes compared with 45 for Tube H (Table 1).

To determine the effects of a reduction in the number of external flutes on tube performance, overall heat transfer data for the double-fluted Tube H* were compared with earlier overall results obtained with the similar double-fluted Tube H.

Overall heat transfer results for the two tubes, obtained at equal water flow rates [3.5×10^{-4} m^3/s (5.5 gpm)], are presented in Figs. 15 and 16 for two water-side arrangements (with and without a 1.27-cm rod inside the tube). The installation of a rod inside the tube increased the overall coefficients for both Tubes H and H*, as a result of higher water velocities. This effect of water velocity on overall heat transfer performance is best shown in Figs. 17 and 18, where data for Tube H* are plotted for a series of water flow rates, with and without a rod installed on the water side, respectively.

Judged on a heat load vs overall temperature difference (Figs. 15 and 16), no appreciable difference in overall performance was found between Tubes H and H* as the result of reducing the number of external flutes from 45 to 36. This is not surprising because the ammonia condensing-side coefficients are probably already quite large (compared to the water-side coefficients, even with a rod inside the tubes) as a result of external enhancement.

In Ref. 16, a comparison of overall coefficients between ORNL single-tube data and ANL large (240-tube) condenser tube bundle tests[5,6] was made for double-fluted Tubes H and H* to determine whether performance anticipated on the basis of single-tube tests can be achieved in tube bundle configurations. Overall heat transfer results from ORNL double-fluted single-tube tests were in approximate agreement with ANL double-fluted condenser tube bundle data. However, for similar heat loads, the ANL overall coefficient ratio between Tubes H and H* differed by 16%; this was contrary to results presented here that show overall performance to be virtually unchanged as the number of external flutes is reduced from 45 (Tube H) to 36 (Tube H*).

Conclusions from Figs. 15 through 18 include:

1. The overall heat transfer coefficients for Tube H* with a 1.27-cm (0.5-in.) rod installed on the water side were better than those without the rod.

2. This increase in overall coefficients was caused by water-side heat transfer enhancement associated with the higher water velocities existing in the presence of the internal rod.

3. No appreciable difference in overall performance was found when the number of external flutes on the CMU Tube H* was reduced from 45 (Tube H) to 36 (Tube H*).

5.4.2 Tube L* test results

Tests were conducted with Tube L* (60 external and 90 internal flutes) to determine the effect of inside flutes and water velocity on the overall heat transfer performance.

The effect of inside flutes was determined by comparing overall test results for Tube L* with overall data for the single-fluted Tube L, which was externally identical to Tube L* but had a smooth inside tube wall.

Overall heat transfer results for Tubes L* and L, with smooth Tube A, are presented in Figs. 19 and 20 as heat load vs overall temperature difference for two different water flow rates. The experimental overall data presented in these figures for Tube L* were obtained with cooling water flowing through an annulus (1.27-cm-OD rod inside the tube). Such a water-side arrangement was necessary to match the water-side configuration used in testing Tube L earlier in this study.

From Fig. 19, the maximum improvement in heat load achieved with Tube L* was 25% above the comparable Tube L*, occurring at the lowest overall temperature difference of 2.7 K (4.9°F) and a water flow rate of 3.4×10^{-4} m^3/s (5.4 gpm). Even at the higher temperature differences, heat loads for Tube L* were as high as 24% above Tube L values. A similar comparison made on Fig. 20 shows that for a higher water flow rate [6.2×10^{-4} m^3/s (9.8 gpm)], the heat loads were increased by up to 22% for Tube L* as compared with Tube L for the range of temperature differences tested.

Clearly, Figs. 19 and 20 show that the inside flutes enhance the overall heat transfer coefficients of Tube L* over those for Tube L. However, a question arises concerning whether the inside flutes result in water-side heat transfer coefficient enhancement or whether an increase in overall coefficient is merely caused by an increase in inside surface area alone. The inside surface area of Tube L* is ~1.32 times that of Tube L (Table 1). For the test conditions in this report, an area increase of this order could explain the observed increase in overall performance with no increase in water-side heat transfer coefficient.

Figures 21 and 22 show the effect of water velocity on the overall heat transfer performance of Tube L*. Figure 21 presents overall heat transfer data taken with a 1.27-cm-OD rod installed on the water side for a series of water flow rates, whereas Fig. 22 presents overall data at the same water flow rates without the rod in place. As would be expected, the overall heat transfer performance of Tube L* with a rod is significantly better than that without the rod. This is caused by the higher water-side heat transfer coefficients achieved as a result of higher water velocities for the same water flow rates.

When condensing-side coefficients are very large (as for ammonia vapor), water-side coefficient effects will tend to become more dominant (a larger fraction of the total overall resistance) in the heat flow process. Consequently, the use of internal flutes to improve overall performance appears to be desirable. However, any significant performance gains may be realized at the expense of greater pumping power and fabrication costs associated with internal flutes. Clearly, cost trade-off between pumping power and heat transfer performance is an area that requires careful study.

Conclusions from Figs. 19 through 22 include:

1. For the double-fluted Tube L*, the inside flutes enhanced overall heat transfer coefficients up to 25% above those for a tube with identical outside flutes and a smooth inside surface.

2. The overall coefficients of Tube L* with a 1.27-cm (0.5-in.) rod installed on the water-side were significantly better than those without the rod. This was caused by the higher water-side coefficients achieved as a result of higher water velocities for the same water flow rates.

6. CONCLUSIONS

The main conclusions drawn from this study of ammonia condensation on enhanced tubes of several geometries and orientations may be summarized as follows:

1. The effect of tube orientation on the condensing performance of ammonia on a smooth tube (Tube A) was studied in a series of experiments:
   a. Data for condensation on the outside surface of a horizontally oriented tube were found to agree well with analytic predictions based on the equations of Nusselt.[12-14]
   b. Condensing performance was maximum for the horizontal orientation where, for a given heat flux, composite condensing coefficients were 2.1 times vertical smooth tube values.
   c. Condensing performance at a tube orientation of 30° from the horizontal was similar to that obtained with the horizontal tube, when judged on a heat load vs composite temperature difference basis.
   d. Condensing performance at a tube orientation of 60° from the horizontal was worse than that obtained at a 30° tilt; but composite coefficients, for a given heat flux, were still 1.56 times vertical tube values.
2. Several extremes were observed among the tubes tested:
   a. A horizontally oriented, finned, stainless steel Tube V gave the lowest condensing performance found thus far in these studies; reduced fin effectiveness caused by condensate flooding and high wall thermal resistance (low thermal conductivity) contributed to composite coefficients that were 86% below horizontal smooth tube values for a given heat flux.
   b. A vertically oriented, single-fluted, aluminum Tube L gave the highest performance among the tubes studied with composite condensing coefficients, at a given heat flux, up to 5.2 times the vertical smooth tube values.
3. The effects of several independent parameters (flute shape, tube material, number of flutes, and inside fluting) were examined through

various comparisons:

a. Condensing performance was found to be independent of flute shape in a comparison of Tube L (60 rounded flutes) and Tube E (60 square flutes) data; this contradicts earlier results.

b. Condensing performance for a vertical single-fluted, carbon steel Tube T was severely degraded (by about 65%) over that for a geometrically identical aluminum tube but was still 1.8 times that for a vertical, smooth aluminum tube.

c. Overall performance was virtually unchanged for a double-fluted aluminum tube as the number of external flutes was reduced from 45 (Tube H) to 36 (Tube H*).

d. Overall performance for Tube L* with inside and outside flutes was 25% greater than that observed for Tube L with identical outside flutes but a smooth inside surface.

REFERENCES

1. S. K. Combs, *An Experimental Study of Heat Transfer Enhancement for Ammonia Condensing on Vertical Fluted Tubes*, ORNL-5356 (January 1978).

2. S. K. Combs, *Experimental Data for Ammonia Condensation on Vertical and Inclined Fluted Tubes*, ORNL-5488 (January 1979).

3. E. E. Wilson, "Basis for Rational Design of Heat Transfer Apparatus," *Trans. ASME* 37, 47 (1915).

4. R. R. Rothfus and C. P. Neuman, "The OTEC Program at Carnegie-Mellon University," p. VI-55 in *Proceedings of the Fourth Annual Conference on Ocean Thermal Energy Conversion*, University of New Orleans, New Orleans, Louisiana, March 22-24, 1977.

5. J. J. Lorenz et al., *OTEC Performance Tests of the Carnegie-Mellon University Vertical Fluted-Tube Evaporator*, ANL/OTEC-PS-5 (1979).

6. L. G. Lewis and N. F. Sather, *OTEC Performance Tests of the Carnegie-Mellon University Vertical Fluted-Tube Condenser*, ANL/OTEC-PS-4 (1979).

7. American Society of Heating, Refrigerating, and Air-Conditioning Engineers, "Properties of Refrigerants," chap. 14, p. 268 in *ASHRAE Handbook on Fundamentals*, New York, 1972.

8. American Society of Heating, Refrigerating, and Air-Conditioning Engineers, *Thermodynamic Properties of Refrigerants*, pp. 131-150, ASHRAE, New York, 1969.

9. American Society of Heating, Refrigerating, and Air-Conditioning Engineers, *Thermophysical Properties of Refrigerants*, pp. 145-150, ASHRAE, New York, 1976.

10. W. H. McAdams, *Heat Transmission*, 3d ed., McGraw-Hill, New York, 1954.

11. A. P. Colburn, "A Method of Correlating Forced Convection Heat Transfer Data and a Comparison with Fluid Friction," *Trans. Am. Inst. Chem. Eng.* 29, 174 (1933).

12. E. N. Sieder and C. E. Tate, "Heat Transfer and Pressure Drop of Liquids in Tubes," *Ind. Eng. Chem.* 28, 1429 (1936).

13. W. H. McAdams, *Heat Transmission*, 3d ed., McGraw-Hill, New York, 1954.

14. W. M. Rohsenow, *Developments in Heat Transfer*, The M.I.T. Press, Massachusetts, 1964.

15. R. Gregorig, "An Analysis of Film Condensation on Wavy Surfaces Including Surface Tension Effect," *Z. Angew. Math. Phys.* 5, 36 (1954).

16. N. Domingo and J. W. Michel, "Ammonia Condensation Experiments at Oak Ridge National Laboratory," paper presented at the Eighth Ocean Energy Conversion (OTEC) Conference, Washington, D.C., June 7-11, 1981.

Appendix A

SAMPLES OF DATA REDUCTION

A.1 Physical Properties for Ammonia

All property data for ammonia used in data reduction were taken from ASHRAE handbooks,[7-9] where ammonia is designated R-717. The accuracy of these thermophysical properties is discussed in Ref. 9.

A.2 Fluted Tube

A sample of the experimental data required for computing the composite condensing film coefficient for a given vapor temperature and heat flux is listed in Table A.1. Data are for R-717 condensing on Tube L (60 external flutes with a smooth inside wall). Experimental run R-717-007 L is used to demonstrate the data reduction procedure, and the series of runs R-717-007 L through R-717-012 L are used to demonstrate the Wilson-plot technique.

The measured pressure P of the vapor should agree with the saturation pressure P_{sat} of R-717 at the vapor temperature T_v, assuming that neither contamination nor superheat are present. In this study, the pressure data for R-717 from ASHRAE[7-9] were fitted as polynomial functions of temperature for the range of 70 to 110°F, resulting in the following equations:

$$P_{sat} = 28.2069 + 0.844516\ (T_v) + 5.05936 \times 10^{-3}\ (T_v)^2 + 4.86132 \times 10^{-5}\ (T_v)^3\ , \quad (A.1)$$

$$\rho_c = 41.2689 - 4.2225 \times 10^{-2}\ (T_c) - 6.49961 \times 10^{-5}\ (T_c)^2\ , \quad (A.2)$$

$$h_{fg} = 566.348 - 6.84592 \times 10^{-1}\ (T_v) - 2.00778 \times 10^{-3}\ (T_v)^2\ , \quad (A.3)$$

From Eq. (A.1), the saturation pressure P_{sat} corresponding to a temperature of 81.76°F is 157.7 psia; this agrees well (-0.6%), within the experimental accuracy of the instruments, with the measured pressure P of

Table A.1. Sample of experimental data for ammonia R-717 condensing on Tube L

Run No.	Vapor feed to test section		Condensate		Primary cooling water through test section			
	Temperature,[a] T_v (°F)	Pressure,[b] P (psia)	Flow rate,[c] F_c (gpm)	Temperature,[d] T_c (°F)	Flow rate,[e] F_w (gpm)	Inlet temperature,[a] $T_{w,in}$ (°F)	Outlet temperature,[a] $T_{w,out}$ (°F)	Temperature difference,[a,f] ΔT_w (°F)
R-717-007 L	81.78	158.7	0.0302	81.00	35.3	80.04	80.42	0.27
R-717-008 L	82.29	159.7	0.0302	81.42	21.2	80.04	80.53	0.44
R-717-009 L	83.84	164.7	0.0301	82.55	9.8	80.15	81.08	0.88
R-717-010 L	84.51	166.2	0.0303	83.36	7.6	80.01	81.21	1.19
R-717-011 L	85.61	169.2	0.0300	84.17	5.4	79.80	81.46	1.64
R-717-012 L	87.44	174.2	0.0301	85.69	3.8	79.84	82.13	2.28

[a]Measured by thermistors (Thermometrics part No. S-10-4 wire).

[b]Measured by pressure gage.

[c]Measured by turbine flow transducer (Flow Technology, model FTM-NX3-LJS).

[d]Measured by quartz thermometer (Hewlett-Packard, model 2801 A).

[e]Measured by one of two rotameters (Fisher and Porter Company and Brooks Rotameter Company).

[f]Corrected for temperature offset and temperature rise from heat generated by friction between fluid and tube wall.

158.7 psia for run R-717-007 L. This agreement also indicates the absence of appreciable amounts of noncondensables in the condenser during operation. The quantities ρ_c and h_{fg} are used later for calculating the heat transfer rates in the condenser from the condensate flow.

The heat transfer rate or heat load in the condenser can be computed from two independent sets of measurements: one on the ammonia side and the other on the water side. To calculate the heat transfer rate from the ammonia-side condensate flow rate F_c requires the latent heat h_{fg} of R-717 at the vapor temperature T_v and the density of liquid R-717 at the condensate temperature T_c near the condensate flow measuring station. From Eqs. (A.2) and (A.3):

$$T_c = 81.00°F \rightarrow \rho_c = 37.44 \text{ lb}_m/\text{ft}^3 ,$$

$$T_v = 81.78°F \rightarrow h_{fg} = 496.93 \text{ Btu/lb}_m .$$

The heat transfer rate can then be calculated from Eq. (4.3), presented in the main text, where the condensate flow rate is given by:

$$\dot{m}_c = F_c \rho_c , \tag{A.4}$$

so that

$$\begin{aligned} Q_c &= F_c \rho_c h_{fg} \\ &= (0.0302 \text{ gpm})(37.44 \text{ lb}_m/\text{ft}^3)(496.93 \text{ Btu/lb}_m) \\ &\qquad \times (1 \text{ ft}^3/7.481 \text{ gal})(60 \text{ min/h}) \\ &= 4506 \text{ Btu/h} . \end{aligned}$$

The heat transfer rate computed from the primary cooling water is given by:

$$Q_w = F_w \rho_w C_{p_w} \Delta T_w , \tag{A.5}$$

where F_w and ΔT_w are the volume flow rate and temperature rise of the primary cooling water, respectively. The term C_{p_w} is the average heat capacity of the primary cooling water, and ρ_w is the average density of the primary cooling water; both C_{p_w} and ρ_w are calculated at the average temperature of the primary water $T_{w,avg}$. In this particular example, the change in water temperature ΔT_w is so small that the variation in properties is insignificant. The average temperature of the primary cooling water is the average of the inlet temperature (80.04°F) and the outlet temperature (80.42°F). The properties for water at an average temperature of 80.23°F are ρ_w = 61.29 lb_m/ft^3 and C_{p_w} = 1.0 $Btu/lb_m \cdot °F$. From Eq. (A.5), the heat transfer rate for run R-717-007 L becomes:

$$Q_w = (35.3\ gpm)(61.29\ lb_m/ft^3)(1\ Btu/lb_m \cdot °F)(0.27°F)$$

$$\times\ (1\ ft^3/7.481\ gal)(60\ min/h)$$

$$= 4685\ Btu/h\ .$$

The percent of difference between the two heat loads is given by:

$$\frac{\Delta Q}{\overline{Q}} \times 100 = \frac{(Q_c - Q_w)}{Q_c} \times 100 = \frac{(4506 - 4685)}{4506} \times 100$$

$$\Delta\% = -4.0\ . \qquad \text{(A.6)}$$

This value illustrates the agreement between the two different methods.

The overall condensing heat transfer coefficient can be computed from Eq. (4.1) using either Q_c or Q_w. However, the heat rate from the condensate flow Q_c has been used in the calculation because it is considered the more accurate of the two. The overall temperature difference $\overline{\Delta T}$ is given by Eq. (4.2):

$$\overline{\Delta T} = T_v - (T_{w,in} + T_{w,out})/2\ .$$

Therefore, with the information for run R-717-006 L:

$$\overline{\Delta T} = 81.78°F - (80.04°F + 80.42°F)/2$$

$$= 1.55°F\ .$$

The outside surface area A_o of Tube L is listed in Table 1 as 1.504 ft². Applying Eq. (4.1) and using the data from run R-717-007 L:

$$U = \frac{Q_c}{A_o \overline{\Delta T}} = \frac{4506 \text{ Btu/h}}{(1.504 \text{ ft}^2)(1.55^\circ\text{F})} = 1930 \frac{\text{Btu}}{\text{h.ft}^2.^\circ\text{F}} .$$

The same calculations illustrated for run R-717-007 L can be used for the other five runs in Table A.1. The results of the calculations for all six runs are shown in Table A.2. The six heat rates can be averaged to obtain an average heat load for the series of runs so that:

$$Q_{c,avg} = 4506 \text{ Btu/h} ,$$

$$Q_{w,avg} = 4685 \text{ Btu/h} .$$

Water velocities v in Table A.2 are calculated from:

$$v = F_w/A_{cs} , \tag{A.7}$$

where A_{cs} is the cross-sectional flow area.

During experimental tests with Tube L, a 0.5-in.-diam solid rod was inserted through the tube center as noted in Sect. 2.3. For Tube L, the cross-sectional flow area is:

$$A_{cs} = \frac{\pi}{4} (D_i^2 - D_r^2) , \tag{A.8}$$

where D_i is the inside diameter of the test tube and D_r is the outside diameter of the solid rod. For Tube L with an inside diameter D_i of 0.87 in.:

$$A_{cs} = \frac{\pi}{4} \left[\left(\frac{0.87}{12}\right)^2 - \left(\frac{0.50}{12}\right)^2\right]$$

$$= 0.002765 \text{ ft}^2 ;$$

Table A.2. Sample information for the Wilson plot for ammonia R-717 condensing on Tube L

Run No.	Condenser heat load			Overall temperature difference,[c] $\overline{\Delta T}$ (°F)	Primary cooling water velocity, v (ft/s)	$\frac{1}{v^{0.8}}$	Overall coefficient, U (Btu/h·ft²·°F)	1/U (h·ft²·°F/Btu)
	Q_c[a] (Btu/h)	Q_w[b] (Btu/h)	ΔT					
R-717-007 L	4506	4685	-4.0	1.55	28.4	0.0688	1930	0.52×10^{-3}
R-717-008 L	4491	4685	-4.3	2.00	17.1	0.1032	1494	0.67×10^{-3}
R-717-009 L	4462	4317	3.3	3.22	7.9	0.1914	921	1.09×10^{-3}
R-717-010 L	4476	4501	-0.5	3.90	6.1	0.2354	763	1.31×10^{-3}
R-717-011-L	4422	4407	0.3	4.97	4.4	0.3057	591	1.69×10^{-3}
R-717-012 L	4406	4381	0.6	6.45	3.1	0.4045	454	2.20×10^{-3}

[a]Calculated from condensate flow.

[b]Calculated from temperature rise and flow of primary cooling water.

[c]Between condensing vapor and primary cooling flow.

the water velocity for run R-717-006 L is

$$v = (35.3 \text{ gpm}) \frac{1 \text{ ft}^3}{7.481 \text{ gal}} \cdot \frac{1 \text{ min}}{60 \text{ s}} \cdot \frac{1}{0.002765 \text{ ft}^2}$$

$$= 28.4 \text{ ft/s} .$$

To generate the Wilson plot, the reciprocal of the overall coefficient must be computed; the water velocity must be raised to the negative 0.8 power. For example, with the values for run R-717-007 L:

$$\frac{1}{v^{0.8}} = (1/28.4 \text{ ft/s})^{0.8} = 0.0688 \text{ (ft/s)}^{-0.8}$$

and

$$\frac{1}{U} = (1/1930 \text{ Btu/h}\cdot\text{ft}^2\cdot{}^\circ\text{F}) = 0.52 \times 10^{-3} \frac{\text{h}\cdot\text{ft}^2\cdot{}^\circ\text{F}}{\text{Btu}} .$$

The values for $v^{-0.8}$ and 1/U are given in Table A.2; these were used to construct the Wilson plot shown in Fig. A.1. The data points shown in Fig. A.1 were fitted by a least squares method of the first order to determine the best linear fit to satisfy the following relationship:

$$\frac{1}{U} = a_0 + a_1 v^{-0.8} ,$$

where a_1 is the slope of the straight line and a_0 is the y-intercept. The reciprocal $1/a_0$ or h* gives the composite heat transfer coefficient of the condensing film and tube wall.

For this particular run series, the values a_0 and h* are:

$$a_0 = 0.1486 \times 10^{-3} \text{ h}\cdot\text{ft}^2\cdot{}^\circ\text{F/Btu} ,$$

$$h^* = 6729 \text{ Btu/h}\cdot\text{ft}^2\cdot{}^\circ\text{F} .$$

The data show good linearity and allow extrapolation, with some confidence, to infinite water velocity (zero water-side resistance) at the plot y-intercept (Fig. A.1).

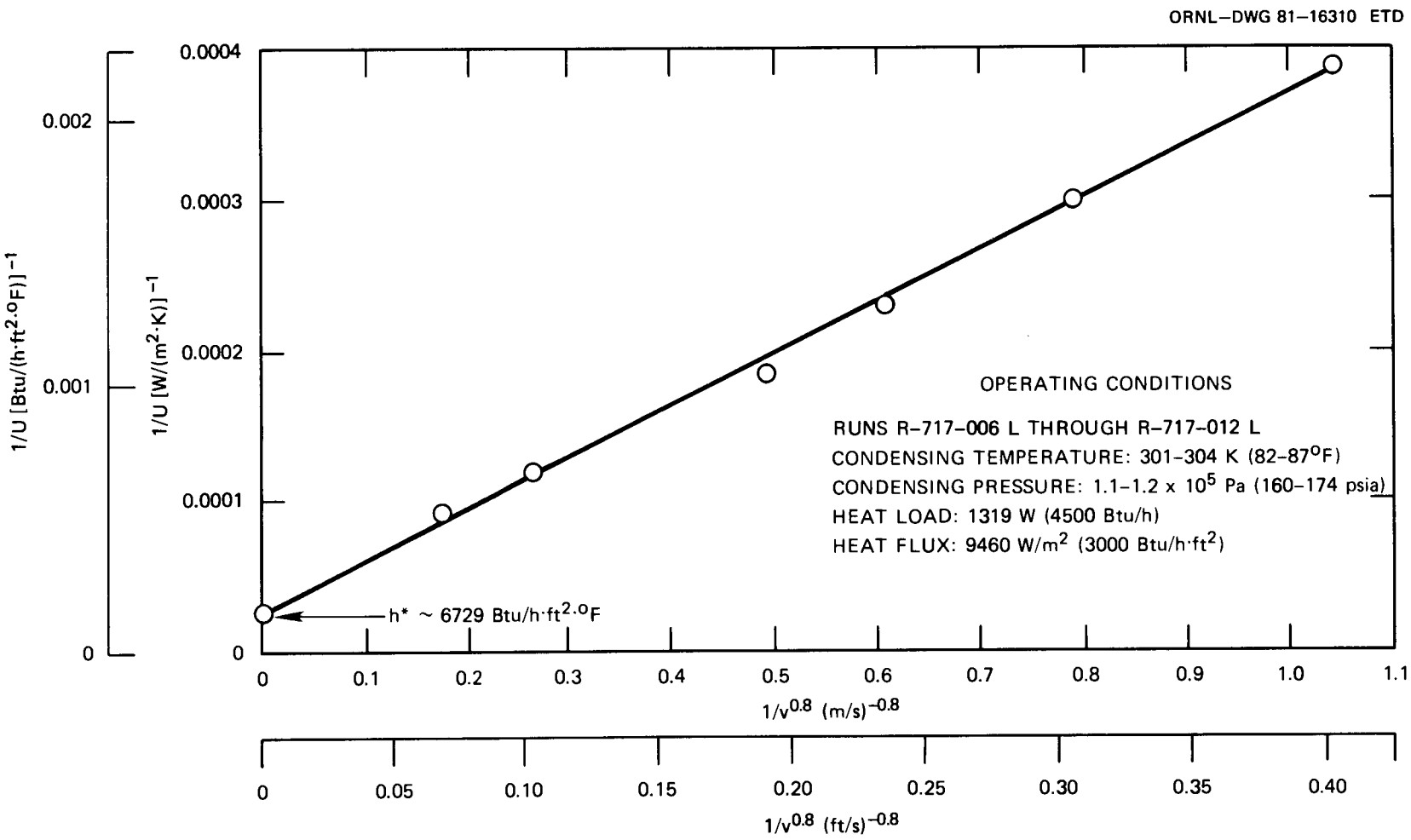

Fig. A.1. Wilson plot for ammonia (R-717) condensing outside fluted Tube L – runs R-717-L to R-717-L.

The corresponding composite temperature difference is calculated using Eq. (4.9). The average heat load value for this series of runs is ~4506 Btu/h; then, from Eq. (4.9):

$$\Delta T^* = \frac{Q_{c,avg}}{h^* A_o} = \frac{(4506 \text{ Btu/h})}{(6729 \text{ Btu/h}\cdot\text{ft}^2\cdot{}^\circ\text{F})(1.504 \text{ ft}^2)}$$

$$= 0.45^\circ\text{F} .$$

The computations outlined in this appendix were followed in reducing all of the experimental data. These Wilson-plot results are presented in graphic and tabular form in Sect. 5 and Appendix C, respectively.

A.3 Nondimensional Quantities

The vapor-side heat transfer coefficient h_v is usually considered equal to the condensing film coefficient because the dominant resistance lies in the condensate film. Therefore, the condensing film heat transfer coefficient can be put into the standard nondimensional form given by Eq. (5.1):

$$H = h_v/(k^3\rho^2 g/\mu^2)^{1/3} ,$$

where all fluid properties are evaluated at the equivalent film temperature T_f, as pointed out by McAdams:[13]

$$T_f = T_v - \frac{3}{4}(T_v - T_{wall}) , \tag{A.7}$$

where T_{wall} is the outside wall temperature. The temperature of the vapor for evaluating film temperatures was chosen as the lowest vapor temperature for the series of runs for a given Wilson plot. For runs R-717-032 AH through R-717-035 AH, the vapor temperature was taken as 87°F (Appendix C, Table C.2) for evaluation of the nondimensional coefficient. The temperature difference across the condensing film (ΔT_f) is given by:

$$\Delta T_f = T_v - T_{wall} = \frac{Q}{h_v A_o} . \tag{A.8}$$

The individual vapor-side coefficient h_v for smooth Tube A can be calculated from the composite heat transfer coefficient h* by solving for h_v in Eq. (4.7):

$$1/h^* = 1/h_v + R_{wall} , \tag{4.7}$$

or

$$h_v = \frac{1}{1/h^* - R_{wall}} ; \tag{A.9}$$

where R_{wall} is given by Eq. (4.6):

$$R_{wall} = \frac{r_o}{k} \ln \frac{r_o}{r_i} . \tag{4.6}$$

The variables for Tube A are

r_o = 0.500 in.,
r_i = 0.435 in.,
k = 99 Btu/h·ft·°F,

so that

$$R_{wall} = \left(\frac{0.500 \text{ in.}}{99 \text{ Btu/h·ft·°F}}\right)\left(\frac{1 \text{ ft}}{12 \text{ in.}}\right) \times \ln \left(\frac{0.500 \text{ in.}}{0.435 \text{ in.}}\right)$$

$$= 5.9 \times 10^{-5} \text{ (Btu/h·ft}^2\text{·°F)}^{-1} .$$

For the runs R-717-032 AH through R-717-035 AH, the value of the composite coefficient h* obtained from the Wilson plot is 2477 Btu/h·ft²·°F (Table C.2). Thus, the vapor-side heat transfer coefficient obtained from Eq. (A.9) is:

$$h_v = \frac{1}{(1/2477 \text{ Btu/h·ft}^2\text{·°F}) - 5.9 \times 10^{-5} \text{ (Btu/h·ft}^2\text{·°F)}^{-1}}$$

$$= 2900 \text{ Btu/h·ft}^2\text{·°F} .$$

The outside surface area A_o of Tube A is listed in Table 1 as 1.047 ft². Substituting the computed value of h_v and the average heat load runs

R-717-032 AH through R-717-035 AH into Eq. (A.7), the temperature difference across the condensing film ΔT_f is found to be

$$\Delta T_f = (T_v - T_{wall}) = \frac{(2823\ \text{Btu/h})}{(2900\ \text{Btu/h}\cdot\text{ft}^2\cdot{}^\circ\text{F})(1.047\ \text{ft}^2)}$$

$$= 0.93^\circ\text{F} ,$$

so that

$$T_f = 87^\circ\text{F} - 3/4\ (0.93^\circ\text{F})$$

$$= 86.30^\circ\text{F} .$$

Evaluating the fluid properties at the film temperature of 86.3°F,

$k = 0.272$ Btu/h·ft·°F ,
$\rho = 37.15\ \text{lb}_m/\text{ft}^3$,
$\mu = 0.328\ \text{lb}_m/\text{h}\cdot\text{ft}$, and
$g = 4.17 \times 10^8\ \text{ft/h}^2$,

so that for $h_v = 2900\ \text{Btu/h}\cdot\text{ft}^2\cdot{}^\circ\text{F}$,

$$H = 2900/[(0.272)^3(37.15)^2(4.17 \times 10^8)/(0.328)^2]^{1/3} = 0.61 .$$

The liquid film Reynolds number is given by Eq. (5.2):

$$Re = \frac{4\Gamma}{\mu} , \tag{5.2}$$

where for a horizontal tube, Γ is the mass flow of condensate at the bottom of the tube per unit length of tube. The mass flow per unit length can be calculated from the heat load Q, latent heat of ammonia h_{fg}, and the length of the tube ℓ:

$$\Gamma = \frac{Q}{h_{fg}\ \ell} . \tag{A.10}$$

The test length of Tube A is 48 in. The latent heat of ammonia is evaluated at the equivalent film temperature using Eq. (A.7). For runs

R-717-032 AH through R-717-035 AH,

$$\Gamma = \frac{(2823\ \text{Btu/h})}{(491.70\ \text{Btu/lb}_m)(48\ \text{in.})(1\ \text{ft/12 in.})}$$

$$= 1.44\ \text{lb}_m/\text{h}\cdot\text{ft}\ ,$$

so that

$$\text{Re} = \frac{4\Gamma}{\mu} = \frac{4\ (1.44\ \text{lb}_m/\text{h}\cdot\text{ft})}{(0.328\ \text{lb}_m/\text{h}\cdot\text{ft})} = 17.6\ .$$

The nondimensional heat transfer coefficients and liquid film Reynolds numbers were used to construct Fig. 8.

The nondimensional quantities H and Re were not found to be very sensitive to the temperature at which the properties were evaluated; therefore, the variation in vapor temperatures during a series of runs should not have affected the heat transfer results significantly. For horizontal Tube A, the vapor temperature variation ranged from 3 to 20°F for a given series of runs (a set heat load).

Appendix B

DROPWISE CONDENSATION ON SMOOTH TUBE A

Though the experimental test loop performed well throughout this study, some unusually high condensing coefficients were noted during the earlier phases of the test series. This condition was first detected after reinstallation of a gasket that had failed during shakedown tests. Observation through existing view ports in the test section revealed what looked like a dropwise condensation phenomenon on the outer surface of horizontal smooth Tube A (Fig. B.1). Condensing coefficients for horizontal Tube A were estimated by the Nusselt[13,14] analysis and compared to those obtained during the presence of the dropwise phenomenon. The latter coefficients were much higher than those obtained from the Nusselt analysis.

Dropwise condensation was thought to be likely caused by impurities associated with the gasket failure. In an attempt to explain the cause of the phenomenon, an ammonia liquid sample was collected from the bottom of the boiler and analyzed for contaminants such as water and oil. Gas chromatographic analysis of the sample indicated only a very small amount of water traceable to the alcohol solvent used with the ammonia in preparation for the analysis. However, flashing all liquid ammonia in the sample and leaching the container with acetone revealed the presence of an amber-like oil residue, with a small amount of insoluble solids. Analysis of the oil residue determined it to be made up of aliphatic and aromatic hydrocarbon oils, in addition to polyacrylamides and other unidentified organics. Qualitative x-ray diffraction analyses of the solids disclosed major concentrations of molybdenum disulfide (MoS_2) with an intermediate amount of hydrous iron oxide [FeO(OH)].

Based on these results, a sample piece of rubber gasket that had been used in the test section prior to failure was analyzed in an attempt to identify the origin of oil contamination. The material, separated into soluble components by acetone leaching, yielded an amber-like oil substance, which, when analyzed, proved to be practically identical to the oil residue collected from the liquid ammonia sample. Surprisingly, this gasket material was identified as butadiene-styrene rubber, which is not

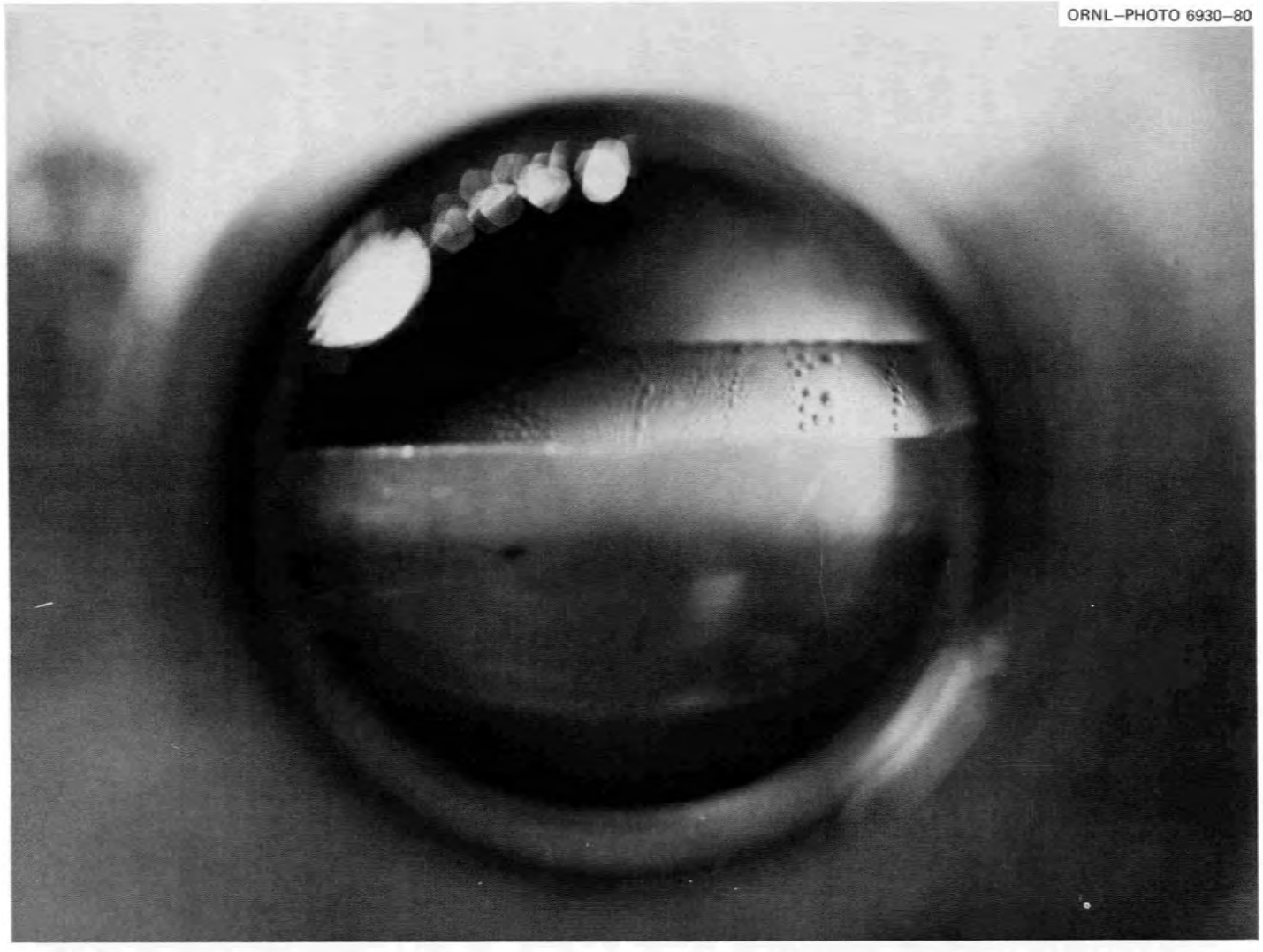

Fig. B.1. Dropwise condensation of ammonia outside horizontal Tube A.

recommended for ammonia. It is not clear why this material was employed; most probably it was used accidentally.

On the basis of the above chemical analyses, the test loop was flushed, evacuated, and recharged with ammonia. All gaskets were serviced and replaced with asbestos-neoprene material, which was verified to be compatible with ammonia. In addition, the test tube was removed and replaced by one of similar design. These steps were successful in correcting the earlier operating difficulties caused by the presence of dropwise condensation.

These findings do not clearly indicate what agent triggered dropwise condensation on the outside surface of Tube A. The most probable explanation is that some combination of impurities found in the ammonia caused this phenomenon.

Appendix C

WILSON-PLOT RESULTS

Tables C.1 through C.8 summarize the Wilson-plot results from condensation experiments performed on the single tubes used in this study. Tables C.1 and C.5 (from Ref. 1) present the results for vertical Tubes A and E, respectively, which served as a baseline for comparisons with other tubes tested. The condenser heat load was taken as the average heat load based on the condensate flow $Q_{c,avg}$ for a series of runs (Appendix A). Individual runs are documented in Appendix D.

Table C.1. Summary of experimental conditions and results from Wilson plots for ammonia condensing on vertical Tube A

Series of runs	Condenser heat load [W (Btu/h)]		Difference (%)	Vapor temperature range	Condensing temperature difference	Condensing heat transfer coefficient
	Q_c	Q_w		[K (°F)]	[K (°F)]	[W/m²·K (Btu/h·ft²·°F)]
R-717-001A to 004A	3,800 (13,100)	3,700 (12,600)	3.9	302-309 (84-96)	7.5 (13.5)	5,200 (920)
R-717-005A to 007A	2,400 (8,200)	2,400 (8,100)	-0.3	296-301 (74-82)	4.5 (8.1)	5,500 (970)
R-717-009A to 011A	2,800 (9,600)	2,800 (9,600)	0	299-303 (78-86)	6.0 (10.9)	4,800 (850)
R-717-013A to 015A	3,200 (10,800)	3,200 (10,900)	-0.7	300-306 (80-90)	6.3 (11.4)	5,200 (910)
R-717-017A to 019A	3,800 (12,900)	3,800 (13,100)	-1.3	302-309 (83-97)	7.5 (13.5)	5,200 (920)
R-717-021A to 023A	2,900 (9,800)	2,900 (9,800)	0	299-303 (78-87)	5.9 (10.6)	5,100 (890)
R-717-025A to 029A	2,800 (9,500)	2,800 (9,700)	-2.6	299-306 (78-90)	5.2 (9.4)	5,500 (960)
R-717-030A to 033A	3,500 (11,900)	3,600 (12,100)	-1.8	300-309 (81-96)	7.2 (13.0)	5,000 (880)
R-717-034A to 037A	1,600 (5,400)	1,600 (5,500)	-0.8	296-300 (72-80)	2.6 (4.6)	6,300 (1,100)
R-717-038A to 041A	1,050 (3,600)	1,050 (3,600)	0	296-299 (74-78)	1.6 (2.8)	6,800 (1,200)
R-717-042A to 045A	1,000 (3,500)	1,100 (3,700)	-5.7	296-299 (74-78)	1.6 (2.8)	6,800 (1,200)
R-717-046A to 050A	800 (2,800)	900 (3,000)	-7.7	294-296 (70-74)	1.1 (2.0)	7,700 (1,350)
R-717-051A to 055A	800 (2,800)	800 (2,800)	0	293-296 (69-72)	1.1 (2.0)	7,900 (1,400)
R-717-056A to 059A	1,700 (5,700)	1,700 (5,800)	-0.8	295-300 (72-80)	2.8 (5.1)	6,300 (1,100)
R-717-060A to 063A	1,400 (4,700)	1,400 (4,700)	0	295-299 (71-78)	2.1 (3.8)	6,800 (1,200)
R-717-064A to 073A	1,400 (4,800)	1,400 (4,900)	-3.0	295-298 (71-77)	2.3 (4.1)	6,300 (1,100)
R-717-074A to 084A	900 (3,100)	900 (3,100)	0	299-302 (79-84)	1.2 (2.2)	7,400 (1,300)
R-717-085A to 088A	560 (1,900)	600 (2,100)	-8.2	298-299 (77-79)	0.7 (1.3)	7,900 (1,400)
R-717-089A to 092A	500 (1,700)	560 (1,900)	-10.4	298-299 (76-78)	0.7 (1.2)	7,900 (1,400)
R-717-098A to 102A	510 (1,700)	570 (2,000)	-11.8	298-300 (77-80)	0.7 (1.2)	7,700 (1,350)
R-717-103A to 106A	3,950 (13,500)	4,050 (13,800)	-2.5	300-310 (81-99)	8.9 (16.0)	4,600 (800)
R-717-107A to 110A	5,000 (17,100)	5,200 (17,800)	-3.7	305-313 (89-104)	12.6 (22.7)	4,100 (720)
R-717-111A to 114A	4,200 (14,200)	4,500 (15,200)	-6.9	306-313 (91-103)	10.2 (18.3)	4,200 (740)
R-717-119A to 122A	3,300 (11,100)	3,400 (11,500)	-3.6	300-308 (81-95)	6.6 (12.0)	5,100 (890)
R-717-123A to 126A	2,000 (6,800)	2,050 (7,000)	-3.0	301-306 (83-90)	3.8 (6.9)	5,400 (940)
R-717-127A to 130A	2,900 (9,900)	3,000 (10,200)	-2.8	300-308 (80-94)	5.9 (10.6)	5,050 (890)
R-717-131A to 134A	2,000 (6,900)	2,000 (6,900)	0	299-304 (78-87)	3.6 (6.6)	5,700 (1,000)
R-717-135A to 138A	4,300 (14,800)	4,400 (15,000)	-1.4	305-316 (89-109)	9.7 (17.4)	4,600 (810)
R-717-139A to 142A	760 (2,600)	800 (2,800)	-8.5	302-304 (83-88)	1.1 (2.0)	7,100 (1,250)
R-717-143A to 145A	1,400 (4,800)	1,450 (4,900)	-2.2	304-306 (87-91)	2.6 (4.7)	5,600 (990)
R-717-146A to 149A	1,100 (3,700)	1,130 (3,800)	-2.9	302-305 (84-89)	1.8 (3.2)	6,300 (1,100)
R-717-150A to 153A	1,700 (5,700)	1,700 (5,700)	0	304-309 (88-96)	3.0 (5.4)	5,700 (1,000)

Table C.2. Summary of experimental conditions and results from Wilson plots for ammonia condensing on horizontal Tube A

Series of runs	Condenser heat load [W (Btu/h)]		Difference (%)	Vapor temperature range	Condensing temperature difference	Condensing heat transfer coefficient
	Q_c	Q_w		[K (°F)]	[K (°F)]	[W/m²·K (Btu/h·ft²·°F)]
R-717-001AH to 006AH	3,271 (11,165)	3,263 (11,137)	0.3	304–311 (88–101)	3.8 (6.8)	8,856 (1,562)
R-717-007AH to 012AH	1,237 (4,221)	1,230 (4,198)	0.6	303–306 (85–91)	1.0 (1.8)	12,651 (2,231)
R-717-013AH to 017AH	4,183 (14,276)	4,164 (14,212)	0.5	307–315 (93–107)	5.0 (9.1)	8,540 (1,507)
R-717-018AH to 023AH	3,821 (13,041)	3,788 (12,927	0.9	306–315 (90–107)	4.5 (8.0)	8,788 (1,550)
R-717-024AH to 027AH	2,283 (7,792)	2,205 (7,527)	3.5	303–308 (86–95)	2.2 (4.0)	10,653 (1,879)
R-717-028AH to 031AH	1,692 (5,773)	1,659 (5,663)	2.0	304–308 (88–94)	1.7 (3.0)	10,454 (1,844)
R-717-032AH to 035AH	827 (2,823)	834 (2,847)	−0.8	304–306 (87–90)	0.6 (1.1)	14,044 (2,477)
R-717-036AH to 039AH	2,694 (9,194)	2,656 (9,065)	1.44	303–309 (85–96)	2.8 (5.1)	9,766 (1,722)
R-717-040AH to 043AH	1,690 (5,768)	1,680 (5,734)	0.6	304–308 (88–96)	1.5 (2.8)	11,346 (2,001)

Table C.3. Summary of experimental conditions and results from Wilson plots for ammonia condensing on Tube A (30° from the horizontal)

Series of runs	Condenser heat load [W (Btu/h)]		Difference (%)	Vapor temperature range [K (°F)]	Condensing temperature difference [K (°F)]	Condensing heat transfer coefficient [W/m²·K (Btu/h·ft²·°F)]
	Q_c	Q_w				
R-717-001A30 to 006A30	3,661 (12,497)	3,588 (12,247)	2.1	306–314 (90–106)	4.4 (8.0)	8,490 (1,497)
R-717-007A30 to 012A30	938 (3,203)	929 (3,171)	1.0	304–306 (87–91)	0.7 (1.3)	13,210 (2,330)
R-717-013A30 to 018A30	2,323 (7,929)	2,243 (7,655)	3.5	304–309 (87–97)	2.3 (4.2)	10,292 (1,815)
R-717-019A30 to 024A30	1,419 (4,842)	1,413 (4,821)	0.4	304–308 (88–94)	1.3 (2.3)	11,244 (1,983)
R-717-025A30 to 030A30	3,156 (10,771)	3,142 (10,725)	0.4	305–313 (90–103)	3.7 (6.7)	8,661 (1,527)
R-717-031A30 to 035A30	4,110 (14,028)	4,080 (13,927)	0.7	307–315 (93–108)	5.2 (9.4)	8,073 (1,424)
R-717-036A30 to 041A30	2,657 (9,069)	2,634 (8,988)	0.9	304–311 (88–100)	3.0 (5.4)	9,101 (1,605)
R-717-042A30 to 047A30	1,832 (6,252)	1,782 (6,083)	2.8	304–308 (87–95)	1.9 (3.3)	10,165 (1,793)

Table C.4. Summary of experimental conditions and results from Wilson plots for ammonia condensing on vertical Tube A (60° from the horizontal)

Series of runs	Condenser heat load [W (But/h)]		Differ-ence (%)	Vapor temperature range [K (°F)]	Condensing temperature difference [K (°F)]	Condensing heat transfer coefficient [W/m²·K (Btu/h·ft²·°F)]
	Q_c	Q_w				
R-717-001A60 to 006A60	1,030 (3,514)	996 (3,401)	-3.3	304-307 (88-92)	1.0 (1.9)	10,141 (1,788)
R-717-007A60 to 011A60	4,004 (13,664)	3,921 (13,380)	-2.2	307-315 (93-107)	5.9 (10.6)	7,005 (1,235)
R-717-012A60 to 017A60	2,634 (8,989)	2,587 (8,830)	-1.9	303-310 (86-98)	3.4 (6.0)	8,080 (1,425)
R-717-018A60 to 023A60	3,503 (11,955)	3,425 (11,689)	-2.3	306-314 (91-106)	4.9 (8.8)	2,330 (1,293)
R-717-024A60 to 029A60	3,145 (10,733)	3,085 (10,530)	-2.0	304-312 (88-102)	4.2 (7.6)	7,698 (1,358)
R-717-030A60 to 035A60	1,785 (6,091)	1,720 (5,872)	-3.7	304-308 (87-95)	2.0 (3.6)	9,192 (1,621)
R-717-036A60 to 041A60	1,421 (4,850)	1,386 (4,730)	-2.5	305-308 (89-95)	1.5 (2.6)	9,936 (1,752)
R-717-042A60 to 047A60	2,260 (7,713)	2,141 (7,306)	-5.4	304-309 (88-97)	2.7 (4.8)	8,747 (1,543)

Table C.5. Summary of experimental conditions and results from Wilson plots for ammonia condensing on vertical Tube E

Series of runs	Condenser heat load [W (Btu/h)]		Difference (%)	Vapor temperature range [K (°F)]	Condensing temperature difference [K (°F)]	Condensing heat transfer coefficient [W/m²·K (Btu/h·ft²·°F)]
	Q_c	Q_w				
R-717-009E to 016E	3,300 (11,300)	3,300 (11,400)	-1.0	297-306 (76-92)	0.8 (1.5)	27,000 (4,700)
R-717-017E to 024E	5,000 (16,900)	5,100 (17,300)	-2.0	300-313 (81-104)	1.6 (2.8)	21,000 (3,700)
R-717-025E to 031E	4,200 (14,400)	4,200 (14,500)	-0.7	298-310 (77-98)	1.1 (2.1)	24,000 (4,300)
R-717-032E to 038E	2,400 (8,100)	2,400 (8,100)	-0.9	296-302 (73-84)	0.5 (0.9)	32,000 (5,700)
R-717-039E to 045E	2,050 (7,000)	2,100 (7,100)	-0.7	296-302 (73-84)	0.4 (0.7)	34,000 (5,900)
R-717-046E to 050E	1,700 (5,800)	1,700 (5,800)	-0.3	296-301 (73-82)	0.4 (0.7)	30,000 (5,300)
R-717-051E to 056E	1,400 (4,700)	1,400 (4,800)	-2.3	298-301 (77-83)	0.2 (0.4)	37,000 (6,600)
R-717-057E to 062E	1,000 (3,500)	1,100 (3,600)	-3.6	298-301 (76-82)	0.2 (0.3)	41,000 (7,200)
R-717-063E to 068E	1,700 (5,700)	1,700 (5,800)	-2.0	298-302 (77-84)	0.3 (0.6)	36,000 (6,300)
R-717-069E to 074E	2,900 (9,900)	3,000 (10,100)	-2.2	299-307 (78-92)	0.7 (1.3)	27,000 (48,000)
R-717-075E to 081E	3,800 (12,800)	3,800 (13,100)	-1.8	301-310 (82-99)	1.0 (1.8)	26,000 (4,600)
R-717-082E to 086E	2,900 (9,900)	2,900 (9,900)	0.3	299-307 (79-92)	0.7 (1.2)	29,000 (5,100)
R-717-087E to 093E	4,300 (14,600)	4,400 (14,900)	-2.1	302-313 (83-104)	1.6 (2.9)	18,000 (3,100)
R-717-094E to 099E	2,700 (9,200)	2,700 (9,200)	-0.7	300-307 (80-93)	0.6 (1.1)	29,000 (5,100)
R-717-100E to 106E	4,400 (15,100)	4,500 (15,500)	-2.7	303-314 (85-105)	1.8 (3.2)	17,000 (3,000)

Table C.6. Summary of experimental conditions and results from Wilson plots for ammonia condensing on vertical Tube L

Series of runs	Condenser heat load [W (Btu/h)]		Difference (%)	Vapor temperature range [K (°F)]	Condensing temperature difference [K (°F)]	Condensing heat transfer coefficient [W/m²·K (Btu/h·ft²·°F)]
	Q_c	Q_w				
R-717-007L to 012L	1,307 (4,461)	1,317 (4,495)	-0.8	301-304 (82-87)	0.2 (0.4)	38,154 (6,729)
R-717-013L to 018L	3,148 (10,745)	3,101 (10,583)	1.5	299-307 (79-93)	0.8 (1.5)	27,100 (4,781)
R-717-019L to 024L	4,152 (14,171)	4,099 (13,939)	1.3	300-310 (81-99)	1.2 (2.1)	25,326 (4,467)
R-717-025L to 030L	3,657 (12,482)	3,581 (12,221	2.1	300-309 (81-97)	1.0 (1.8)	26,141 (4,610)
R-717-031L to 036L	1,594 (5,442)	1,562 (5,331)	2.1	301-305 (82-89)	0.3 (0.6)	33,633 (5,932)
R-717-037L to 042L	2,093 (7,142)	2,021 (6,896)	3.1	301-306 (83-92)	0.5 (0.9)	30,481 (5,376)
R-717-043L to 048L	2,632 (8,983)	2,595 (8,857)	1.4	302-308 (83-94)	0.7 (1.2)	28,032 (4,944)
R-717-049L to 054L	4,697 (16,030)	4,604 (15,713)	2.0	298-310 (78-99)	1.4 (2.5)	23,830 (4,203)

Table C.7. Summary of experimental conditions and results from Wilson plots for ammonia condensing on vertical Tube T

Series of runs	Condenser heat load [W (Btu/h)]		Difference (%)	Vapor temperature range	Condensing temperature difference	Condensing heat transfer coefficient
	Q_c	Q_w		[K (°F)]	[K (°F)]	[W/m²·K (Btu/h·ft²·°F)]
R-717-001T to 006T	4,741 (16,182)	4,720 (16,109)	0.5	300–311 (80–100)	3.0 (5.3)	17,758 (1,897)
R-717-007T to 012T	2,629 (8,972)	2,612 (8,913)	0.7	300–306 (80–91)	1.5 (2.7)	11,791 (2,080)
R-717-013T to 018T	1,250 (4,266)	1,258 (4,293)	–0.6	301–304 (82–87)	0.6 (1.2)	13,081 (2,307)
R-717-019T to 024T	4,140 (14,131)	4,095 (13,975)	1.1	301–311 (83–100)	2.6 (4.7)	10,667 (1,881)
R-717-025T to 030T	3,645 (12,440)	3,598 (12,280)	1.3	301–310 (83–98)	2.2 (4.0)	10,968 (1,934)
R-717-031T to 036T	3,100 (10,579)	3,075 (10,497)	0.8	301–308 (82–95)	1.8 (3.3)	11,260 (1,986)
R-717-037T to 042T	1,979 (6,754)	1,953 (6,665)	1.4	300–304 (80–88)	1.1 (1.9)	12,455 (2,197)
R-717-043T to 048T	1,550 (5,289)	1,558 (5,319)	–0.6	300–303 (80–86)	0.8 (1.5)	12,789 (2,256)
R-717-049T to 054T	3,053 (10,421)	3,029 (10,339)	0.8	300–308 (81–94)	1.8 (3.2)	11,387 (2,008)

Table C.8. Summary of experimental conditions and results from Wilson plots for ammonia condensing on horizontal Tube V

Series of runs	Condenser heat load [W (Btu/h)]		Difference (%)	Vapor temperature range	Condensing temperature difference	Condensing heat transfer coefficient
	Q_c	Q_w		[K (°F)]	[K (°F)]	[W/m²·K (Btu/h·ft²·°F)]
R-717-001V to 006V	2,988 (10,197)	3,004 (10,252)	−0.6	305–313 (88–104)	8.7 (15.7)	1,883 (332)
R-717-007V to 012V	1,140 (3,891)	1,161 (3,963)	−1.9	301–305 (82–89)	3.1 (5.5)	2,031 (358)
R-717-013V to 018V	2,119 (7,291)	2,101 (7,172)	0.8	304–310 (88–99)	5.9 (10.6)	1,979 (349)
R-717-019V to 024V	2,414 (8,238)	2,401 (8,195)	0.5	304–311 (88–101)	6.7 (12.0)	1,979 (349)
R-717-025V to 030V	2,692 (9,189)	2,713 (9,258)	−0.8	303–311 (87–101)	7.8 (14.0)	1,902 (336)
R-717-031V to 036V	1,435 (4,897)	1,460 (4,981)	−1.8	302–307 (84–92)	4.0 (7.1)	1,984 (350)
R-717-037V to 042V	1,715 (5,852)	1,745 (5,957)	−1.8	303–309 (86–96)	4.8 (8.6)	1,975 (348)

Appendix D

EXPERIMENTAL DATA

Tables D.1 through D.14 document 153 runs that yielded 864 heat transfer data points. The tables summarize experimental data used in data reduction and for the construction of Wilson plots. Tables D.1 and D.5 were taken from Ref. 1, whereas Tables D.6 and D.7 were obtained from Ref. 2. The tables list overall heat transfer coefficients, in addition to saturation pressures and heat balance checks. Water velocities are presented with Reynolds numbers for the various water flow rates. The information was generated by computer code used for data reduction, and the runs are grouped in series corresponding to Wilson plots.

Table D.1. Experimental data for ammonia condensing on Tube A (vertical)

Run No.	T_v (°F)	P (psia)	P_{sat} (psia)	F_c (gpm)	T_c (°F)	m_c (lb_m/h)	F_w (gpm)	v (ft/s)	Re	$T_{w,in}$ (°F)	$T_{w,out}$ (°F)	ΔT_w (°F)	$\overline{\Delta T}$ (°F)	Q_c (Btu/h)	Q_w (Btu/h)	Δ (%)	U (Btu/h·ft²·°F)
R-717-001A	84.42	165.7	164.8	0.0896	79.38	26.96	32.6	26.3	73894.	66.94	67.81	0.78	17.05	13324.	12739.	4.4	746.
R-717-002A	91.89	186.7	186.3	0.0892	84.04	26.65	7.4	6.0	17056.	66.92	70.26	3.34	23.30	12963.	12336.	4.8	531.
R-717-003A	95.87	197.7	198.5	0.0893	86.77	26.59	5.1	4.1	11901.	66.70	71.43	4.72	26.81	12825.	12089.	5.7	457.
R-717-004A	89.10	178.7	178.0	0.0898	82.69	26.90	11.8	9.5	27139.	67.30	69.57	2.25	20.67	13163.	13255.	-0.7	608.
R-717-005A	73.72	138.7	137.4	0.0540	72.76	16.40	32.6	26.3	69924.	63.13	63.73	0.51	10.29	8282.	8357.	-0.9	769.
R-717-006A	78.73	150.7	149.8	0.0535	76.39	16.17	7.5	6.0	16343.	63.46	65.63	2.16	14.19	8086.	8103.	-0.2	544.
R-717-007A	81.81	159.2	157.8	0.0540	78.51	16.26	5.2	4.2	11421.	63.56	66.65	3.09	16.71	8079.	8027.	0.7	462.
R-717-009A	78.24	147.2	148.5	0.0653	76.17	19.73	32.6	26.3	71213.	64.38	65.06	0.60	13.52	9876.	9709.	1.7	698.
R-717-010A	82.81	161.7	160.4	0.0644	80.09	19.37	7.4	6.0	16355.	64.04	66.67	2.62	17.45	9605.	9711.	-1.1	526.
R-717-011A	85.75	169.2	168.5	0.0635	82.42	19.02	5.2	4.2	11525.	63.93	67.59	3.65	19.99	9376.	9484.	-1.2	448.
R-717-013A	79.71	152.7	152.3	0.0729	78.05	21.98	32.6	26.3	71837.	64.96	65.72	0.68	14.37	10967.	11094.	-1.1	729.
R-717-014A	85.65	169.2	168.2	0.0728	82.70	21.80	7.9	6.4	17680.	64.79	67.57	2.77	19.47	10745.	10992.	-2.3	527.
R-717-015A	90.28	182.7	181.5	0.0742	86.95	22.08	5.2	4.2	11734.	64.98	69.11	4.13	23.24	10781.	10729.	0.5	443.
R-717-017A	83.23	163.2	161.6	0.0881	81.04	26.43	32.6	26.3	72503.	65.54	66.46	0.83	17.23	13095.	13488.	-3.0	726.
R-717-018A	87.79	175.2	174.2	0.0879	84.63	26.25	12.0	9.7	27077.	65.93	68.15	2.20	20.75	12882.	13222.	-2.6	593.
R-717-019A	91.51	186.2	185.1	0.0882	87.70	26.24	7.9	6.4	18208.	66.50	69.76	3.26	23.38	12774.	12943.	-1.3	522.
R-717-021A	77.92	147.7	147.7	0.0663	76.31	20.02	32.6	26.3	71146.	64.30	65.01	0.63	13.27	10027.	10181.	-1.5	722.
R-717-022A	82.77	161.7	160.3	0.0653	79.96	19.62	7.7	6.2	16964.	64.04	66.61	2.56	17.44	9729.	9835.	-1.1	533.
R-717-023A	86.53	172.2	170.7	0.0656	83.00	19.64	5.1	4.1	11394.	64.04	67.78	3.73	20.63	9663.	9569.	1.0	447.
R-717-025A	78.02	148.7	148.0	0.0638	76.15	19.29	32.6	26.3	72141.	65.30	65.99	0.61	12.38	9658.	9921.	-2.7	745.
R-717-026A	80.41	154.7	154.1	0.0636	78.17	19.17	13.8	11.1	30656.	65.18	66.65	1.45	14.50	9552.	10033.	-5.0	629.
R-717-027A	83.29	162.7	161.7	0.0636	80.40	19.11	8.0	6.4	17889.	65.17	67.61	2.44	16.90	9467.	9758.	-3.1	535.
R-717-028A	88.00	175.7	174.8	0.0638	84.17	19.06	4.7	3.8	10599.	64.98	69.02	4.02	21.00	9350.	9448.	-1.0	425.
R-717-029A	90.27	182.7	181.4	0.0644	86.27	19.19	4.0	3.2	9061.	64.96	69.69	4.73	22.94	9369.	9448.	-0.8	390.
R-717-030A	80.75	154.2	155.0	0.0806	78.27	24.29	32.5	26.2	70458.	63.75	64.61	0.77	16.57	12096.	12570.	-3.9	697.
R-717-031A	86.42	169.7	170.3	0.0816	83.27	24.40	9.8	7.9	21704.	64.08	66.59	2.49	21.08	12011.	12280.	-2.2	544.
R-717-032A	91.28	184.2	184.4	0.0816	87.51	24.25	5.4	4.4	12034.	63.26	67.72	4.45	25.79	11815.	12113.	-2.5	438.
R-717-033A	96.04	199.7	199.0	0.0825	91.60	24.38	3.9	3.2	8760.	63.16	69.16	5.99	29.88	11753.	11761.	-0.1	376.
R-717-034A	72.25	135.2	134.0	0.0350	71.22	10.64	32.6	26.3	72622.	65.91	66.33	0.33	6.13	5386.	5425.	-0.7	840.
R-717-035A	74.69	140.7	139.8	0.0355	72.85	10.78	9.8	7.9	22013.	65.78	66.92	1.13	8.34	5432.	5572.	-2.6	622.
R-717-036A	77.23	146.2	146.0	0.0358	74.72	10.84	5.4	4.4	12214.	65.53	67.58	2.04	10.68	5436.	5550.	-2.1	486.
R-717-037A	79.92	153.7	152.8	0.0365	76.90	11.01	3.9	3.2	8873.	65.70	68.48	2.78	12.83	5490.	5453.	0.7	409.
R-717-038A	73.86	138.7	137.8	0.0236	70.68	7.19	32.6	26.3	76619.	69.88	70.18	0.21	3.83	3630.	3356.	7.6	905.
R-717-039A	75.47	142.2	141.7	0.0234	72.12	7.11	9.8	7.9	23210.	69.84	70.60	0.76	5.25	3577.	3746.	-4.7	651.
R-717-040A	77.00	146.2	145.4	0.0234	73.09	7.11	5.4	4.4	12845.	69.55	70.92	1.36	6.76	3569.	3715.	-4.1	504.
R-717-041A	78.20	148.7	148.4	0.0237	74.12	7.19	3.9	3.2	9251.	69.23	71.06	1.82	8.05	3596.	3582.	0.4	427.
R-717-042A	73.95	138.7	138.0	0.0231	70.11	7.03	32.6	26.3	76717.	69.97	70.28	0.23	3.82	3547.	3698.	-4.3	886.
R-717-043A	75.53	142.2	141.8	0.0227	71.47	6.91	9.8	7.9	23215.	69.85	70.63	0.77	5.29	3479.	3810.	-9.5	628.
R-717-044A	77.00	146.2	145.4	0.0228	72.24	6.93	5.4	4.4	12839.	69.53	70.89	1.36	6.79	3479.	3696.	-6.2	489.
R-717-045A	78.31	149.2	148.7	0.0231	73.39	7.00	3.9	3.2	9256.	69.26	71.11	1.86	8.12	3504.	3647.	-4.1	412.

Table D.1 (continued)

Run No.	T_v (°F)	P (psia)	P_{sat} (psia)	F_c (gpm)	T_c (°F)	m_c (lb_m/h)	F_w (gpm)	v (ft/s)	Re	$T_{w,in}$ (°F)	$T_{w,out}$ (°F)	ΔT_w (°F)	$\overline{\Delta T}$ (°F)	Q_c (Btu/h)	Q_w (Btu/h)	Δ (%)	U (Btu/h·ft²·°F)
R-717-046A	69.65	128.7	128.0	0.0176	67.64	5.37	32.6	26.3	73482.	66.84	67.09	0.17	2.68	2735.	2737.	-0.1	974.
R-717-047A	70.31	130.2	129.5	0.0177	68.46	5.40	23.0	18.5	52142.	67.25	67.52	0.22	2.92	2744.	2551.	7.0	897.
R-717-048A	71.29	132.2	131.7	0.0178	69.41	5.42	9.8	7.9	22368.	67.21	67.80	0.58	3.78	2751.	2850.	-3.6	695.
R-717-049A	72.43	134.7	134.4	0.0179	69.88	5.45	5.4	4.4	12386.	67.07	68.06	0.98	4.87	2759.	2677.	3.0	541.
R-717-050A	73.55	137.7	137.0	0.0179	70.75	5.46	3.9	3.2	8939.	66.93	68.31	1.37	5.93	2760.	2683.	2.8	445.
R-717-051A	68.99	127.2	126.5	0.0183	67.86	5.60	32.6	26.3	72712.	66.08	66.34	0.17	2.78	2855.	2851.	0.1	980.
R-717-052A	69.41	128.2	127.5	0.0183	68.43	5.60	23.0	18.5	51442.	66.26	66.55	0.24	3.00	2852.	2793.	2.1	908.
R-717-053A	70.22	130.2	129.3	0.0184	68.84	5.63	9.8	7.9	22007.	66.04	66.62	0.56	3.89	2860.	2771.	3.1	702.
R-717-054A	71.33	132.7	131.8	0.0183	69.46	5.58	5.4	4.4	12165.	65.74	66.78	1.03	5.07	2833.	2800.	1.2	534.
R-717-055A	72.43	135.2	134.4	0.0182	69.93	5.53	3.9	3.2	8781.	65.63	67.04	1.40	6.10	2802.	2753.	1.7	439.
R-717-056A	72.05	134.7	133.5	0.0378	71.68	11.48	32.6	26.3	71657.	64.94	65.38	0.35	6.89	5818.	5783.	0.6	807.
R-717-057A	74.33	140.2	138.9	0.0377	73.41	11.44	9.8	7.9	21696.	64.70	65.92	1.21	9.02	5772.	5946.	-3.0	611.
R-717-058A	77.03	146.7	145.5	0.0377	75.43	11.41	5.4	4.4	12070.	64.62	66.78	2.14	11.33	5723.	5839.	-2.0	482.
R-717-059A	79.73	153.7	152.4	0.0377	77.53	11.39	3.8	3.1	8577.	64.64	67.61	2.96	13.61	5682.	5700.	-0.3	399.
R-717-060A	71.07	131.7	131.2	0.0301	68.55	9.19	32.6	26.3	72439.	65.75	66.12	0.29	5.13	4666.	4659.	0.2	869.
R-717-061A	73.48	137.2	136.9	0.0308	70.42	9.39	9.8	7.9	21802.	65.88	66.90	1.01	7.09	4742.	4935.	-4.1	639.
R-717-062A	75.98	143.7	142.9	0.0310	72.67	9.41	5.4	4.3	12100.	65.91	67.70	1.78	9.18	4731.	4791.	-1.3	492.
R-717-063A	77.79	147.7	147.4	0.0309	73.73	9.38	3.8	3.1	8664.	65.64	68.06	2.41	10.94	4699.	4636.	1.3	410.
R-717-064A	70.94	132.2	130.9	0.0316	70.96	9.62	32.6	26.3	71823.	65.13	65.52	0.31	5.61	4884.	4985.	-2.1	832.
R-717-065A	72.16	135.2	133.8	0.0315	72.26	9.58	12.6	10.2	27827.	65.10	65.90	0.79	6.66	4850.	4974.	-2.6	695.
R-717-066A	72.86	136.7	135.4	0.0308	72.98	9.35	9.8	7.9	21757.	64.99	66.03	1.02	7.36	4731.	5035.	-6.4	614.
R-717-067A	71.83	134.7	133.0	0.0302	71.92	9.18	17.7	14.3	39156.	65.31	65.93	0.58	6.21	4651.	5174.	-11.3	715.
R-717-068A	73.59	138.7	137.1	0.0311	73.10	9.43	7.7	6.2	17023.	64.92	66.22	1.29	8.02	4762.	4971.	-4.4	567.
R-717-069A	74.15	139.7	138.5	0.0313	73.66	9.49	6.4	5.2	14182.	64.75	66.28	1.53	8.63	4790.	4895.	-2.2	530.
R-717-070A	74.81	141.2	140.1	0.0311	73.90	9.42	5.4	4.4	11931.	64.64	66.42	1.77	9.28	4744.	4781.	-0.8	488.
R-717-071A	75.54	143.2	141.8	0.0313	74.48	9.47	4.8	3.9	10742.	64.70	66.71	2.00	9.84	4767.	4845.	-1.6	463.
R-717-072A	75.95	144.2	142.8	0.0313	74.78	9.47	4.5	3.6	9969.	64.65	66.80	2.14	10.23	4763.	4814.	-1.1	445.
R-717-073A	76.82	146.2	145.0	0.0309	75.10	9.35	3.9	3.2	8720.	64.61	67.05	2.43	10.99	4695.	4772.	-1.6	408.
R-717-074A	78.57	150.2	149.4	0.0201	75.85	6.08	33.0	26.6	83222.	75.37	75.62	0.18	3.08	3041.	3013.	0.9	943.
R-717-075A	79.34	152.2	151.3	0.0201	76.70	6.07	17.7	14.3	44816.	75.61	76.00	0.34	3.53	3033.	3046.	-0.5	821.
R-717-076A	79.96	153.9	152.9	0.0204	78.08	6.15	12.6	10.2	31980.	75.73	76.26	0.52	3.97	3067.	3281.	-7.0	739.
R-717-077A	80.34	154.7	153.9	0.0204	78.56	6.16	9.8	7.9	25015.	75.72	76.36	0.64	4.30	3070.	3135.	-2.1	682.
R-717-078A	80.65	155.7	154.7	0.0207	78.28	6.22	7.6	6.1	19305.	75.42	76.28	0.85	4.80	3100.	3231.	-4.2	617.
R-717-079A	81.06	156.2	155.8	0.0205	78.36	6.17	6.4	5.1	16148.	75.40	76.40	0.99	5.16	3072.	3156.	-2.7	569.
R-717-080A	81.47	157.2	156.9	0.0205	78.57	6.17	5.4	4.4	13815.	75.31	76.48	1.16	5.58	3069.	3165.	-3.1	526.
R-717-081A	81.72	157.7	157.5	0.0206	78.93	6.21	4.9	3.9	12414.	75.21	76.49	1.28	5.87	3085.	3119.	-1.1	502.
R-717-082A	82.18	159.7	158.8	0.0207	79.26	6.22	4.4	3.6	11291.	75.26	76.68	1.42	6.22	3087.	3144.	-1.8	474.
R-717-083A	82.68	161.2	160.1	0.0206	79.57	6.20	3.9	3.2	9976.	75.20	76.80	1.60	6.67	3075.	3137.	-2.0	440.
R-717-084A	83.54	162.7	162.4	0.0206	80.05	6.19	3.2	2.6	8173.	75.03	76.97	1.93	7.54	3067.	3100.	-1.1	389.
R-717-085A	76.78	146.2	144.9	0.0125	74.59	3.78	33.0	26.6	82580.	74.79	75.00	0.13	1.89	1899.	2190.	-15.3	961.
R-717-086A	77.51	147.7	146.7	0.0127	75.29	3.85	9.8	7.9	24642.	74.67	75.08	0.41	2.63	1930.	2025.	-4.9	701.
R-717-087A	78.28	149.7	148.6	0.0126	75.72	3.80	5.4	4.3	13396.	74.42	75.18	0.76	3.48	1901.	2043.	-7.5	521.
R-717-088A	79.05	151.7	150.6	0.0125	76.25	3.77	3.9	3.2	9836.	74.40	75.42	1.01	4.14	1883.	1986.	-5.5	434.
R-717-089A	76.21	144.7	143.5	0.0114	74.97	3.46	33.0	26.6	82150.	74.39	74.60	0.13	1.72	1739.	2140.	-23.1	967.
R-717-090A	76.88	145.7	145.1	0.0113	75.35	3.43	9.8	7.9	24276.	74.32	74.70	0.38	2.37	1722.	1848.	-7.4	693.
R-717-091A	77.48	147.2	146.6	0.0113	75.93	3.43	5.4	4.3	13366.	74.00	74.68	0.68	3.14	1718.	1822.	-6.1	523.
R-717-092A	77.97	149.0	147.9	0.0112	76.35	3.40	3.9	3.1	9671.	73.74	74.66	0.92	3.77	1700.	1792.	-5.4	431.

Table D.1 (continued)

Run No.	T_v (°F)	P (psia)	P_{sat} (psia)	F_c (gpm)	T_c (°F)	m_c (lb_m/h)	F_w (gpm)	v (ft/s)	Re	$T_{w,in}$ (°F)	$T_{w,out}$ (°F)	ΔT_w (°F)	$\overline{\Delta T}$ (°F)	Q_c (Btu/h)	Q_w (Btu/h)	Δ (%)	U (Btu/h·ft²·°F)
R-717-098A	77.79	148.7	147.4	0.0114	77.14	3.43	9.8	7.9	24675.	75.18	75.57	0.38	2.42	1717.	1882.	-9.6	678.
R-717-099A	78.45	150.2	149.1	0.0114	77.40	3.45	5.3	4.2	13221.	74.88	75.60	0.72	3.21	1728.	1884.	-9.0	514.
R-717-100A	77.20	147.4	145.9	0.0119	77.19	3.59	33.0	26.6	83119.	75.30	75.50	0.13	1.80	1799.	2074.	-15.3	955.
R-717-101A	77.76	148.2	147.3	0.0117	77.19	3.54	18.0	14.5	45536.	75.61	75.86	0.23	2.02	1775.	2083.	-17.4	840.
R-717-102A	79.60	153.2	152.0	0.0114	78.19	3.43	3.9	3.1	9871.	75.30	76.26	0.96	3.82	1712.	1860.	-8.7	428.
R-717-103A	81.17	153.7	156.1	0.0911	79.18	27.42	32.6	26.3	67488.	60.48	61.44	0.88	20.21	13645.	14254.	-4.5	645.
R-717-104A	87.16	170.4	172.4	0.0920	85.26	27.44	9.8	7.9	20726.	60.66	63.52	2.84	25.07	13486.	13974.	-3.6	514.
R-717-105A	93.58	189.7	191.4	0.0938	91.01	27.75	5.4	4.4	11448.	60.05	65.16	5.10	30.97	13452.	13775.	-2.4	415.
R-717-106A	98.84	206.7	208.1	0.0943	95.01	27.72	3.9	3.1	8342.	59.79	66.68	6.88	35.61	13282.	13416.	-1.0	356.
R-717-107A	95.27	192.7	196.6	0.1191	91.98	35.20	9.8	7.9	21033.	61.32	64.91	3.59	32.16	16998.	17670.	-4.0	505.
R-717-108A	88.60	171.7	176.6	0.1174	85.31	35.04	32.6	26.3	68752.	61.66	62.83	1.09	26.36	17165.	17740.	-3.4	622.
R-717-109A	104.13	221.7	225.9	0.1232	100.34	35.95	5.4	4.4	11749.	61.22	67.65	6.42	39.70	17013.	17334.	-1.9	409.
R-717-110A	94.44	184.7	194.0	0.1211	89.80	35.88	17.7	14.3	38106.	62.63	64.75	2.10	30.75	17360.	18600.	-7.1	539.
R-717-111A	90.93	178.9	183.4	0.0987	87.84	29.35	32.6	26.3	75569.	68.49	69.53	0.94	21.92	14308.	15362.	-7.4	623.
R-717-112A	94.30	189.2	193.6	0.0997	90.69	29.50	17.7	14.3	41623.	69.19	70.95	1.75	24.23	14276.	15460.	-8.3	563.
R-717-113A	97.37	199.2	203.3	0.1004	93.74	29.59	9.8	7.9	22867.	68.29	71.46	3.17	27.50	14222.	15435.	-8.5	494.
R-717-114A	103.36	218.7	223.2	0.1018	99.48	29.76	5.4	4.4	12901.	67.84	73.28	5.44	32.80	14108.	14818.	-5.0	411.
R-717-119A	80.76	154.7	155.0	0.0754	79.74	22.67	32.6	26.3	71961.	65.06	65.87	0.72	15.29	11290.	11713.	-3.7	705.
R-717-120A	85.51	168.2	167.8	0.0761	84.16	22.73	9.8	7.9	21981.	65.05	67.44	2.38	19.27	11208.	11709.	-4.5	556.
R-717-121A	90.17	182.2	181.1	0.0763	88.32	22.67	5.4	4.4	12240.	64.58	68.83	4.24	23.47	11071.	11539.	-4.2	451.
R-717-122A	95.05	197.2	195.9	0.0772	92.92	22.79	3.9	3.2	8925.	64.60	70.42	5.82	27.54	11009.	11421.	-3.7	382.
R-717-123A	82.48	158.7	159.6	0.0468	80.57	14.06	32.6	26.3	80043.	73.19	73.69	0.43	9.04	6978.	7042.	-0.9	737.
R-717-124A	84.58	166.7	165.2	0.0459	82.61	13.75	9.8	7.9	24377.	73.31	74.77	1.45	10.53	6795.	7135.	-5.0	616.
R-717-125A	87.51	174.7	173.4	0.0458	84.98	13.66	5.4	4.4	13558.	73.16	75.72	2.55	13.07	6710.	6944.	-3.5	490.
R-717-126A	90.40	183.2	181.8	0.0462	87.80	13.74	3.9	3.2	9879.	73.09	76.62	3.52	15.54	6707.	6933.	-3.4	412.
R-717-127A	79.96	153.7	152.9	0.0665	79.15	20.01	33.3	26.8	74501.	66.08	66.78	0.62	13.53	9979.	10250.	-2.7	705.
R-717-128A	85.66	168.7	168.2	0.0677	84.30	20.21	9.6	7.7	21723.	66.17	68.33	2.15	18.41	9965.	10338.	-3.7	517.
R-717-129A	90.19	181.7	181.2	0.0678	88.24	20.15	5.4	4.4	12414.	65.88	69.59	3.70	22.46	9840.	10087.	-2.5	419.
R-717-130A	94.17	193.7	193.2	0.0681	91.89	20.12	3.9	3.2	9026.	65.76	70.90	5.13	25.84	9741.	10080.	-3.5	360.
R-717-131A	78.25	149.7	148.6	0.0468	77.36	14.11	33.4	26.9	77790.	69.10	69.62	0.42	8.89	7062.	7043.	0.3	759.
R-717-132A	81.08	157.2	155.8	0.0464	79.67	13.95	9.8	7.9	23012.	68.88	70.29	1.41	11.49	6944.	6925.	0.3	577.
R-717-133A	84.55	166.7	165.2	0.0461	82.78	13.80	5.4	4.4	12793.	68.66	71.21	2.54	14.61	6819.	6915.	-1.4	446.
R-717-134A	87.08	173.7	172.2	0.0455	84.87	13.57	3.9	3.2	9269.	68.54	72.03	3.50	16.79	6670.	6873.	-3.0	379.
R-717-135A	88.55	176.7	176.4	0.1025	86.31	30.53	33.4	26.9	75162.	66.35	67.35	0.91	21.70	14961.	15121.	-1.1	659.
R-717-136A	95.37	197.7	196.9	0.1049	93.22	30.94	9.8	7.9	22447.	66.34	69.48	3.12	27.46	14936.	15321.	-2.6	519.
R-717-137A	101.94	219.7	218.4	0.1055	99.34	30.83	5.4	4.4	12593.	66.04	71.51	5.46	33.17	14665.	14864.	-1.4	422.
R-717-138A	108.53	242.2	241.6	0.1079	105.66	31.23	3.8	3.1	8926.	65.88	73.71	7.83	38.74	14626.	14907.	-1.9	361.
R-717-139A	83.03	162.2	161.0	0.0175	80.40	5.26	34.0	27.4	91169.	80.22	80.47	0.18	2.69	2607.	3036.	-16.5	926.
R-717-140A	85.10	168.2	166.7	0.0172	82.24	5.16	9.8	7.9	26445.	80.98	81.55	0.56	3.83	2547.	2719.	-6.8	635.
R-717-141A	86.50	171.7	170.6	0.0174	83.34	5.19	5.4	4.4	14697.	81.05	82.05	1.00	4.95	2556.	2683.	-5.0	493.
R-717-142A	87.78	175.7	174.2	0.0175	84.28	5.23	3.9	3.2	10746.	81.23	82.62	1.39	5.86	2569.	2727.	-6.2	419.
R-717-143A	86.60	171.7	170.9	0.0337	84.92	10.06	34.0	27.4	91501.	80.45	80.82	0.31	5.97	4952.	5241.	-5.8	793.
R-717-144A	88.63	177.7	176.6	0.0328	85.89	9.79	9.8	7.9	26649.	80.56	81.56	0.99	7.56	4797.	4885.	-1.8	606.
R-717-145A	90.77	184.2	182.9	0.0326	87.39	9.69	5.5	4.4	14951.	80.59	82.31	1.71	9.32	4725.	4687.	0.8	484.

Table D.1 (continued)

Run No.	T_v (°F)	P (psia)	P_{sat} (psia)	F_c (gpm)	T_c (°F)	m_c (lb_m/h)	F_w (gpm)	v (ft/s)	Re	$T_{w,in}$ (°F)	$T_{w,out}$ (°F)	ΔT_w (°F)	$\overline{\Delta T}$ (°F)	Q_c (Btu/h)	Q_w (Btu/h)	Δ (%)	U (Btu/h·ft^2·°F)
R-717-146A	84.53	167.2	165.1	0.0257	82.72	7.71	34.0	27.4	91091.	80.12	80.43	0.24	4.26	3808.	4020.	-5.6	854.
R-717-147A	86.18	170.7	169.7	0.0256	83.59	7.66	9.8	7.9	26427.	79.99	80.79	0.79	5.79	3772.	3867.	-2.5	622.
R-717-148A	87.89	175.7	174.5	0.0253	84.39	7.55	5.4	4.4	14660.	79.89	81.30	1.40	7.29	3705.	3820.	-3.1	485.
R-717-149A	89.25	179.7	178.4	0.0250	85.70	7.46	3.9	3.2	10609.	79.94	81.83	1.88	8.37	3648.	3688.	-1.1	416.
R-717-150A	88.20	177.2	175.4	0.0396	85.97	11.81	34.0	27.4	92240.	81.07	81.50	0.35	6.91	5793.	5954.	-2.8	801.
R-717-151A	90.98	184.7	183.5	0.0394	88.42	11.69	9.8	7.9	26877.	81.16	82.34	1.17	9.23	5698.	5749.	-0.9	590.
R-717-152A	93.88	193.7	192.3	0.0399	90.92	11.80	5.4	4.4	15012.	81.50	83.54	2.04	11.35	5714.	5541.	3.0	481.
R-717-153A	95.90	199.7	198.6	0.0399	92.42	11.77	3.9	3.2	10836.	81.15	84.05	2.90	13.30	5676.	5688.	-0.2	408.

Table D.2. Experimental data for ammonia condensing on Tube A (horizontal)

Run No.	T_v (°F)	P (psia)	P_{sat} (psia)	F_c (gpm)	T_c (°F)	m_c (lb_m/h)	F_w (gpm)	v (ft/s)	Re	$T_{w,in}$ (°F)	$T_{w,out}$ (°F)	ΔT_w (°F)	$\overline{\Delta T}$ (°F)	Q_c (Btu/h)	Q_w (Btu/h)	Δ (%)	U (Btu/h·ft²·°F)
R-717-001AH	87.53	173.7	173.5	0.0779	87.17	23.17	35.0	28.2	90776.	77.30	78.08	0.64	9.84	11376.	11263.	1.0	1104.
R-717-002AH	89.62	180.2	179.5	0.0782	89.51	23.19	17.7	14.3	46361.	77.80	79.14	1.27	11.15	11339.	11250.	0.8	971.
R-717-003AH	92.55	189.7	188.2	0.0783	92.31	23.11	9.8	7.9	25860.	77.89	80.23	2.27	13.49	11228.	11123.	0.9	795.
R-717-004AH	94.20	194.7	193.3	0.0782	93.92	23.03	7.6	6.1	20095.	77.71	80.72	2.97	14.99	11148.	11269.	-1.1	711.
R-717-005AH	97.10	203.2	202.4	0.0780	96.52	22.88	5.4	4.4	14490.	77.62	81.71	4.04	17.43	11003.	10990.	0.1	603.
R-717-006AH	100.89	215.7	214.8	0.0783	100.09	22.85	4.0	3.2	10721.	77.55	83.07	5.47	20.59	10894.	10922.	-0.3	505.
R-717-007AH	85.15	167.2	166.8	0.0288	84.89	8.61	35.0	28.2	96135.	82.11	82.47	0.24	2.85	4248.	4121.	3.0	1423.
R-717-008AH	86.01	169.7	169.2	0.0288	85.52	8.60	17.7	14.3	48789.	82.31	82.85	0.47	3.43	4236.	4141.	2.2	1180.
R-717-009AH	86.88	172.7	171.7	0.0290	86.45	8.62	9.9	8.0	27260.	82.05	82.95	0.86	4.39	4241.	4243.	-0.0	924.
R-717-010AH	87.71	174.7	174.0	0.0291	87.27	8.66	7.6	6.1	20984.	82.14	83.30	1.12	4.99	4253.	4243.	0.2	814.
R-717-011AH	89.12	179.2	178.1	0.0288	88.52	8.54	5.3	4.3	14850.	82.35	83.96	1.58	5.96	4181.	4220.	-0.9	670.
R-717-012AH	90.70	183.7	182.7	0.0288	89.86	8.54	3.9	3.2	11011.	82.42	84.59	2.14	7.20	4164.	4221.	-1.4	552.
R-717-013AH	92.65	189.7	188.6	0.1009	91.90	29.81	35.0	28.2	93669.	79.72	80.66	0.80	12.47	14479.	14039.	3.0	1109.
R-717-014AH	95.72	198.7	198.0	0.1016	94.74	29.90	17.7	14.3	47879.	80.20	81.90	1.64	14.67	14424.	14482.	-0.4	939.
R-717-015AH	99.29	210.7	209.5	0.1020	98.21	29.86	9.8	7.9	26815.	80.09	83.04	2.91	17.72	14292.	14285.	0.0	770.
R-717-016AH	101.69	218.7	217.5	0.1025	100.52	29.90	7.6	6.1	20823.	80.21	83.97	3.72	19.60	14233.	14124.	0.8	694.
R-717-017AH	106.79	237.7	235.3	0.1024	105.36	29.66	5.1	4.1	14199.	80.62	86.19	5.55	23.38	13949.	14126.	-1.3	570.
R-717-018AH	90.34	183.2	181.6	0.0905	89.87	26.82	35.0	28.2	92557.	78.79	79.67	0.75	11.11	13092.	13044.	0.4	1125.
R-717-019AH	93.36	192.2	190.7	0.0928	92.74	27.37	17.7	14.3	47357.	79.39	80.94	1.48	13.19	13274.	13060.	1.6	961.
R-717-020AH	96.68	202.2	201.1	0.0931	95.88	27.34	9.8	7.9	26370.	79.27	81.98	2.66	16.05	13160.	12986.	1.3	783.
R-717-021AH	98.78	209.7	207.8	0.0932	97.87	27.31	7.6	6.2	20685.	79.29	82.74	3.41	17.76	13085.	13026.	0.5	704.
R-717-022AH	102.15	220.7	219.1	0.0932	101.04	27.17	5.4	4.4	14837.	79.18	83.96	4.73	20.58	12916.	12858.	0.5	599.
R-717-023AH	106.74	236.7	235.1	0.0934	105.41	27.04	3.9	3.1	10744.	79.28	85.80	6.47	24.20	12717.	12589.	1.0	502.
R-717-024AH	85.56	169.2	168.0	0.0538	85.44	16.05	35.0	28.2	93198.	79.50	80.06	0.43	5.78	7912.	7543.	4.7	1307.
R-717-025AH	87.20	173.7	172.5	0.0536	86.88	15.95	23.0	18.5	62052.	80.46	81.21	0.66	6.36	7835.	7619.	2.8	1177.
R-717-026AH	89.27	179.7	178.5	0.0538	88.87	15.96	9.8	7.9	26549.	79.97	81.55	1.54	8.52	7809.	7582.	2.9	876.
R-717-027AH	95.21	197.7	196.4	0.0535	94.10	15.76	3.9	3.1	10648.	79.91	83.71	3.78	13.40	7610.	7357.	3.3	542.
R-717-028AH	87.67	174.7	173.9	0.0403	87.72	11.98	35.0	28.2	97143.	82.92	83.38	0.34	4.52	5882.	5884.	-0.0	1244.
R-717-029AH	88.66	177.7	176.7	0.0398	88.54	11.82	23.0	18.5	64543.	83.78	84.33	0.47	4.61	5788.	5370.	7.2	1200.
R-717-030AH	90.01	182.2	180.7	0.0399	89.79	11.83	9.9	8.0	27687.	83.18	84.38	1.16	6.23	5777.	5734.	0.7	886.
R-717-031AH	94.24	194.7	193.4	0.0396	93.24	11.66	3.8	3.1	10823.	82.72	85.68	2.94	10.04	5645.	5655.	-0.2	537.
R-717-032AH	86.90	172.7	171.7	0.0193	85.58	5.74	35.4	28.5	100660.	85.01	85.29	0.16	1.74	2824.	2773.	1.8	1548.
R-717-033AH	87.29	173.7	172.8	0.0194	85.89	5.79	22.9	18.5	65228.	85.13	85.47	0.25	1.99	2847.	2902.	-1.9	1366.
R-717-034AH	88.32	176.7	175.8	0.0194	86.75	5.79	9.8	7.9	28139.	85.23	85.86	0.59	2.78	2837.	2899.	-2.2	974.
R-717-035AH	90.44	182.7	181.9	0.0192	88.30	5.71	3.9	3.1	11171.	85.03	86.50	1.45	4.68	2785.	2817.	-1.2	569.
R-717-036AH	84.93	166.7	166.2	0.0635	84.84	18.95	35.0	28.2	90558.	77.17	77.83	0.52	7.43	9355.	9150.	2.2	1202.
R-717-037AH	86.03	170.2	169.3	0.0634	85.84	18.91	23.0	18.5	59807.	77.45	78.33	0.79	8.13	9313.	9030.	3.0	1094.
R-717-038AH	89.10	179.2	178.0	0.0633	88.57	18.79	9.8	7.9	25782.	77.45	79.37	1.86	10.69	9197.	9160.	0.4	822.
R-717-039AH	95.97	200.2	198.8	0.0628	94.63	18.48	3.9	3.1	10313.	76.91	81.55	4.59	16.74	8910.	8935.	-0.3	508.
R-717-040AH	88.03	175.7	174.9	0.0400	87.21	11.91	35.0	28.2	98045.	83.68	84.14	0.33	4.12	5840.	5780.	1.0	1354.
R-717-041AH	89.32	179.7	178.7	0.0396	88.33	11.76	23.0	18.5	65128.	84.52	85.10	0.49	4.51	5754.	5634.	2.1	1217.
R-717-042AH	90.96	184.7	183.5	0.0402	89.82	11.91	9.8	7.9	27874.	84.14	85.37	1.19	6.21	5806.	5838.	-0.6	893.
R-717-043AH	95.52	199.2	197.4	0.0399	93.96	11.75	3.8	3.1	10992.	84.00	86.99	2.96	10.02	5673.	5691.	-0.3	541.

Table D.3. Experimental data for ammonia condensing on Tube A (30° for the horizontal)

Run No.	T_v (°F)	P (psia)	P_{sat} (psia)	F_c (gpm)	T_c (°F)	m_c (lb_m/h)	F_w (gpm)	v (ft/s)	Re	$T_{w,in}$ (°F)	$T_{w,out}$ (°F)	ΔT_w (°F)	$\overline{\Delta T}$ (°F)	Q_c (Btu/h)	Q_w (Btu/h)	Δ (%)	U (Btu/h·ft²·°F)
R-717-001A30	90.23	182.2	181.3	0.0872	89.59	25.85	35.0	28.2	92650.	78.89	79.73	0.71	10.92	12619.	12415.	1.6	1104.
R-717-002A30	92.88	190.7	189.2	0.0890	92.10	26.28	23.0	18.5	62014.	80.21	81.37	1.06	12.09	12759.	12209.	4.3	1008.
R-717-003A30	96.36	201.7	200.1	0.0893	95.41	26.25	9.8	7.9	26380.	79.36	81.96	2.54	15.71	12644.	12433.	1.7	769.
R-717-004A30	98.36	208.2	206.5	0.0888	97.38	26.04	7.6	6.1	20635.	79.49	82.78	3.25	17.23	12487.	12374.	0.9	692.
R-717-005A30	101.48	217.7	216.8	0.0888	100.22	25.91	5.4	4.4	14698.	79.28	83.82	4.49	19.93	12340.	12099.	2.0	592.
R-717-006A30	105.90	233.7	232.1	0.0887	104.33	25.74	3.9	3.2	10812.	79.55	85.71	6.11	23.27	12131.	11949.	1.5	498.
R-717-007A30	87.08	172.7	172.2	0.0220	85.95	6.57	35.0	28.2	99336.	84.84	85.15	0.18	2.08	3227.	3213.	0.4	1482.
R-717-008A30	87.71	174.7	174.0	0.0221	86.49	6.59	23.0	18.5	65558.	85.19	85.52	0.25	2.36	3233.	2915.	9.9	1311.
R-717-009A30	88.56	177.2	176.4	0.0221	87.42	6.56	9.8	7.9	28059.	84.96	85.65	0.66	3.25	3216.	3238.	-0.7	945.
R-717-010A30	89.12	179.2	178.1	0.0219	87.98	6.51	7.6	6.1	21748.	85.03	85.90	0.83	3.65	3184.	3171.	0.4	832.
R-717-011A30	90.01	181.7	180.7	0.0219	88.85	6.51	5.4	4.4	15576.	84.97	86.19	1.20	4.43	3180.	3255.	-2.4	686.
R-717-012A30	91.44	186.7	184.9	0.0220	90.09	6.52	3.9	3.1	11202.	85.16	86.84	1.66	5.44	3176.	3230.	-1.7	557.
R-717-013A30	86.82	172.7	171.5	0.0547	86.38	16.28	35.0	28.2	94329.	80.48	81.03	0.43	6.07	8008.	7526.	6.0	1260.
R-717-014A30	88.23	176.7	175.5	0.0551	87.66	16.38	23.0	18.5	62576.	81.14	81.89	0.66	6.71	8029.	7596.	5.4	1142.
R-717-015A30	90.39	182.7	181.8	0.0551	89.62	16.33	9.8	7.9	26779.	80.64	82.27	1.59	8.94	7972.	7838.	1.7	852.
R-717-016A30	91.73	187.2	185.8	0.0549	90.87	16.25	7.5	6.1	20612.	80.76	82.84	2.04	9.93	7906.	7691.	2.7	761.
R-717-017A30	93.80	193.7	192.1	0.0550	92.69	16.22	5.4	4.4	14929.	80.65	83.49	2.81	11.73	7860.	7646.	2.7	640.
R-717-018A30	97.04	203.7	202.2	0.0552	95.78	16.21	3.9	3.2	10857.	81.01	84.94	3.90	14.06	7795.	7629.	2.1	529.
R-717-019A30	88.17	176.2	175.3	0.0336	87.16	10.00	35.0	28.2	98973.	84.49	84.90	0.28	3.48	4904.	4907.	-0.1	1347.
R-717-020A30	88.82	178.2	177.2	0.0337	87.83	10.02	23.0	18.5	65239.	84.70	85.19	0.41	3.87	4905.	4682.	4.6	1210.
R-717-021A30	90.30	182.7	181.5	0.0334	89.12	9.92	9.8	7.9	27993.	84.59	85.63	1.00	5.19	4841.	4904.	-1.3	891.
R-717-022A30	91.26	185.2	184.4	0.0335	90.24	9.91	7.5	6.1	21519.	84.69	86.02	1.29	5.91	4829.	4859.	-0.6	781.
R-717-023A30	92.50	189.2	188.1	0.0334	91.30	9.87	5.4	4.4	15575.	84.67	86.47	1.77	6.93	4795.	4821.	-0.5	661.
R-717-024A30	94.40	195.2	193.9	0.0335	92.95	9.87	3.9	3.2	11247.	84.82	87.27	2.43	8.35	4776.	4752.	0.5	546.
R-717-025A30	89.50	179.7	179.2	0.0758	87.92	22.53	35.0	28.2	93447.	79.63	80.36	0.61	9.50	11015.	10669.	3.1	1108.
R-717-026A30	91.91	187.7	186.3	0.0755	90.08	22.36	23.0	18.5	62722.	81.21	82.21	0.91	10.20	10879.	10499.	3.5	1018.
R-717-027A30	94.74	196.7	195.0	0.0760	92.82	22.43	9.7	7.8	26327.	80.18	82.46	2.24	13.42	10845.	10840.	0.0	772.
R-717-028A30	96.05	200.7	199.1	0.0752	94.07	22.14	7.6	6.1	20656.	80.01	82.86	2.82	14.61	10672.	10692.	-0.2	698.
R-717-029A30	99.47	211.2	210.1	0.0761	97.00	22.32	5.2	4.2	14295.	79.92	84.18	4.24	17.42	10677.	11039.	-3.4	585.
R-717-030A30	103.36	224.7	223.2	0.0762	100.52	22.23	3.8	3.1	10491.	79.91	85.52	5.60	20.64	10539.	10609.	-0.7	488.
R-717-031A30	93.29	191.7	190.5	0.0988	91.58	29.20	35.0	28.2	94159.	80.15	81.07	0.80	12.68	14163.	13969.	1.4	1066.
R-717-032A30	95.33	197.7	196.8	0.0989	93.35	29.15	23.0	18.5	62628.	80.94	82.24	1.21	13.75	14075.	13919.	1.1	978.
R-717-033A30	100.16	213.7	212.4	0.1012	98.11	29.63	9.8	7.9	26867.	80.68	83.60	2.88	18.02	14153.	14086.	0.5	750.
R-717-034A30	102.56	221.7	220.5	0.1008	100.42	29.41	7.3	5.9	20124.	80.67	84.52	3.81	19.96	13970.	13876.	0.7	668.
R-717-035A30	107.62	239.7	238.3	0.1013	105.13	29.35	4.8	3.9	13378.	80.60	86.38	5.76	24.13	13779.	13784.	-0.0	545.
R-717-036A30	88.28	176.7	175.6	0.0632	86.80	18.81	35.5	28.6	95585.	80.36	80.99	0.51	7.60	9224.	8979.	2.6	1159.
R-717-037A30	90.15	182.2	181.1	0.0636	88.58	18.89	23.0	18.5	62783.	81.35	82.22	0.78	8.36	9222.	9008.	2.3	1053.
R-717-038A30	92.43	189.2	187.9	0.0635	90.60	18.80	9.7	7.8	26431.	80.51	82.43	1.88	10.96	9137.	9131.	0.1	796.
R-717-039A30	94.45	195.2	194.1	0.0632	92.50	18.66	7.3	5.9	20078.	80.92	83.43	2.47	12.27	9026.	9027.	-0.0	702.
R-717-040A30	96.63	202.2	200.9	0.0630	94.49	18.55	5.4	4.4	14884.	80.91	84.25	3.31	14.04	8931.	8931.	0.0	607.
R-717-041A30	100.36	214.7	213.1	0.0635	98.06	18.58	3.9	3.1	10886.	81.33	85.90	4.55	16.75	8872.	8855.	0.2	506.
R-717-042A30	87.09	172.7	172.2	0.0436	85.82	13.00	35.0	28.2	96026.	81.97	82.43	0.34	4.89	6387.	5972.	6.5	1247.
R-717-043A30	87.65	174.7	173.8	0.0430	86.43	12.81	23.0	18.5	63206.	82.04	82.64	0.51	5.31	6289.	5909.	6.0	1130.
R-717-044A30	89.75	180.7	179.9	0.0432	88.14	12.85	9.9	8.0	27328.	82.05	83.35	1.27	7.05	6279.	6253.	0.4	851.
R-717-045A30	90.83	184.2	183.1	0.0432	89.18	12.82	7.4	6.0	20522.	82.01	83.71	1.66	7.97	6251.	6156.	1.5	749.
R-717-046A30	92.47	189.2	188.0	0.0431	90.46	12.76	5.3	4.3	14847.	81.98	84.29	2.29	9.33	6199.	6102.	1.6	635.
R-717-047A30	95.28	197.7	196.6	0.0429	93.14	12.65	3.8	3.1	10655.	82.37	85.61	3.22	11.29	6109.	6104.	0.1	517.

Table D.4. Experimental data for ammonia condensing on Tube A (60° for the horizontal)

Run No.	T_v (°F)	P (psia)	P_{sat} (psia)	F_c (gpm)	T_c (°F)	m_c (lb_m/h)	F_w (gpm)	v (ft/s)	Re	$T_{w,in}$ (°F)	$T_{w,out}$ (°F)	ΔT_w (°F)	$\overline{\Delta T}$ (°F)	Q_c (Btu/h)	Q_w (Btu/h)	Δ (%)	U (Btu/h·ft²·°F)
R-717-001A60	87.51	174.7	173.4	0.0241	86.38	7.17	35.0	28.2	99176.	84.70	85.02	0.20	2.65	3520.	3457.	1.8	1269.
R-717-002A60	87.82	175.7	174.3	0.0238	86.64	7.07	23.0	18.5	65184.	84.69	85.07	0.29	2.94	3471.	3374.	2.8	1128.
R-717-003A60	89.18	179.7	178.2	0.0245	87.67	7.28	9.9	8.0	28199.	84.94	85.65	0.67	3.88	3564.	3324.	6.7	877.
R-717-004A60	89.73	181.7	179.9	0.0247	88.16	7.33	7.6	6.1	21760.	84.93	85.87	0.90	4.33	3583.	3441.	4.0	790.
R-717-005A60	90.78	184.7	182.9	0.0239	89.14	7.10	5.4	4.4	15598.	85.06	86.34	1.26	5.09	3461.	3420.	1.2	650.
R-717-006A60	92.42	189.7	187.8	0.0242	90.51	7.17	3.8	3.1	10981.	85.30	87.11	1.78	6.21	3485.	3396.	2.6	536.
R-717-007A60	93.07	190.7	189.8	0.0975	92.20	28.79	35.0	28.2	92507.	78.73	79.65	0.78	13.88	13970.	13672.	2.1	961.
R-717-008A60	94.95	197.2	195.6	0.0978	93.96	28.82	23.0	18.5	61386.	79.33	80.61	1.18	14.98	13928.	13551.	2.7	888.
R-717-009A60	99.25	210.7	209.4	0.0982	98.06	28.75	9.8	7.9	26476.	79.13	81.94	2.75	18.71	13760.	13529.	1.7	702.
R-717-010A60	101.71	218.7	217.6	0.0976	100.43	28.46	7.3	5.8	19611.	79.19	82.90	3.67	20.66	13547.	13289.	1.9	626.
R-717-011A60	106.51	235.7	234.3	0.0962	104.95	27.86	4.7	3.8	12895.	79.43	84.97	5.49	24.31	13114.	12873.	1.8	515.
R-717-012A60	86.36	171.7	170.2	0.0617	86.16	18.39	35.0	28.2	91321.	77.84	78.48	0.50	8.20	9052.	8678.	4.1	1054.
R-717-013A60	88.06	176.7	175.0	0.0626	87.67	18.62	23.0	18.5	60691.	78.62	79.50	0.78	9.00	9131.	9008.	1.4	969.
R-717-014A60	90.93	185.7	183.4	0.0626	90.24	18.55	9.8	7.9	26085.	78.41	80.28	1.81	11.59	9041.	8880.	1.8	745.
R-717-015A60	92.20	188.7	187.2	0.0623	91.44	18.41	7.6	6.1	20222.	78.33	80.70	2.33	12.68	8949.	8873.	0.9	674.
R-717-016A60	95.01	197.2	195.8	0.0632	93.81	18.61	5.4	4.4	14560.	78.39	81.71	3.27	14.96	8991.	8899.	1.0	574.
R-717-017A60	97.90	206.7	205.0	0.0623	96.56	18.27	3.8	3.1	10331.	78.13	82.68	4.50	17.49	8770.	8636.	1.5	479.
R-717-018A60	90.83	184.7	183.1	0.0842	90.01	24.94	35.0	28.2	92371.	78.67	79.47	0.67	11.76	12159.	11699.	3.8	987.
R-717-019A60	92.18	189.2	187.1	0.0847	91.38	25.03	23.0	18.5	60999.	78.90	80.02	1.03	12.72	12171.	11807.	3.0	914.
R-717-020A60	96.46	201.7	200.4	0.0849	95.20	24.96	9.8	7.9	26344.	79.15	81.62	2.41	16.08	12021.	11817.	1.7	714.
R-717-021A60	98.38	208.2	206.6	0.0848	97.14	24.86	7.6	6.1	20501.	79.26	82.39	3.10	17.56	11922.	11762.	1.3	649.
R-717-022A60	101.25	217.2	216.0	0.0850	99.86	24.81	5.4	4.4	14733.	78.84	83.16	4.28	20.25	11821.	11629.	1.6	558.
R-717-023A60	106.27	234.7	233.4	0.0852	104.33	24.71	3.8	3.1	10628.	79.70	85.70	5.95	23.57	11635.	11421.	1.8	471.
R-717-024A60	88.06	176.2	175.0	0.0748	87.42	22.23	35.0	28.2	90900.	77.43	78.16	0.60	10.27	10906.	10459.	4.1	1015.
R-717-025A60	89.21	179.7	178.3	0.0752	88.55	22.32	23.0	18.5	59917.	77.54	78.54	0.91	11.17	10920.	10430.	4.5	933.
R-717-026A60	93.05	190.7	189.8	0.0750	92.01	22.17	9.8	7.9	25944.	77.80	80.02	2.17	14.14	10757.	10654.	1.0	727.
R-717-027A60	94.93	197.2	195.6	0.0749	93.86	22.08	7.6	6.2	20264.	77.95	80.77	2.78	15.57	10670.	10625.	0.4	654.
R-717-028A60	98.01	207.2	205.4	0.0759	96.85	22.27	5.4	4.4	14484.	77.95	81.89	3.89	18.09	10689.	10541.	1.4	564.
R-717-029A60	101.54	217.7	217.0	0.0752	99.95	21.96	3.9	3.2	10607.	77.79	83.13	5.30	21.08	10455.	10450.	0.0	474.
R-717-030A60	86.65	172.2	171.0	0.0420	85.89	12.52	35.0	28.2	95345.	81.39	81.85	0.34	5.02	6162.	5867.	4.8	1171.
R-717-031A60	87.42	174.7	173.2	0.0420	86.61	12.52	23.0	18.5	62863.	81.60	82.18	0.50	5.53	6147.	5703.	7.2	1061.
R-717-032A60	89.39	179.7	178.8	0.0417	88.29	12.39	9.8	7.9	26999.	81.51	82.74	1.20	7.26	6060.	5877.	3.0	797.
R-717-033A60	90.43	183.2	181.9	0.0424	89.36	12.57	7.5	6.0	20607.	81.51	83.13	1.59	8.10	6133.	5942.	3.1	723.
R-717-034A60	92.01	188.7	186.6	0.0422	90.84	12.49	5.4	4.4	15041.	81.57	83.79	2.19	9.33	6074.	5968.	1.7	622.
R-717-035A60	94.54	196.7	194.3	0.0418	93.10	12.34	3.8	3.1	10700.	81.72	84.80	3.06	11.28	5969.	5870.	1.7	505.
R-717-036A60	88.68	177.7	176.8	0.0337	87.48	10.02	35.0	28.2	99134.	84.63	85.02	0.27	3.85	4909.	4680.	4.7	1217.
R-717-037A60	89.32	179.7	178.7	0.0338	88.05	10.05	23.0	18.5	65356.	84.86	85.34	0.39	4.22	4917.	4532.	7.8	1112.
R-717-038A60	90.72	184.2	182.8	0.0337	89.18	9.99	9.8	7.9	28021.	84.69	85.70	0.97	5.53	4875.	4772.	2.1	843.
R-717-039A60	91.94	187.7	186.4	0.0336	90.36	9.95	7.4	6.0	21305.	84.97	86.29	1.28	6.31	4840.	4772.	1.4	733.
R-717-040A60	93.26	191.7	190.4	0.0333	91.74	9.85	5.4	4.4	15641.	85.03	86.82	1.77	7.33	4778.	4821.	-0.9	623.
R-717-041A60	95.21	198.2	196.4	0.0336	93.55	9.90	3.9	3.1	11236.	85.14	87.63	2.47	8.82	4782.	4794.	-0.3	518.
R-717-042A60	87.50	174.7	173.4	0.0535	86.97	15.91	35.0	28.2	94531.	80.65	81.20	0.42	6.57	7815.	7334.	6.2	1136.
R-717-043A60	89.20	179.7	178.3	0.0536	88.38	15.93	23.0	18.5	63011.	81.73	82.43	0.62	7.11	7795.	7091.	9.0	1047.
R-717-044A60	90.95	184.7	183.4	0.0539	90.15	15.96	9.8	7.9	26822.	80.81	82.37	1.52	9.36	7781.	7479.	3.9	794.
R-717-045A60	92.08	188.2	186.8	0.0536	91.10	15.86	7.6	6.1	20801.	80.80	82.78	1.95	10.29	7711.	7413.	3.9	716.
R-717-046A60	93.96	194.2	192.5	0.0533	92.78	15.72	5.4	4.4	14786.	80.67	83.41	2.72	11.92	7614.	7320.	3.9	610.
R-717-047A60	96.55	202.2	200.7	0.0534	95.08	15.70	3.9	3.1	10741.	80.65	84.38	3.70	14.03	7562.	7195.	4.9	515.

Table D.5. Experimental data for ammonia condensing on Tube E (vertical)

Run No.	T_v (°F)	P (psia)	P_{sat} (psia)	F_c (gpm)	T_c (°F)	m_c (lb_m/h)	F_w (gpm)	v (ft/s)	Re	$T_{w,in}$ (°F)	$T_{w,out}$ (°F)	ΔT_w (°F)	$\overline{\Delta T}$ (°F)	Q_c (Btu/h)	Q_w (Btu/h)	Δ (%)	U (Btu/h·ft²·°F)
R-717-009E	75.72	143.2	142.3	0.0746	75.58	22.57	33.4	26.9	79349.	70.44	71.22	0.69	4.88	11351.	11599.	-2.2	1448.
R-717-010E	77.63	148.2	147.0	0.0754	77.38	22.75	18.5	14.9	44154.	70.54	71.82	1.24	6.45	11402.	11491.	-0.8	1101.
R-717-011E	79.36	152.7	151.4	0.0755	79.04	22.71	12.6	10.2	30146.	70.44	72.28	1.84	8.00	11343.	11591.	-2.2	884.
R-717-012E	80.87	156.7	155.3	0.0760	80.42	22.83	9.8	7.9	23611.	70.33	72.67	2.33	9.37	11368.	11493.	-1.1	756.
R-717-013E	82.78	161.7	160.4	0.0762	82.22	22.83	7.7	6.2	18516.	70.25	73.23	2.98	11.04	11322.	11454.	-1.2	639.
R-717-014E	86.50	171.7	170.6	0.0772	85.62	23.02	5.4	4.4	13185.	70.23	74.41	4.18	14.18	11327.	11363.	-0.3	498.
R-717-015E	89.53	181.2	179.3	0.0772	88.32	22.93	4.4	3.6	10846.	70.31	75.45	5.14	16.65	11210.	11420.	-1.9	419.
R-717-016E	91.51	186.7	185.1	0.0778	90.12	23.04	3.9	3.2	9611.	70.24	76.03	5.79	18.37	11218.	11356.	-1.2	380.
R-717-017E	80.51	155.2	154.4	0.1137	79.55	34.21	33.4	26.9	81571.	72.47	73.59	1.03	7.48	17042.	17196.	-0.9	1420.
R-717-018E	85.64	168.7	168.2	0.1171	84.48	34.97	17.7	14.3	44561.	74.35	76.38	2.00	10.28	17240.	17643.	-2.3	1045.
R-717-019E	87.27	173.2	172.8	0.1181	86.02	35.19	12.6	10.2	31446.	73.26	76.12	2.85	12.58	17288.	17896.	-3.5	856.
R-717-020E	89.28	178.2	178.5	0.1131	87.58	33.64	9.8	7.9	24561.	72.85	76.40	3.55	14.66	16456.	17430.	-5.9	699.
R-717-021E	91.82	185.7	186.1	0.1182	89.96	35.01	7.8	6.3	19517.	72.67	77.11	4.43	16.93	17037.	17254.	-1.3	627.
R-717-022E	96.92	201.7	201.9	0.1183	94.74	34.81	5.4	4.4	13759.	72.46	78.70	6.22	21.34	16747.	16926.	-1.1	489.
R-717-023E	100.61	214.2	213.9	0.1201	98.17	35.15	4.6	3.7	11707.	72.46	79.95	7.49	24.41	16773.	17184.	-2.5	428.
R-717-024E	103.58	224.7	224.0	0.1193	100.94	34.77	3.9	3.2	10067.	72.43	80.99	8.56	26.87	16478.	16789.	-1.9	382.
R-717-025E	77.32	147.2	146.2	0.0935	76.73	28.23	33.4	26.9	79854.	70.85	71.77	0.83	6.01	14156.	13819.	2.4	1467.
R-717-026E	81.30	157.2	156.4	0.0963	80.37	28.92	17.7	14.3	43134.	72.02	73.71	1.66	8.43	14385.	14658.	-1.9	1063.
R-717-027E	83.02	161.7	161.0	0.0971	82.01	29.09	12.6	10.2	30616.	71.45	73.84	2.39	10.37	14422.	15005.	-4.0	866.
R-717-028E	85.04	167.2	166.5	0.0986	83.90	29.47	9.8	7.9	24059.	71.55	74.53	2.97	12.00	14549.	14605.	-0.4	755.
R-717-029E	87.44	174.2	173.2	0.0991	86.13	29.52	7.7	6.2	18897.	71.51	75.30	3.78	14.03	14496.	14521.	-0.2	644.
R-717-030E	91.57	186.2	185.3	0.0996	89.88	29.53	5.4	4.4	13416.	70.99	76.28	5.28	17.94	14375.	14370.	0.0	499.
R-717-031E	97.57	204.7	203.9	0.1008	95.25	29.63	3.9	3.2	9777.	70.80	78.09	7.30	23.12	14234.	14307.	-0.5	384.
R-717-032E	73.41	137.7	136.7	0.0547	73.22	16.61	33.4	26.9	78511.	69.74	70.34	0.51	3.37	8394.	8529.	-1.6	1553.
R-717-033E	75.00	141.7	140.5	0.0532	74.70	16.10	17.7	14.3	41849.	69.99	70.95	0.93	4.53	8109.	8225.	-1.4	1116.
R-717-034E	76.24	144.7	143.5	0.0536	75.86	16.20	12.6	10.2	29842.	69.93	71.28	1.35	5.64	8138.	8475.	-4.1	899.
R-717-035E	77.27	147.2	146.1	0.0534	76.79	16.12	9.8	7.9	23361.	69.88	71.53	1.65	6.57	8083.	8121.	-0.5	767.
R-717-036E	81.05	156.7	155.8	0.0530	80.03	15.92	5.4	4.4	13018.	69.78	72.69	2.90	9.82	7925.	7898.	0.3	503.
R-717-037E	83.07	162.2	161.1	0.0534	81.82	16.01	4.4	3.6	10646.	69.55	73.16	3.61	11.72	7936.	8027.	-1.1	422.
R-717-038E	84.49	166.7	165.0	0.0535	83.22	16.00	3.9	3.2	9436.	69.60	73.65	4.04	12.87	7909.	7942.	-0.4	383.
R-717-039E	73.42	138.2	136.7	0.0460	73.45	13.97	33.4	26.9	79050.	70.29	70.81	0.43	2.87	7057.	7177.	-1.7	1533.
R-717-040E	74.61	141.2	139.6	0.0463	74.49	14.02	17.7	14.3	41588.	70.31	71.13	0.80	3.89	7065.	7049.	0.2	1131.
R-717-041E	75.81	143.7	142.5	0.0463	75.55	14.00	12.6	10.2	29993.	70.41	71.55	1.14	4.83	7038.	7171.	-1.9	908.
R-717-042E	76.75	146.2	144.8	0.0463	76.52	13.98	10.0	8.1	23860.	70.43	71.88	1.45	5.59	7016.	7231.	-3.1	781.
R-717-043E	78.78	150.7	149.9	0.0461	78.37	13.88	6.5	5.2	15569.	70.26	72.40	2.13	7.45	6941.	6916.	0.4	580.
R-717-044E	80.39	154.7	154.0	0.0465	79.80	13.98	5.4	4.4	13114.	70.51	73.07	2.56	8.60	6967.	6983.	-0.2	505.
R-717-045E	83.80	164.2	163.1	0.0467	82.67	13.98	3.8	3.1	9183.	70.39	74.08	3.69	11.56	6918.	7001.	-1.2	373.
R-717-046E	73.29	137.2	136.4	0.0377	73.34	11.44	33.4	26.9	79475.	70.73	71.17	0.36	2.34	5783.	5942.	-2.7	1540.
R-717-047E	76.14	144.2	143.3	0.0382	76.00	11.56	9.8	7.9	23595.	70.86	72.04	1.16	4.69	5808.	5710.	1.7	772.
R-717-048E	78.24	149.2	148.5	0.0383	78.04	11.55	6.5	5.2	15677.	71.05	72.88	1.83	6.27	5780.	5944.	-2.8	574.
R-717-049E	81.74	158.7	157.6	0.0384	80.99	11.53	3.9	3.2	9527.	71.00	73.94	2.94	9.27	5731.	5762.	-0.5	385.
R-717-050E	79.71	153.7	152.3	0.0386	79.61	11.62	5.3	4.3	12834.	71.29	73.49	2.20	7.32	5800.	5812.	-0.2	494.
R-717-051E	77.16	147.2	145.8	0.0311	77.16	9.40	33.4	26.9	84175.	75.27	75.62	0.28	1.71	4713.	4732.	-0.4	1716.
R-717-052E	78.39	150.2	148.9	0.0312	78.14	9.40	17.7	14.3	44885.	75.64	76.21	0.57	2.47	4703.	5033.	-7.0	1188.
R-717-053E	78.96	151.7	150.4	0.0310	78.68	9.32	9.5	7.7	24015.	74.77	75.78	1.01	3.69	4659.	4812.	-3.3	787.
R-717-054E	79.84	154.2	152.6	0.0310	79.40	9.34	7.7	6.2	19429.	74.92	76.16	1.23	4.30	4660.	4740.	-1.7	674.
R-717-055E	82.02	159.7	158.3	0.0308	81.22	9.25	5.1	4.1	12981.	75.30	77.13	1.83	5.80	4594.	4654.	-1.3	493.
R-717-056E	82.69	161.7	160.1	0.0312	81.81	9.35	4.6	3.7	11862.	75.38	77.40	2.02	6.30	4638.	4688.	-1.1	458.

Table D.5 (continued)

Run No.	T_v (°F)	P (psia)	P_{sat} (psia)	F_c (gpm)	T_c (°F)	m_c (lb_m/h)	F_w (gpm)	v (ft/s)	Re	$T_{w,in}$ (°F)	$T_{w,out}$ (°F)	ΔT_w (°F)	$\overline{\Delta T}$ (°F)	Q_c (Btu/h)	Q_w (Btu/h)	Δ (%)	U (Btu/h·ft²·°F)
R-717-057E	76.37	144.7	143.9	0.0237	75.96	7.16	33.4	26.9	83732.	74.89	75.18	0.22	1.33	3596.	3716.	-3.3	1684.
R-717-058E	76.82	145.7	145.0	0.0235	76.37	7.11	17.7	14.3	44303.	74.70	75.13	0.42	1.90	3569.	3709.	-3.9	1169.
R-717-059E	78.22	149.2	148.5	0.0231	77.63	6.97	9.5	7.7	23937.	75.04	75.82	0.77	2.79	3490.	3645.	-4.4	778.
R-717-060E	79.88	153.7	152.7	0.0231	78.94	6.95	5.4	4.4	13642.	74.95	76.31	1.35	4.25	3466.	3634.	-4.9	508.
R-717-061E	80.85	156.2	155.2	0.0233	79.78	6.99	4.7	3.8	11863.	75.29	76.83	1.54	4.79	3482.	3579.	-2.8	453.
R-717-062E	81.82	158.7	157.8	0.0232	80.60	6.97	3.9	3.2	10014.	75.39	77.21	1.82	5.52	3464.	3574.	-3.2	391.
R-717-063E	77.47	147.7	146.6	0.0380	76.76	11.47	33.4	26.9	83999.	75.07	75.50	0.36	2.19	5751.	5999.	-4.3	1636.
R-717-064E	79.87	153.7	152.7	0.0379	80.18	11.40	9.9	8.0	25080.	74.86	76.05	1.19	4.41	5689.	5917.	-4.0	803.
R-717-065E	82.24	159.7	158.9	0.0379	81.01	11.38	6.6	5.3	16756.	75.49	77.25	1.75	5.87	5649.	5749.	-1.8	599.
R-717-066E	83.26	162.7	161.7	0.0379	82.09	11.37	5.4	4.4	13923.	75.46	77.54	2.08	6.76	5635.	5661.	-0.5	519.
R-717-067E	84.27	165.7	164.4	0.0380	82.97	11.39	4.6	3.7	11877.	75.24	77.72	2.47	7.78	5629.	5737.	-1.9	451.
R-717-068E	85.64	169.2	168.2	0.0382	84.03	11.42	3.9	3.2	10079.	75.36	78.25	2.89	8.84	5632.	5664.	-0.6	397.
R-717-069E	78.43	149.7	149.0	0.0670	77.91	20.19	33.4	26.9	82834.	73.85	74.56	0.64	4.22	10104.	10681.	-5.7	1490.
R-717-070E	81.54	158.2	157.1	0.0667	80.70	20.02	12.6	10.2	31435.	73.83	75.50	1.66	6.88	9953.	10454.	-5.0	901.
R-717-071E	83.75	163.7	163.0	0.0669	82.66	20.03	10.0	8.1	25361.	74.92	76.94	2.02	7.82	9915.	10078.	-1.6	790.
R-717-072E	87.92	175.7	174.6	0.0670	86.36	19.96	5.4	4.4	13842.	74.24	77.85	3.61	11.87	9792.	9818.	-0.3	514.
R-717-073E	90.15	182.2	181.1	0.0672	88.26	19.97	4.6	3.7	11895.	74.47	78.73	4.26	13.55	9750.	9887.	-1.4	448.
R-717-074E	92.34	188.7	187.6	0.0677	90.22	20.04	3.9	3.2	10073.	74.26	79.25	4.99	15.59	9741.	9776.	-0.4	389.
R-717-075E	82.29	159.7	159.1	0.0885	81.26	26.55	33.4	26.9	85674.	76.37	77.27	0.83	5.48	13180.	13897.	-5.4	1500.
R-717-076E	86.40	170.7	170.3	0.0877	84.97	26.17	12.6	10.2	32562.	76.34	78.47	2.11	8.99	12881.	13295.	-3.2	892.
R-717-077E	87.88	175.2	174.5	0.0879	86.24	26.19	10.0	8.1	25904.	76.29	78.89	2.60	10.29	12851.	12986.	-1.1	778.
R-717-078E	91.77	186.7	185.9	0.0891	89.89	26.40	6.4	5.2	16668.	75.86	79.92	4.05	13.88	12845.	12968.	-1.0	577.
R-717-079E	93.61	191.7	191.5	0.0894	91.56	26.44	5.4	4.4	14148.	75.37	80.15	4.78	15.85	12815.	12991.	-1.4	504.
R-717-080E	95.85	198.7	198.4	0.0894	93.64	26.35	4.6	3.7	11985.	75.24	80.85	5.60	17.80	12706.	12861.	-1.2	445.
R-717-081E	98.65	207.7	207.4	0.0897	96.10	26.35	3.9	3.1	10122.	75.05	81.65	6.60	20.29	12631.	12743.	-0.9	388.
R-717-082E	78.81	150.2	150.0	0.0668	77.79	20.13	33.4	26.9	83517.	74.50	75.17	0.60	3.97	10062.	9964.	1.0	1580.
R-717-083E	82.48	160.2	159.6	0.0672	81.34	20.17	12.6	10.2	31853.	74.86	76.51	1.65	6.80	10007.	10372.	-3.6	918.
R-717-084E	83.84	163.7	163.2	0.0673	82.56	20.16	9.8	7.9	25027.	75.07	77.08	2.01	7.76	9975.	9897.	0.8	801.
R-717-085E	88.40	176.7	176.0	0.0676	86.65	20.12	5.5	4.4	14147.	74.98	78.53	3.55	11.64	9863.	9765.	1.0	528.
R-717-086E	92.09	187.2	186.9	0.0679	89.90	20.11	4.0	3.2	10299.	74.70	79.52	4.82	14.98	9779.	9623.	1.6	407.
R-717-087E	83.38	161.2	162.0	0.1002	82.14	30.03	33.4	26.9	85465.	76.14	77.12	0.91	6.76	14873.	15163.	-2.0	1371.
R-717-088E	88.38	175.2	175.9	0.1015	86.83	30.21	12.6	10.2	32594.	76.24	78.72	2.47	10.90	14807.	15558.	-5.1	846.
R-717-089E	90.09	180.2	180.9	0.1015	88.47	30.14	10.0	8.1	25972.	76.29	79.31	3.02	12.29	14717.	15077.	-2.4	746.
R-717-090E	94.94	195.2	195.6	0.1023	93.10	30.18	6.5	5.2	17127.	76.64	81.24	4.59	16.00	14587.	14888.	-2.1	568.
R-717-091E	97.70	203.7	204.3	0.1032	95.80	30.31	5.4	4.4	14338.	76.82	82.29	5.47	18.15	14560.	14731.	-1.2	500.
R-717-092E	100.10	213.2	212.2	0.1036	98.05	30.34	4.7	3.8	12632.	77.07	83.30	6.22	19.92	14495.	14654.	-1.1	453.
R-717-093E	103.49	223.7	223.7	0.1043	101.25	30.39	3.9	3.2	10606.	77.17	84.56	7.39	22.63	14406.	14491.	-0.6	397.
R-717-094E	79.61	152.7	152.0	0.0624	79.79	18.76	33.4	26.9	84706.	75.60	76.26	0.58	3.67	9363.	9748.	-4.1	1588.
R-717-095E	82.86	161.2	160.6	0.0623	82.70	18.67	12.6	10.2	32253.	75.91	77.40	1.49	6.20	9257.	9341.	-0.9	930.
R-717-096E	84.38	165.7	164.7	0.0623	84.15	18.63	9.8	7.9	25399.	76.29	78.18	1.89	7.15	9209.	9273.	-0.7	803.
R-717-097E	88.69	178.2	176.8	0.0626	88.09	18.59	5.4	4.4	14037.	76.18	79.55	3.36	10.82	9108.	9055.	0.6	524.
R-717-098E	90.79	184.2	183.0	0.0626	89.98	18.54	4.7	3.8	12221.	76.63	80.50	3.87	12.22	9043.	8997.	0.5	461.
R-717-099E	92.91	190.7	189.3	0.0626	91.84	18.49	3.9	3.2	10375.	76.82	81.37	4.55	13.81	8977.	8923.	0.6	405.

Table D.5 (continued)

Run No.	T_v (°F)	P (psia)	P_{sat} (psia)	F_c (gpm)	T_c (°F)	m_c (lb_m/h)	F_w (gpm)	v (ft/s)	Re	$T_{w,in}$ (°F)	$T_{w,out}$ (°F)	ΔT_w (°F)	$\overline{\Delta T}$ (°F)	Q_c (Btu/h)	Q_w (Btu/h)	Δ (%)	U (Btu/h·ft²·°F)
R-717-100E	84.94	164.7	166.2	0.1037	83.87	31.00	33.4	26.9	86634.	77.19	78.20	0.94	7.25	15305.	15647.	-2.2	1316.
R-717-101E	89.82	179.2	180.1	0.1044	88.56	30.99	12.6	10.2	33004.	77.19	79.75	2.55	11.35	15144.	16029.	-5.8	831.
R-717-102E	91.79	185.2	186.0	0.1054	90.44	31.22	10.0	8.1	26347.	77.37	80.50	3.13	12.85	15192.	15635.	-2.9	736.
R-717-103E	93.84	191.7	192.2	0.1060	92.51	31.29	7.7	6.2	20308.	76.70	80.71	4.00	15.14	15157.	15441.	-1.9	624.
R-717-104E	98.40	207.2	206.6	0.1063	96.85	31.19	5.4	4.4	14445.	76.58	82.23	5.65	18.99	14957.	15351.	-2.6	491.
R-717-105E	100.69	214.2	214.2	0.1067	99.05	31.19	4.6	3.7	12389.	76.57	83.08	6.50	20.87	14881.	15086.	-1.4	444.
R-717-106E	104.69	227.2	227.8	0.1089	102.87	31.66	3.9	3.2	10598.	76.91	84.68	7.77	23.89	14966.	15244.	-1.9	390.

Table D.6. Experimental data for ammonia condensing on Tube H (vertical)

Run No.	T_v (°F)	P (psia)	P_{sat} (psia)	F_c (gpm)	T_c (°F)	m_c (lb_m/h)	F_w (gpm)	v (ft/s)	Re	$T_{w,in}$ (°F)	$T_{w,out}$ (°F)	ΔT_w (°F)	$\overline{\Delta T}$ (°F)	Q_c (Btu/h)	Q_w (Btu/h)	Δ (%)	U (Btu/h·ft²·°F)
R-717-001H	85.71	169.2	168.4	0.0387	85.24	11.54	34.0	23.7	91994.	83.50	83.90	0.33	2.01	5688.	5615.	1.3	1607.
R-717-002H	87.05	172.7	172.1	0.0387	86.41	11.53	17.1	11.9	46622.	83.99	84.68	0.69	2.71	5669.	5921.	-4.4	1188.
R-717-003H	88.01	175.2	174.9	0.0390	87.23	11.60	9.8	6.9	26888.	83.85	85.02	1.18	3.58	5692.	5818.	-2.2	904.
R-717-004H	89.52	179.7	179.2	0.0388	88.49	11.53	5.5	3.9	15196.	83.81	85.87	2.08	4.68	5636.	5763.	-2.2	684.
R-717-005H	90.12	181.7	181.0	0.0389	89.00	11.53	4.7	3.3	12864.	83.79	86.24	2.48	5.11	5631.	5797.	-2.9	626.
R-717-006H	90.64	183.2	182.5	0.0388	89.29	11.51	4.0	2.8	10948.	83.65	86.50	2.88	5.56	5616.	5728.	-2.0	574.
R-717-007H	86.75	171.7	171.3	0.0773	86.29	23.02	34.0	23.7	90626.	82.09	82.85	0.69	4.28	11323.	11721.	-3.5	1503.
R-717-008H	88.32	176.7	175.7	0.0776	87.92	23.06	17.4	12.1	46480.	81.97	83.33	1.34	5.67	11305.	11676.	-3.3	1133.
R-717-009H	90.83	184.2	183.1	0.0777	90.12	23.03	10.0	7.0	27002.	82.38	84.68	2.30	7.30	11228.	11499.	-2.4	874.
R-717-010H	94.80	196.7	195.1	0.0790	93.90	23.27	5.5	3.8	15230.	83.10	87.26	4.20	9.62	11249.	11590.	-3.0	664.
R-717-011H	96.05	199.7	199.1	0.0791	95.04	23.26	4.7	3.3	12958.	83.18	88.06	4.92	10.43	11211.	11492.	-2.5	611.
R-717-012H	97.05	203.7	202.3	0.0789	96.02	23.17	4.0	2.8	11041.	82.95	88.61	5.69	11.28	11144.	11290.	-1.3	562.
R-717-013H	89.09	179.2	178.0	0.1255	88.85	37.26	33.3	23.2	88103.	81.28	82.45	1.10	7.23	18237.	18258.	-0.1	1433.
R-717-014H	90.93	184.7	183.4	0.1253	90.49	37.11	17.7	12.3	46722.	80.63	82.73	2.10	9.25	18090.	18535.	-2.5	1111.
R-717-015H	94.88	196.7	195.4	0.1271	94.22	37.42	9.8	6.9	26372.	80.96	84.71	3.76	12.05	18085.	18482.	-2.2	853.
R-717-016H	100.59	213.7	213.8	0.1290	99.60	37.67	5.5	3.9	15261.	81.74	88.35	6.65	15.55	17974.	18421.	-2.5	657.
R-717-017H	102.82	221.7	221.4	0.1311	101.61	38.17	4.7	3.3	13012.	82.07	89.87	7.84	16.85	18119.	18314.	-1.1	611.
R-717-018H	86.87	172.2	171.6	0.0312	85.46	9.32	34.0	23.7	93796.	85.15	85.48	0.26	1.55	4581.	4461.	2.6	1675.
R-717-019H	88.18	175.7	175.4	0.0313	86.67	9.31	17.7	12.3	49168.	85.75	86.31	0.55	2.15	4567.	4840.	-6.0	1207.
R-717-020H	89.14	178.2	178.1	0.0311	87.55	9.26	9.9	6.9	27725.	85.82	86.75	0.93	2.85	4531.	4614.	-1.8	902.
R-717-021H	90.15	181.2	181.1	0.0311	88.44	9.24	5.5	3.9	15496.	85.64	87.29	1.69	3.69	4510.	4672.	-3.6	694.
R-717-022H	90.70	183.2	182.7	0.0310	89.14	9.20	4.7	3.3	13106.	85.75	87.66	1.95	4.00	4486.	4550.	-1.4	638.
R-717-023H	91.34	185.2	184.6	0.0307	89.74	9.11	3.9	2.7	10952.	85.81	88.07	2.28	4.40	4437.	4439.	-0.0	573.
R-717-024H	88.10	175.2	175.1	0.0570	87.24	16.96	34.0	23.7	93518.	84.78	85.35	0.50	3.04	8319.	8532.	-2.6	1556.
R-717-025H	89.39	179.2	178.9	0.0577	88.37	17.14	18.4	12.8	50810.	84.92	85.87	0.94	4.00	8381.	8638.	-3.1	1192.
R-717-026H	91.86	186.7	186.1	0.0578	90.60	17.12	9.8	6.9	27520.	85.67	87.36	1.70	5.34	8330.	8350.	-0.2	886.
R-717-027H	93.94	193.2	192.5	0.0579	92.53	17.10	5.4	3.8	15306.	85.42	88.49	3.11	6.99	8282.	8437.	-1.9	673.
R-717-028H	94.81	196.2	195.2	0.0580	93.37	17.09	4.7	3.3	13255.	85.54	89.08	3.58	7.51	8262.	8390.	-1.6	625.
R-717-029H	95.90	199.2	198.6	0.0585	94.33	17.23	3.9	2.7	11127.	85.54	89.74	4.23	8.26	8307.	8272.	0.4	571.
R-717-030H	87.75	174.2	174.1	0.0676	87.03	20.12	34.0	23.7	92364.	83.71	84.36	0.58	3.72	9876.	9906.	-0.3	1509.
R-717-031H	89.25	178.7	178.4	0.0682	88.37	20.26	17.7	12.3	48284.	83.81	84.95	1.14	4.87	9912.	10067.	-1.6	1156.
R-717-032H	91.61	186.2	185.4	0.0687	90.61	20.33	9.9	6.9	27310.	84.22	86.24	2.02	6.38	9894.	9982.	-0.9	881.
R-717-033H	94.62	195.2	194.6	0.0686	93.40	20.23	5.4	3.8	15187.	84.49	88.10	3.66	8.32	9783.	9930.	-1.5	668.
R-717-034H	95.32	197.7	196.8	0.0686	94.13	20.21	4.7	3.3	13077.	84.25	88.44	4.23	8.97	9758.	9891.	-1.4	618.
R-717-035H	96.55	201.2	200.7	0.0689	95.20	20.27	3.9	2.7	11005.	84.22	89.19	4.99	9.84	9760.	9764.	-0.0	563.
R-717-036H	86.38	170.7	170.2	0.0470	85.72	14.00	34.0	23.7	92140.	83.60	84.07	0.40	2.55	6891.	6802.	1.3	1536.
R-717-037H	87.48	173.7	173.4	0.0472	86.75	14.06	18.5	12.9	50329.	83.76	84.54	0.77	3.33	6904.	7125.	-3.2	1179.
R-717-038H	89.45	179.2	179.0	0.0475	88.61	14.10	9.8	6.9	27069.	84.29	85.70	1.41	4.46	6896.	6939.	-0.6	878.
R-717-039H	91.21	185.2	184.2	0.0474	90.30	14.03	5.4	3.8	14910.	84.11	86.66	2.59	5.82	6835.	6983.	-2.2	667.
R-717-040H	91.69	186.2	185.7	0.0472	90.77	13.98	4.7	3.3	12934.	84.00	86.93	2.97	6.23	6803.	6932.	-1.9	621.
R-717-041H	92.85	190.2	189.2	0.0478	91.82	14.13	3.9	2.7	10927.	84.24	87.71	3.49	6.88	6860.	6851.	0.1	566.
R-717-042H	86.02	169.2	169.2	0.0899	85.78	26.79	34.0	23.7	88836.	80.42	81.28	0.79	5.17	13197.	13349.	-1.2	1451.
R-717-043H	87.89	174.7	174.5	0.0905	87.48	26.91	17.7	12.3	46420.	80.37	81.93	1.55	6.74	13205.	13714.	-3.9	1113.
R-717-044H	90.85	183.7	183.1	0.0912	90.26	27.03	9.8	6.9	26123.	80.70	83.42	2.72	8.79	13178.	13386.	-1.6	852.
R-717-045H	94.85	196.2	195.3	0.0918	93.97	27.04	5.4	3.8	14707.	81.05	85.91	4.91	11.37	13069.	13339.	-2.1	653.
R-717-046H	95.96	199.2	198.8	0.0922	94.97	27.13	4.7	3.3	12664.	80.88	86.54	5.70	12.24	13082.	13313.	-1.8	607.
R-717-047H	97.17	203.2	202.6	0.0917	96.11	26.93	3.9	2.7	10651.	80.51	87.17	6.68	13.33	12948.	13091.	-1.1	552.

Table D.6 (continued)

Run No.	T_v (°F)	P (psia)	P_{sat} (psia)	F_c (gpm)	T_c (°F)	m_c (lb_m/h)	F_w (gpm)	v (ft/s)	Re	$T_{w,in}$ (°F)	$T_{w,out}$ (°F)	ΔT_w (°F)	$\overline{\Delta T}$ (°F)	Q_c (Btu/h)	Q_w (Btu/h)	Δ (%)	U (Btu/h·ft²·°F)
R-717-048H	84.73	165.7	165.7	0.0239	83.85	7.13	34.0	23.7	91583.	83.19	83.48	0.22	1.40	3523.	3681.	-4.5	1433.
R-717-049H	85.37	168.2	167.4	0.0240	84.52	7.18	17.7	12.3	47879.	83.46	83.90	0.43	1.69	3542.	3824.	-8.0	1194.
R-717-050H	86.43	171.2	170.4	0.0238	85.53	7.10	9.8	6.9	26819.	83.86	84.59	0.73	2.20	3495.	3587.	-2.6	901.
R-717-051H	87.15	173.2	172.4	0.0235	86.09	7.01	5.4	3.8	14836.	83.56	84.85	1.33	2.95	3447.	3630.	-5.3	665.
R-717-052H	87.42	173.7	173.2	0.0231	86.31	6.89	4.6	3.2	12526.	83.46	85.00	1.57	3.19	3382.	3610.	-6.7	602.
R-717-053H	87.85	175.2	174.4	0.0236	86.80	7.02	3.9	2.7	10717.	83.46	85.24	1.79	3.50	3445.	3519.	-2.2	560.
R-717-054H	86.50	171.2	170.6	0.1017	86.16	30.30	34.0	23.7	88549.	80.11	81.07	0.90	5.91	14909.	15198.	-1.9	1433.
R-717-055H	88.46	176.7	176.1	0.1019	87.96	30.29	17.7	12.3	46273.	80.03	81.76	1.72	7.56	14843.	15224.	-2.6	1115.
R-717-056H	91.82	187.2	186.1	0.1030	91.22	30.46	9.8	6.9	26075.	80.37	83.45	3.08	9.91	14821.	15160.	-2.3	849.
R-717-057H	96.10	200.2	199.2	0.1032	95.23	30.33	5.4	3.8	14690.	80.66	86.12	5.49	12.71	14621.	14941.	-2.2	653.
R-717-058H	97.76	205.2	204.5	0.1040	96.71	30.50	4.7	3.3	12742.	80.89	87.20	6.34	13.71	14648.	14841.	-1.3	607.
R-717-059H	99.90	212.7	211.5	0.1047	98.77	30.63	3.9	2.7	10789.	81.16	88.66	7.51	14.99	14639.	14734.	-0.7	555.
R-717-060H	84.43	166.2	164.8	0.0288	83.68	8.61	34.0	23.7	91176.	82.81	83.12	0.24	1.47	4254.	4088.	3.9	1647.
R-717-061H	85.11	167.7	166.7	0.0288	84.06	8.61	17.7	12.3	47582.	82.92	83.42	0.49	1.94	4251.	4362.	-2.6	1244.
R-717-062H	85.90	169.7	168.9	0.0281	84.91	8.40	9.8	6.9	26522.	82.87	83.74	0.88	2.60	4139.	4305.	-4.0	904.
R-717-063H	87.56	174.2	173.6	0.0287	86.22	8.56	5.5	3.8	15002.	83.30	84.84	1.58	3.49	4203.	4354.	-3.6	685.
R-717-064H	88.09	176.2	175.1	0.0286	86.85	8.53	4.7	3.3	12792.	83.46	85.27	1.84	3.72	4182.	4315.	-3.2	638.
R-717-065H	88.72	178.2	176.9	0.0286	87.32	8.51	3.9	2.7	10750.	83.54	85.67	2.14	4.11	4166.	4204.	-0.9	576.
R-717-066H	86.90	172.7	171.7	0.1064	86.50	31.68	34.0	23.7	88703.	80.23	81.22	0.92	6.17	15578.	15690.	-0.7	1434.
R-717-067H	88.61	177.2	176.6	0.1071	88.07	31.82	18.0	12.5	46935.	79.79	81.58	1.78	7.93	15591.	15958.	-2.4	1117.
R-717-068H	92.62	189.7	188.4	0.1076	91.85	31.80	9.8	6.9	26194.	80.68	83.89	3.22	10.33	15444.	15809.	-2.4	849.
R-717-069H	97.17	203.7	202.6	0.1080	96.19	31.71	5.4	3.8	14788.	81.10	86.78	5.72	13.23	15248.	15553.	-2.0	655.
R-717-070H	98.59	208.7	207.2	0.1088	98.55	31.82	4.7	3.3	12848.	81.10	87.65	6.59	14.22	15252.	15483.	-1.5	610.
R-717-071H	101.17	216.7	215.8	0.1090	100.00	31.83	3.9	2.7	10865.	81.57	89.43	7.88	15.67	15167.	15448.	-1.9	550.

Table D.7. Experimental data for ammonia condensing on Tube H (vertical, no rod on water side)

Run No.	T_v (°F)	P (psia)	P_{sat} (psia)	F_c (gpm)	T_c (°F)	m_c (lb_m/h)	F_w (gpm)	v (ft/s)	Re	$T_{w,in}$ (°F)	$T_{w,out}$ (°F)	ΔT_w (°F)	$\overline{\Delta T}$ (°F)	Q_c (Btu/h)	Q_w (Btu/h)	Δ (%)	U (Btu/h·ft²·°F)
R-717-001HW	83.75	164.7	163.0	0.0493	82.91	14.76	33.3	16.2	134382.	80.52	80.99	0.44	3.00	7304.	7277.	0.4	1385.
R-717-002HW	84.10	164.7	163.9	0.0491	83.13	14.68	17.7	8.6	70897.	79.73	80.58	0.79	3.95	7262.	6950.	4.3	1046.
R-717-003HW	84.39	165.7	164.7	0.0495	83.42	14.80	13.3	6.5	53083.	79.30	80.44	1.10	4.52	7318.	7305.	0.2	919.
R-717-004HW	85.77	169.2	168.5	0.0491	84.58	14.67	8.3	4.1	33426.	79.43	81.17	1.71	5.47	7229.	7111.	1.6	751.
R-717-005HW	88.27	176.7	175.6	0.0492	86.68	14.65	4.9	2.4	19967.	79.42	82.35	2.91	7.39	7184.	7162.	0.3	553.
R-717-006HW	88.84	178.2	177.3	0.0497	87.20	14.78	4.6	2.3	18840.	79.49	82.66	3.14	7.77	7238.	7282.	-0.6	529.
R-717-007HW	87.00	173.7	172.0	0.1173	86.32	34.96	33.3	16.2	131663.	78.57	79.66	1.05	7.89	17184.	17477.	-1.7	1238.
R-717-008HW	89.68	180.7	179.7	0.1181	89.07	35.04	17.7	8.6	70312.	78.48	80.50	1.98	10.19	17127.	17511.	-2.2	955.
R-717-009HW	91.74	186.7	185.8	0.1178	90.80	34.87	13.3	6.5	53433.	79.05	81.75	2.67	11.34	16968.	17696.	-4.3	850.
R-717-010HW	95.05	196.7	195.9	0.1176	93.90	34.65	8.3	4.0	33613.	79.22	83.45	4.20	13.71	16742.	17316.	-3.4	694.
R-717-011HW	100.10	213.2	212.2	0.1184	98.71	34.64	5.1	2.5	21013.	79.04	85.86	6.79	17.65	16546.	17276.	-4.4	532.
R-717-012HW	101.77	217.7	217.8	0.1189	100.20	34.69	4.5	2.2	18815.	78.90	86.59	7.66	19.03	16510.	17379.	-5.3	493.
R-717-013HW	83.41	162.7	162.1	0.0249	82.09	7.46	34.0	16.6	139231.	81.82	82.08	0.22	1.47	3693.	3817.	-3.3	1430.
R-717-014HW	83.74	163.2	163.0	0.0252	82.30	7.54	17.7	8.6	72325.	81.54	82.00	0.42	1.97	3731.	3718.	0.4	1075.
R-717-015HW	83.95	164.7	163.5	0.0252	82.46	7.54	13.3	6.5	54302.	81.41	82.00	0.55	2.24	3729.	3623.	2.8	944.
R-717-016HW	84.87	166.7	166.0	0.0254	83.15	7.59	8.2	4.0	33441.	81.53	82.49	0.93	2.86	3747.	3786.	-1.0	744.
R-717-017HW	86.21	169.7	169.8	0.0253	84.24	7.55	5.1	2.5	21024.	81.75	83.23	1.45	3.72	3716.	3689.	0.7	568.
R-717-018HW	86.72	171.7	171.2	0.0252	84.50	7.52	4.6	2.2	19072.	81.96	83.60	1.61	3.94	3697.	3701.	-0.1	533.
R-717-019HW	85.53	169.2	167.9	0.0669	84.72	19.98	17.7	8.6	70837.	79.53	80.65	1.08	5.44	9851.	9537.	3.2	1029.
R-717-020HW	86.54	171.7	170.7	0.0668	85.72	19.91	13.3	6.5	53439.	79.67	81.15	1.43	6.14	9795.	9515.	2.9	907.
R-717-021HW	88.43	177.2	176.1	0.0668	87.47	19.86	8.3	4.1	33674.	79.72	82.08	2.33	7.53	9732.	9679.	0.5	734.
R-717-022HW	91.16	185.2	184.1	0.0665	89.81	19.72	5.1	2.5	20764.	79.58	83.37	3.76	9.69	9609.	9557.	0.5	564.
R-717-023HW	92.16	188.2	187.1	0.0666	90.65	19.72	4.6	2.3	18910.	79.60	83.86	4.23	10.43	9590.	9762.	-1.8	523.
R-717-024HW	85.43	166.2	167.6	0.0670	83.89	20.04	33.3	16.2	133485.	79.92	80.52	0.57	5.21	9886.	9469.	4.2	1078.
R-717-025HW	86.22	170.7	169.8	0.0303	84.66	9.03	33.3	16.2	140606.	84.32	84.61	0.26	1.76	4449.	4402.	1.0	1440.
R-717-026HW	86.91	172.7	171.7	0.0302	85.10	9.01	17.7	8.6	74844.	84.33	84.84	0.48	2.33	4432.	4212.	5.0	1082.
R-717-027HW	87.36	173.7	173.0	0.0303	85.54	9.04	13.3	6.5	56326.	84.38	85.05	0.65	2.65	4439.	4300.	3.1	952.
R-717-028HW	88.40	176.7	176.0	0.0306	86.42	9.12	8.3	4.1	35435.	84.54	85.63	1.05	3.31	4472.	4376.	2.1	767.
R-717-029HW	89.72	180.7	179.8	0.0304	87.57	9.05	5.1	2.5	21765.	84.47	86.24	1.73	4.37	4425.	4409.	0.3	575.
R-717-030HW	90.14	181.7	181.0	0.0306	87.99	9.09	4.6	2.3	19876.	84.51	86.46	1.91	4.65	4439.	4433.	0.1	542.
R-717-031HW	86.46	171.7	170.5	0.0839	85.76	25.00	34.0	16.6	137876.	80.78	81.52	0.71	5.31	12304.	12128.	1.4	1318.
R-717-032HW	88.17	175.2	175.3	0.0835	87.13	24.84	17.7	8.6	71930.	80.63	82.02	1.37	6.84	12181.	12080.	0.8	1012.
R-717-033HW	89.45	179.2	179.0	0.0843	88.39	25.04	13.3	6.5	54270.	80.73	82.58	1.82	7.80	12248.	12109.	1.1	892.
R-717-034HW	91.74	186.2	185.8	0.0842	90.42	24.94	8.4	4.1	34700.	80.79	83.75	2.93	9.47	12138.	12333.	-1.6	728.
R-717-035HW	95.70	198.7	198.0	0.0843	94.08	24.84	5.1	2.5	21249.	80.95	85.78	4.81	12.33	11982.	12236.	-2.1	552.
R-717-036HW	96.60	201.2	200.8	0.0846	94.81	24.89	4.6	2.3	19426.	80.96	86.21	5.22	13.02	11984.	12105.	-1.0	523.
R-717-037HW	86.05	169.7	169.3	0.0999	85.25	29.82	33.3	16.2	132295.	79.02	79.97	0.92	6.55	14688.	15267.	-3.9	1275.
R-717-038HW	88.24	175.7	175.5	0.1011	87.25	30.07	17.7	8.6	70489.	78.83	80.56	1.70	8.55	14741.	14985.	-1.7	980.
R-717-039HW	89.53	179.7	179.3	0.1011	88.59	30.01	13.3	6.5	53095.	78.73	81.04	2.27	9.65	14672.	15075.	-2.7	864.
R-717-040HW	92.51	188.7	188.1	0.1019	91.32	30.14	8.4	4.1	34131.	79.02	82.64	3.57	11.68	14641.	15054.	-2.8	712.
R-717-041HW	97.78	205.2	204.6	0.1036	96.27	30.42	5.0	2.4	20377.	79.15	85.27	6.09	15.57	14609.	15067.	-3.1	533.
R-717-042HW	98.86	208.7	208.1	0.1051	97.17	30.82	4.6	2.3	19168.	79.16	85.81	6.62	16.38	14763.	15364.	-4.1	512.
R-717-043HW	87.15	173.2	172.4	0.0676	86.34	20.13	33.3	16.2	138113.	82.68	83.30	0.59	4.16	9894.	9802.	0.9	1350.
R-717-044HW	88.58	176.7	176.5	0.0675	87.52	20.09	17.7	8.6	73553.	82.58	83.71	1.09	5.43	9841.	9669.	1.7	1029.
R-717-045HW	89.44	179.2	179.0	0.0676	88.36	20.09	13.3	6.5	55376.	82.57	84.04	1.43	6.13	9825.	9488.	3.4	910.
R-717-046HW	91.69	186.2	185.7	0.0675	90.36	20.00	8.3	4.1	35033.	82.95	85.32	2.34	7.56	9735.	9712.	0.2	732.
R-717-047HW	94.69	195.2	194.8	0.0680	93.02	20.06	5.2	2.5	21995.	83.03	86.84	3.78	9.75	9701.	9771.	-0.7	565.
R-717-048HW	95.63	198.7	197.7	0.0681	93.95	20.06	4.6	2.3	19806.	83.07	87.32	4.22	10.43	9680.	9785.	-1.1	527.

Table D.7 (continued)

Run No.	T_v (°F)	P (psia)	P_{sat} (psia)	F_c (gpm)	T_c (°F)	m_c (lb_m/h)	F_w (gpm)	v (ft/s)	Re	$T_{w,in}$ (°F)	$T_{w,out}$ (°F)	ΔT_w (°F)	$\overline{\Delta T}$ (°F)	Q_c (Btu/h)	Q_w (Btu/h)	Δ (%)	U (Btu/h·ft²·°F)
R-717-049HN	84.41	165.7	164.8	0.0176	81.90	5.28	34.0	16.6	141702.	83.30	83.48	0.15	1.02	2610.	2493.	4.5	1455.
R-717-050HN	84.94	167.2	166.2	0.0180	82.96	5.40	17.7	8.6	73885.	83.35	83.68	0.30	1.42	2667.	2631.	1.3	1064.
R-717-051HN	85.25	168.2	167.1	0.0183	83.30	5.46	13.3	6.5	55569.	83.37	83.82	0.42	1.66	2695.	2800.	-3.9	922.
R-717-052HN	85.77	169.2	168.5	0.0177	83.56	5.30	8.3	4.0	34740.	83.39	84.08	0.66	2.03	2614.	2725.	-4.2	731.
R-717-053HN	86.35	171.2	170.2	0.0182	84.02	5.43	5.1	2.5	21316.	83.07	84.18	1.08	2.73	2672.	2753.	-3.0	556.
R-717-054HN	86.50	171.7	170.6	0.0181	84.13	5.41	4.5	2.2	18662.	82.91	84.15	1.22	2.97	2664.	2712.	-1.8	509.

Table D.8. Experimental data for ammonia condensing on Tube H* (vertical)

Run No.	T_v (°F)	P (psia)	P_{sat} (psia)	F_c (gpm)	T_c (°F)	m_c (lb_m/h)	F_w (gpm)	v (ft/s)	Re	$T_{w,in}$ (°F)	$T_{w,out}$ (°F)	ΔT_w (°F)	$\overline{\Delta T}$ (°F)	Q_c (Btu/h)	Q_w (Btu/h)	Δ (%)	U (Btu/h·ft²·°F)
R-717-001H*	87.20	173.7	172.5	0.1032	86.25	30.74	35.3	24.6	92618.	80.69	81.68	0.89	6.01	15106.	15744.	-4.2	1554.
R-717-002H*	88.28	176.7	175.6	0.1034	87.29	30.75	21.0	14.6	55150.	80.51	82.01	1.44	7.01	15075.	15087.	-0.1	1329.
R-717-003H*	92.60	189.7	188.4	0.1039	91.21	30.73	9.8	6.9	26470.	81.61	84.67	3.04	9.46	14929.	14934.	-0.0	976.
R-717-004H*	94.43	195.2	194.0	0.1043	92.84	30.77	7.6	5.3	20682.	82.01	85.91	3.89	10.47	14885.	14781.	0.7	879.
R-717-005H*	96.53	201.7	200.6	0.1050	94.98	30.89	5.3	3.7	14457.	81.56	87.18	5.60	12.16	14877.	14815.	0.4	757.
R-717-006H*	99.73	212.7	211.0	0.1057	97.97	30.95	3.8	2.7	10650.	81.69	89.39	7.70	14.19	14799.	14786.	0.1	645.
R-717-007H*	77.79	148.2	147.4	0.0343	77.29	10.34	35.3	24.6	86576.	75.62	76.04	0.32	1.96	5180.	5600.	-8.1	1637.
R-717-008H*	79.06	151.2	150.6	0.0341	78.21	10.27	21.0	14.6	52128.	76.48	77.06	0.52	2.29	5133.	5469.	-6.5	1384.
R-717-009H*	79.93	154.2	152.8	0.0345	79.19	10.39	9.8	6.9	24433.	76.15	77.28	1.11	3.21	5182.	5479.	-5.7	998.
R-717-010H*	80.18	154.7	153.5	0.0343	79.45	10.33	7.6	5.3	18773.	75.88	77.31	1.41	3.58	5151.	5336.	-3.6	889.
R-717-011H*	81.28	157.2	156.4	0.0344	80.33	10.33	5.4	3.8	13600.	76.20	78.16	1.95	4.10	5139.	5302.	-3.2	775.
R-717-012H*	82.92	161.7	160.7	0.0344	81.73	10.31	3.8	2.6	9578.	76.61	79.35	2.73	4.94	5111.	5172.	-1.2	640.
R-717-013H*	82.50	160.7	159.6	0.0691	81.85	20.73	35.3	24.6	89554.	78.12	78.86	0.64	4.01	10285.	11306.	-9.9	1585.
R-717-014H*	83.12	162.2	161.3	0.0690	82.40	20.68	21.0	14.6	53212.	77.86	78.93	1.02	4.73	10250.	10655.	-3.9	1340.
R-717-015H*	86.00	170.2	169.2	0.0688	84.93	20.53	9.8	6.8	25220.	78.56	80.70	2.12	6.37	10113.	10375.	-2.6	982.
R-717-016H*	87.00	172.7	172.0	0.0688	85.89	20.50	7.6	5.3	19691.	78.61	81.32	2.69	7.04	10078.	10234.	-1.5	885.
R-717-017H*	88.15	176.2	175.3	0.0688	86.98	20.47	5.5	3.8	14242.	78.29	81.96	3.65	8.03	10038.	10013.	0.3	773.
R-717-018H*	90.80	183.7	183.0	0.0690	89.33	20.47	3.8	2.6	9964.	78.50	83.78	5.28	9.66	9980.	10006.	-0.3	639.
R-717-019H*	84.52	165.7	165.1	0.0858	83.80	25.66	35.3	24.6	90745.	79.11	79.97	0.77	4.98	12679.	13578.	-7.1	1574.
R-717-020H*	85.35	168.2	167.4	0.0860	84.55	25.67	21.0	14.6	53940.	78.83	80.13	1.24	5.87	12664.	13023.	-2.8	1334.
R-717-021H*	88.76	177.7	177.0	0.0866	87.76	25.75	9.8	6.9	25716.	79.48	82.09	2.59	7.97	12614.	12732.	-0.9	978.
R-717-022H*	89.73	180.7	179.9	0.0865	88.71	25.67	7.5	5.3	19746.	79.24	82.61	3.35	8.81	12544.	12607.	-0.5	881.
R-717-023H*	91.63	186.7	185.5	0.0857	90.44	25.37	5.4	3.8	14378.	79.34	83.92	4.55	10.00	12351.	12385.	-0.3	764.
R-717-024H*	94.29	194.7	193.6	0.0865	92.88	25.54	3.9	2.7	10399.	79.33	85.67	6.33	11.79	12358.	12324.	0.3	648.
R-717-025H*	77.54	147.7	146.8	0.0576	77.08	17.40	35.3	24.6	84814.	73.94	74.55	0.51	3.29	8719.	9034.	-3.6	1637.
R-717-026H*	78.68	150.2	149.7	0.0577	77.99	17.39	21.0	14.6	50801.	74.33	75.21	0.82	3.92	8693.	8580.	1.3	1373.
R-717-027H*	80.63	155.7	154.7	0.0577	79.84	17.36	9.8	6.9	24001.	74.45	76.20	1.73	5.30	8646.	8501.	1.7	1009.
R-717-028H*	81.43	157.7	156.8	0.0578	80.52	17.35	7.6	5.3	18624.	74.45	76.68	2.21	5.86	8627.	8413.	2.5	910.
R-717-029H*	82.46	160.7	159.5	0.0579	81.48	17.35	5.4	3.8	13218.	74.12	77.24	3.10	6.78	8612.	8365.	2.9	785.
R-717-030H*	84.49	166.2	165.0	0.0581	83.49	17.39	3.9	2.7	9637.	74.27	78.56	4.28	8.07	8594.	8322.	3.2	658.
R-717-031H*	85.53	168.7	167.9	0.1137	84.72	33.95	35.3	24.6	89914.	78.27	79.35	0.99	6.73	16742.	17417.	-4.0	1539.
R-717-032H*	87.12	173.2	172.3	0.1138	86.29	33.92	21.0	14.6	53804.	78.44	80.11	1.62	7.85	16668.	16972.	-1.8	1313.
R-717-033H*	91.16	185.2	184.1	0.1152	89.98	34.13	9.8	6.9	25631.	78.81	82.22	3.39	10.64	16632.	16664.	-0.2	966.
R-717-034H*	92.71	189.7	188.7	0.1138	91.44	33.66	7.6	5.3	19917.	78.92	83.26	4.32	11.62	16348.	16365.	-0.1	870.
R-717-035H*	94.99	196.7	195.7	0.1143	93.63	33.70	5.5	3.8	14538.	78.83	84.75	5.91	13.20	16284.	16222.	0.4	763.
R-717-036H*	98.36	207.7	206.5	0.1161	96.74	34.07	3.9	2.7	10417.	78.46	86.82	8.36	15.72	16340.	16268.	0.4	643.
R-717-037H*	76.92	145.7	145.2	0.0260	76.26	7.86	35.3	24.6	86172.	75.29	75.64	0.25	1.45	3943.	4350.	-10.3	1677.
R-717-038H*	77.28	146.7	146.1	0.0262	76.67	7.90	21.0	14.6	51309.	75.31	75.77	0.41	1.74	3964.	4254.	-7.3	1410.
R-717-039H*	78.35	149.7	148.8	0.0261	77.47	7.87	9.8	6.8	24071.	75.52	76.38	0.83	2.41	3937.	4068.	-3.3	1012.
R-717-040H*	78.62	150.2	149.5	0.0259	77.77	7.81	7.6	5.3	18616.	75.40	76.48	1.07	2.68	3907.	4046.	-3.6	900.
R-717-041H*	79.16	151.7	150.9	0.0258	78.19	7.77	5.4	3.8	13409.	75.34	76.82	1.46	3.09	3880.	3983.	-2.7	778.
R-717-042H*	79.95	153.7	152.9	0.0258	78.86	7.77	3.9	2.7	9616.	75.24	77.26	2.01	3.70	3876.	3909.	-0.8	648.
R-717-043H*	79.13	151.7	150.8	0.0457	78.37	13.76	35.3	24.6	87344.	76.26	76.78	0.42	2.61	6877.	7326.	-6.5	1632.
R-717-044H*	79.85	153.7	152.7	0.0465	79.11	14.00	21.0	14.6	52093.	76.35	77.08	0.67	3.13	6983.	7051.	-1.0	1379.
R-717-045H*	81.64	158.2	157.3	0.0460	80.64	13.83	9.8	6.9	24646.	76.68	78.12	1.42	4.24	6873.	6958.	-1.2	1002.
R-717-046H*	82.22	159.7	158.9	0.0463	81.25	13.88	7.6	5.3	19037.	76.56	78.41	1.83	4.74	6892.	6946.	-0.8	900.
R-717-047H*	83.29	162.7	161.7	0.0463	82.19	13.88	5.4	3.8	13709.	76.55	79.08	2.52	5.47	6879.	6844.	0.5	777.
R-717-048H*	84.44	165.7	164.9	0.0464	83.24	13.89	3.9	2.7	9827.	76.20	79.70	3.48	6.49	6864.	6773.	1.3	654.

Table D.9. Experimental data for ammonia condensing on Tube H* (vertical, no rod on water side)

Run No.	T_v (°F)	P (psia)	P_{sat} (psia)	F_c (gpm)	T_c (°F)	m_c (lb_m/h)	F_w (gpm)	v (ft/s)	Re	$T_{w,in}$ (°F)	$T_{w,out}$ (°F)	ΔT_w (°F)	$\overline{\Delta T}$ (°F)	Q_c (Btu/h)	Q_w (Btu/h)	Δ (%)	U (Btu/h·ft²·°F)
R-717-049H*N	81.09	156.7	155.9	0.0236	80.60	7.10	41.2	20.1	164029.	79.54	79.80	0.19	1.42	3534.	3844.	-8.8	1540.
R-717-050H*N	81.35	157.2	156.6	0.0237	80.84	7.11	21.0	10.2	83406.	79.28	79.67	0.36	1.87	3537.	3772.	-6.6	1168.
R-717-051H*N	82.34	159.7	159.2	0.0235	81.52	7.04	9.8	4.8	39287.	79.44	80.19	0.71	2.52	3494.	3509.	-0.4	856.
R-717-052H*N	82.70	161.2	160.2	0.0235	81.91	7.05	7.6	3.7	30405.	79.37	80.33	0.94	2.85	3495.	3585.	-2.6	757.
R-717-053H*N	83.55	163.2	162.4	0.0233	82.52	6.99	5.4	2.6	21617.	79.44	80.77	1.31	3.44	3460.	3540.	-2.3	622.
R-717-054H*N	84.58	165.7	165.2	0.0233	83.37	6.98	3.8	1.9	15455.	79.42	81.25	1.82	4.24	3448.	3490.	-1.2	502.
R-717-055H*N	81.56	157.7	157.1	0.0234	80.41	7.02	25.0	12.2	99758.	79.68	80.02	0.30	1.71	3492.	3779.	-8.2	1265.
R-717-056H*N	81.91	159.2	158.1	0.0229	80.75	6.89	16.7	8.1	66702.	79.69	80.16	0.44	1.99	3421.	3658.	-6.9	1065.
R-717-057H*N	82.23	159.7	158.9	0.0233	81.03	7.00	13.4	6.5	53588.	79.75	80.30	0.50	2.21	3477.	3369.	3.1	975.
R-717-058H*N	82.54	160.7	159.7	0.0234	81.34	7.03	10.0	4.9	40014.	79.72	80.43	0.68	2.47	3486.	3392.	2.7	874.
R-717-059H*N	84.13	164.7	164.0	0.0232	82.68	6.95	5.0	2.4	20126.	79.84	81.26	1.40	3.58	3435.	3505.	-2.0	594.
R-717-060H*N	84.75	166.2	165.7	0.1128	84.04	33.70	41.2	20.1	159237.	76.86	77.77	0.83	7.43	16646.	16998.	-2.1	1385.
R-717-061H*N	87.44	174.2	173.2	0.1134	86.55	33.76	21.0	10.2	81940.	77.24	78.89	1.62	9.37	16579.	16972.	-2.4	1094.
R-717-062H*N	91.48	186.2	185.0	0.1144	90.38	33.89	9.8	4.8	38878.	77.27	80.68	3.39	12.50	16501.	16683.	-1.1	817.
R-717-063H*N	93.96	193.7	192.5	0.1154	92.74	34.06	7.5	3.7	30033.	77.71	82.13	4.39	14.03	16497.	16477.	0.1	727.
R-717-064H*N	97.10	203.2	202.4	0.1164	95.67	34.19	5.4	2.6	21712.	77.39	83.53	6.11	16.63	16445.	16474.	-0.2	611.
R-717-065H*N	101.18	216.7	215.8	0.1159	99.48	33.85	3.9	1.9	15842.	77.13	85.44	8.28	19.90	16132.	16114.	0.1	501.
R-717-066H*N	84.27	165.2	164.4	0.0838	83.54	25.06	41.2	20.1	162461.	78.56	79.25	0.63	5.37	12391.	12847.	-3.7	1428.
R-717-067H*N	86.81	172.2	171.4	0.0838	85.90	24.97	21.0	10.2	83992.	79.43	80.65	1.18	6.77	12278.	12404.	-1.0	1121.
R-717-068H*N	89.02	179.2	177.8	0.0838	87.93	24.89	9.8	4.8	39132.	78.65	81.16	2.47	9.12	12185.	12096.	0.7	827.
R-717-069H*N	90.28	182.2	181.5	0.0834	89.02	24.75	7.6	3.7	30509.	78.51	81.73	3.21	10.16	12080.	12199.	-1.0	735.
R-717-070H*N	92.79	189.7	189.0	0.0842	91.35	24.90	5.4	2.7	21996.	78.54	82.99	4.42	12.03	12090.	12031.	0.5	622.
R-717-071H*N	96.23	200.7	199.7	0.0845	94.51	24.88	3.8	1.9	15684.	78.45	84.60	6.14	14.71	11988.	11788.	1.7	504.
R-717-072H*N	82.05	159.2	158.4	0.0959	81.33	28.79	41.2	20.1	156085.	75.36	76.15	0.70	6.29	14297.	14491.	-1.4	1405.
R-717-073H*N	85.62	168.7	168.1	0.0960	84.61	28.68	21.2	10.3	82374.	77.04	78.43	1.36	7.89	14139.	14352.	-1.5	1109.
R-717-074H*N	87.71	174.7	174.0	0.0963	86.55	28.68	9.8	4.8	37942.	75.60	78.50	2.89	10.66	14077.	14202.	-0.9	817.
R-717-075H*N	89.59	180.2	179.4	0.0964	88.25	28.62	7.6	3.7	29639.	75.99	79.65	3.64	11.78	13993.	13830.	1.2	735.
R-717-076H*N	92.31	188.7	187.5	0.0968	90.77	28.65	5.4	2.6	21129.	75.71	80.86	5.13	14.03	13925.	13812.	0.8	614.
R-717-077H*N	97.15	203.7	202.6	0.0984	95.17	28.93	3.8	1.9	15353.	76.18	83.42	7.22	17.35	13911.	13862.	0.4	496.
R-717-078H*N	83.00	161.7	161.0	0.0606	81.86	18.18	41.2	20.1	162964.	78.89	79.41	0.46	3.85	9011.	9373.	-4.0	1447.
R-717-079H*N	84.45	165.7	164.9	0.0603	83.07	18.04	21.0	10.2	83524.	79.15	80.04	0.86	4.86	8915.	9010.	-1.1	1134.
R-717-080H*N	86.44	171.7	170.4	0.0606	84.89	18.09	9.8	4.8	39092.	78.90	80.75	1.82	6.61	8902.	8884.	0.2	832.
R-717-081H*N	87.18	173.7	172.5	0.0604	85.54	18.02	7.6	3.7	30471.	78.64	80.98	2.32	7.37	8853.	8847.	0.1	743.
R-717-082H*N	88.80	177.7	177.1	0.0604	86.94	17.97	5.4	2.7	21796.	78.41	81.65	3.23	8.77	8798.	8777.	0.2	620.
R-717-083H*N	91.54	186.2	185.2	0.0607	89.35	18.00	3.9	1.9	15755.	78.61	83.08	4.46	10.70	8762.	8676.	1.0	506.
R-717-084H*N	77.68	147.7	147.1	0.0353	76.53	10.66	41.2	20.1	155459.	75.27	75.61	0.26	2.24	5339.	5344.	-0.1	1475.
R-717-085H*N	78.43	149.7	149.0	0.0354	77.22	10.67	21.0	10.2	79308.	75.23	75.79	0.53	2.92	5339.	5563.	-4.2	1132.
R-717-086H*N	79.61	152.7	152.0	0.0353	78.21	10.63	9.8	4.8	37098.	75.13	76.26	1.12	3.92	5305.	5476.	-3.2	837.
R-717-087H*N	80.14	153.7	153.4	0.0351	78.71	10.58	7.6	3.7	28866.	75.04	76.46	1.40	4.39	5276.	5307.	-0.6	743.
R-717-088H*N	81.73	158.2	157.6	0.0352	79.99	10.57	5.4	2.7	20840.	75.50	77.46	1.94	5.25	5255.	5275.	-0.4	619.
R-717-089H*N	82.80	161.2	160.4	0.0346	81.02	10.39	3.9	1.9	14823.	75.07	77.75	2.65	6.39	5150.	5133.	0.3	499.
R-717-090H*N	78.59	150.2	149.4	0.0478	77.37	14.42	41.2	20.1	155731.	75.36	75.79	0.35	3.01	7211.	7215.	-0.0	1482.
R-717-091H*N	79.95	153.2	152.9	0.0480	78.59	14.47	21.0	10.2	79880.	75.70	76.43	0.70	3.88	7215.	7313.	-1.3	1149.
R-717-092H*N	81.41	157.2	156.7	0.0478	79.97	14.37	9.8	4.8	37522.	75.44	76.92	1.46	5.23	7148.	7199.	-0.7	845.
R-717-093H*N	82.26	159.7	159.0	0.0476	80.77	14.30	7.5	3.7	28845.	75.46	77.35	1.87	5.85	7100.	7036.	0.9	751.
R-717-094H*N	83.67	163.7	162.8	0.0474	81.98	14.21	5.4	2.7	20914.	75.49	78.02	2.51	6.92	7034.	6827.	2.9	629.
R-717-095H*N	85.78	169.2	168.6	0.0478	83.81	14.28	3.9	1.9	15269.	75.58	79.08	3.48	8.45	7039.	6854.	2.6	515.

Table D.9 (continued)

Run No.	T_v (°F)	P (psia)	P_{sat} (psia)	F_c (gpm)	T_c (°F)	m_c (lb_m/h)	F_w (gpm)	v (ft/s)	Re	$T_{w,in}$ (°F)	$T_{w,out}$ (°F)	ΔT_w (°F)	$\overline{\Delta T}$ (°F)	Q_c (Btu/h)	Q_w (Btu/h)	Δ (%)	U (Btu/h·ft^2·°F)
R-717-096H*N	80.60	155.2	154.6	0.0722	79.72	21.71	41.2	20.1	156427.	75.61	76.24	0.55	4.68	10314.	11264.	-4.2	1430.
R-717-097H*N	82.37	159.7	159.3	0.0722	81.16	21.68	21.0	10.2	80217.	75.84	76.96	1.08	5.97	10760.	11357.	-5.5	1115.
R-717-098H*N	85.17	167.2	166.9	0.0730	83.71	21.83	9.8	4.8	37563.	75.94	78.19	2.23	8.11	10772.	10872.	-0.9	821.
R-717-099H*N	86.54	171.7	170.7	0.0733	85.05	21.88	7.6	3.7	29530.	76.10	78.95	2.83	9.01	10767.	10762.	0.0	739.
R-717-100H*N	88.31	176.2	175.7	0.0731	86.73	21.76	5.4	2.7	21152.	75.70	79.59	3.86	10.66	10668.	10498.	1.6	619.
R-717-101H*N	91.66	186.7	185.6	0.0736	89.81	21.81	3.9	1.9	15401.	75.92	81.30	5.36	13.05	10616.	10486.	1.2	503.
R-717-102H*N	81.89	158.7	158.0	0.0225	79.73	6.76	25.0	12.2	100237.	80.07	80.40	0.29	1.65	3361.	3654.	-8.7	1258.
R-717-103H*N	82.05	159.2	158.4	0.0225	79.93	6.76	16.5	8.1	66042.	79.87	80.33	0.43	1.95	3358.	3523.	-4.9	1065.
R-717-104H*N	82.11	159.7	158.6	0.0225	80.11	6.77	13.4	6.5	53580.	79.74	80.29	0.50	2.10	3364.	3363.	0.0	991.
R-717-105H*N	82.09	159.7	158.5	0.0225	80.22	6.76	10.0	4.9	39835.	79.37	80.06	0.66	2.37	3357.	3303.	1.6	875.
R-717-106H*N	83.75	163.7	163.0	0.0221	81.36	6.63	4.9	2.4	19737.	79.58	80.98	1.38	3.47	3280.	3395.	-3.5	584.
R-717-107H*N	82.92	161.7	160.7	0.0303	81.30	9.09	25.0	12.2	100818.	80.49	80.91	0.38	2.22	4506.	4802.	-6.6	1257.
R-717-108H*N	82.97	161.7	160.9	0.0302	81.38	9.05	16.7	8.1	67059.	80.06	80.66	0.57	2.62	4485.	4749.	-5.9	1061.
R-717-109H*N	82.91	161.7	160.7	0.0301	81.43	9.02	13.4	6.5	53614.	79.70	80.43	0.68	2.84	4473.	4553.	-1.8	974.
R-717-110H*N	83.67	164.2	162.8	0.0298	81.91	8.92	10.0	4.9	40238.	80.07	80.98	0.88	3.15	4417.	4385.	0.7	868.
R-717-111H*N	85.38	168.2	167.4	0.0293	83.40	8.76	5.0	2.4	20215.	80.02	81.80	1.76	4.47	4321.	4400.	-1.8	598.

Table D.10. Experimental data for ammonia condensing on Tube L (vertical)

Run No.	T_v (°F)	P (psia)	P_{sat} (psia)	F_c (gpm)	T_c (°F)	m_c (lb_m/h)	F_w (gpm)	v (ft/s)	Re	$T_{w,in}$ (°F)	$T_{w,out}$ (°F)	ΔT_w (°F)	$\overline{\Delta T}$ (°F)	Q_c (Btu/h)	Q_w (Btu/h)	Δ (%)	U (Btu/h·ft²·°F)
R-717-007L	81.78	158.7	157.7	0.0302	81.00	9.07	35.3	28.4	94523.	80.04	80.42	0.27	1.55	4506.	4685.	-4.0	1930.
R-717-008L	82.29	159.7	159.0	0.0302	81.42	9.05	21.2	17.1	56808.	80.04	80.53	0.44	2.00	4491.	4685.	-4.3	1494.
R-717-009L	83.84	164.7	163.2	0.0301	82.55	9.02	9.8	7.9	26367.	80.15	81.08	0.88	3.22	4462.	4317.	3.3	921.
R-717-010L	84.51	166.2	165.0	0.0303	83.36	9.06	7.6	6.1	20446.	80.01	81.21	1.19	3.90	4476.	4501.	-0.5	763.
R-717-011L	85.61	169.2	168.1	0.0300	84.17	8.97	5.4	4.4	14532.	79.80	81.46	1.64	4.97	4422.	4407.	0.3	591.
R-717-012L	87.44	174.2	173.2	0.0301	85.69	8.97	3.8	3.1	10406.	79.84	82.13	2.28	6.45	4406.	4381.	0.6	454.
R-717-013L	78.68	150.2	149.7	0.0725	78.34	21.85	35.3	28.4	87941.	74.19	74.92	0.62	4.13	10924.	10866.	0.5	1758.
R-717-014L	80.13	154.2	153.4	0.0726	79.62	21.83	21.0	16.9	52494.	74.27	75.35	1.01	5.31	10886.	10582.	2.8	1362.
R-717-015L	83.52	164.2	162.4	0.0726	82.79	21.72	9.8	7.9	24777.	74.20	76.40	2.17	8.22	10756.	10649.	1.0	870.
R-717-016L	85.26	167.7	167.1	0.0726	84.31	21.68	7.6	6.1	19177.	74.13	76.94	2.79	9.72	10695.	10575.	1.1	731.
R-717-017L	88.73	177.7	176.9	0.0731	87.50	21.75	5.4	4.4	13906.	74.46	78.35	3.87	12.32	10654.	10528.	1.2	575.
R-717-018L	92.74	189.7	188.8	0.0735	91.10	21.73	3.9	3.2	10098.	74.50	79.80	5.27	15.59	10552.	10304.	2.3	450.
R-717-019L	81.09	156.7	155.9	0.0972	80.57	29.18	35.3	28.4	88931.	74.95	75.88	0.82	5.67	14522.	14476.	0.3	1702.
R-717-020L	83.91	164.7	163.4	0.0964	82.92	28.86	21.0	16.9	53897.	76.15	77.58	1.36	7.04	14277.	14301.	-0.2	1348.
R-717-021L	87.47	174.7	173.3	0.0979	86.60	29.15	9.8	7.9	25144.	75.00	77.88	2.84	11.03	14314.	13951.	2.5	863.
R-717-022L	89.70	180.7	179.8	0.0976	88.61	28.97	7.6	6.1	19485.	74.94	78.63	3.66	12.92	14159.	13896.	1.9	729.
R-717-023L	93.96	194.2	192.5	0.0979	92.54	28.89	5.4	4.4	14163.	75.31	80.38	5.06	16.11	13994.	13753.	1.7	577.
R-717-024L	98.95	209.7	208.4	0.0980	97.14	28.72	3.9	3.1	10215.	74.97	81.96	6.96	20.49	13757.	13550.	1.5	446.
R-717-025L	80.71	156.2	154.9	0.0848	80.31	25.48	35.3	28.4	89398.	75.42	76.23	0.69	4.89	12687.	12222.	3.7	1724.
R-717-026L	82.18	159.7	158.8	0.0844	81.54	25.32	21.0	16.9	53306.	75.38	76.62	1.16	6.18	12574.	12205.	2.9	1353.
R-717-027L	86.39	171.2	170.3	0.0853	85.49	25.44	9.8	7.9	25267.	75.55	78.09	2.50	9.57	12520.	12310.	1.7	870.
R-717-028L	88.51	177.7	176.3	0.0858	87.59	25.51	7.6	6.1	19517.	75.47	78.76	3.26	11.39	12499.	12332.	1.3	729.
R-717-029L	92.01	188.2	186.6	0.0858	90.81	25.40	5.4	4.4	14165.	75.61	80.10	4.47	14.16	12354.	12167.	1.5	580.
R-717-030L	97.04	203.7	202.2	0.0867	95.41	25.48	3.9	3.2	10320.	75.77	81.97	6.18	18.17	12256.	12082.	1.4	449.
R-717-031L	82.19	159.7	158.8	0.0372	81.15	11.16	35.3	28.4	94530.	80.03	80.44	0.30	1.96	5540.	5354.	3.4	1882.
R-717-032L	82.89	161.7	160.7	0.0370	81.70	11.11	21.0	16.9	56316.	80.07	80.63	0.52	2.54	5507.	5448.	1.1	1441.
R-717-033L	84.90	166.7	166.1	0.0372	83.60	11.13	9.8	7.9	26588.	80.31	81.45	1.08	4.03	5496.	5312.	3.4	908.
R-717-034L	85.94	169.7	169.0	0.0365	84.39	10.90	7.6	6.1	20614.	80.56	81.97	1.39	4.67	5372.	5259.	2.1	765.
R-717-035L	86.96	172.7	171.9	0.0367	85.43	10.95	5.4	4.4	14720.	79.94	81.90	1.94	6.03	5386.	5283.	1.9	594.
R-717-036L	89.07	179.2	177.9	0.0367	87.22	10.93	3.9	3.2	10640.	79.96	82.69	2.73	7.75	5348.	5335.	0.2	459.
R-717-037L	82.89	161.7	160.7	0.0485	81.91	14.55	35.3	28.4	94642.	80.08	80.58	0.39	2.56	7215.	6921.	4.1	1874.
R-717-038L	84.05	164.7	163.8	0.0487	82.97	14.57	21.0	16.9	56593.	80.39	81.11	0.68	3.30	7208.	7114.	1.3	1453.
R-717-039L	86.01	170.2	169.2	0.0487	84.69	14.55	9.8	7.9	26572.	80.11	81.55	1.39	5.18	7169.	6826.	4.8	919.
R-717-040L	87.14	173.2	172.4	0.0485	85.74	14.45	7.6	6.1	20554.	80.12	81.94	1.81	6.11	7100.	6848.	3.6	773.
R-717-041L	89.31	179.7	178.6	0.0491	87.62	14.60	5.4	4.4	14828.	80.25	82.80	2.53	7.78	7140.	6884.	3.6	610.
R-717-042L	91.54	186.2	185.2	0.0486	89.44	14.42	3.9	3.2	10682.	79.91	83.38	3.47	9.90	7020.	6786.	3.3	471.
R-717-043L	83.05	162.2	161.1	0.0612	82.47	18.34	35.3	28.4	93873.	79.37	79.99	0.51	3.38	9089.	9017.	0.8	1789.
R-717-044L	84.30	165.2	164.5	0.0614	83.59	18.38	21.0	16.9	56043.	79.50	80.42	0.87	4.34	9084.	9094.	-0.1	1393.
R-717-045L	87.06	172.7	172.2	0.0613	85.97	18.27	9.8	7.9	26418.	79.46	81.26	1.75	6.70	8982.	8619.	4.0	891.
R-717-046L	88.54	177.2	176.4	0.0617	87.27	18.36	7.6	6.1	20422.	79.33	81.69	2.34	8.03	8996.	8891.	1.2	745.
R-717-047L	90.87	184.2	183.2	0.0617	89.36	18.29	5.4	4.4	14701.	79.19	82.45	3.24	10.04	8918.	8799.	1.3	590.
R-717-048L	94.11	194.2	193.0	0.0618	93.32	18.24	3.9	3.2	10634.	79.05	83.52	4.46	12.83	8829.	8732.	1.1	457.
R-717-049L	77.59	147.7	146.9	0.1079	77.31	32.54	35.3	28.4	84037.	70.47	71.50	0.91	6.60	16309.	15981.	2.0	1643.
R-717-050L	80.04	154.2	153.1	0.1088	79.63	32.71	21.2	17.1	50954.	70.90	72.50	1.51	8.34	16312.	15986.	2.0	1301.
R-717-051L	84.85	166.7	166.0	0.1092	84.07	32.63	9.8	7.9	23761.	70.47	73.72	3.20	12.75	16111.	15730.	2.4	840.
R-717-052L	87.77	174.7	174.2	0.1096	86.80	32.62	7.6	6.1	18507.	70.73	74.89	4.13	14.96	16009.	15663.	2.2	712.
R-717-053L	92.65	189.7	188.6	0.1103	91.42	32.61	5.4	4.4	13478.	71.11	76.86	5.72	18.67	15840.	15566.	1.7	564.
R-717-054L	98.60	208.7	207.3	0.1109	96.89	32.53	3.9	3.1	9740.	70.78	78.70	7.88	23.86	15595.	15342.	1.6	435.

Table D.11. Experimental data for ammonia condensing on Tube L* (vertical)

Run No.	T_v (°F)	P (psia)	P_{sat} (psia)	F_c (gpm)	T_c (°F)	m_c (lb_m/h)	F_w (gpm)	v (ft/s)	Re	$T_{w,in}$ (°F)	$T_{w,out}$ (°F)	ΔT_w (°F)	$\overline{\Delta T}$ (°F)	Q_c (Btu/h)	Q_w (Btu/h)	Δ (%)	U (Btu/h·ft²·°F)
R-717-001L*	88.42	177.2	176.0	0.1049	87.62	31.19	34.0	30.5	96064.	82.27	83.28	0.90	5.64	15287.	15334.	-0.3	1803.
R-717-002L*	89.86	180.7	180.2	0.1046	88.94	31.05	21.0	18.8	59497.	82.25	83.76	1.46	6.86	15171.	15328.	-1.0	1471.
R-717-003L*	93.71	192.7	191.8	0.1055	92.58	31.14	9.8	8.7	27989.	82.56	85.63	3.05	9.62	15088.	14821.	1.8	1043.
R-717-004L*	95.79	199.2	198.3	0.1054	94.62	31.03	7.6	6.8	22074.	82.88	86.81	3.91	10.95	14967.	14857.	0.7	909.
R-717-005L*	99.69	211.7	210.8	0.1050	98.12	30.74	5.4	4.8	15855.	83.38	88.83	5.44	13.58	14696.	14627.	0.5	719.
R-717-006L*	104.09	226.7	225.7	0.1069	102.27	31.11	3.9	3.5	11451.	82.34	89.87	7.52	17.98	14724.	14604.	0.8	544.
R-717-007L*	86.81	172.2	171.4	0.0345	85.71	10.27	34.0	30.5	98835.	84.93	85.34	0.31	1.68	5052.	5343.	-5.8	2005.
R-717-008L*	87.27	173.7	172.8	0.0345	86.16	10.29	21.0	18.8	61103.	84.94	85.48	0.48	2.06	5056.	5071.	-0.3	1632.
R-717-009L*	88.38	176.7	175.9	0.0340	87.15	10.12	9.8	8.8	28586.	84.90	85.94	1.02	2.96	4959.	4987.	-0.6	1113.
R-717-010L*	89.35	179.7	178.7	0.0343	88.07	10.18	7.3	6.6	21540.	85.13	86.50	1.35	3.54	4981.	4943.	0.8	936.
R-717-011L*	90.44	182.7	181.9	0.0339	89.02	10.05	5.4	4.9	15997.	85.17	86.99	1.81	4.36	4904.	4903.	0.0	748.
R-717-012L*	92.48	189.2	188.0	0.0339	90.90	10.03	3.9	3.5	11527.	85.40	87.92	2.51	5.82	4875.	4878.	-0.1	557.
R-717-013L*	88.62	177.7	176.6	0.0689	87.89	20.47	34.4	30.8	99990.	84.77	85.48	0.61	3.49	10028.	10537.	-5.1	1910.
R-717-014L*	90.22	182.7	181.3	0.0690	89.43	20.45	17.0	15.2	49649.	84.93	86.12	1.15	4.69	9984.	9728.	2.6	1415.
R-717-015L*	92.33	189.2	187.6	0.0697	91.37	20.60	9.8	8.8	28931.	85.10	87.17	2.04	6.20	10014.	10028.	-0.1	1074.
R-717-016L*	99.57	211.7	210.4	0.0695	97.85	20.37	3.8	3.4	11357.	85.04	90.17	5.12	11.96	9741.	9691.	0.5	541.
R-717-017L*	88.12	175.7	175.2	0.0874	87.68	25.97	34.7	31.1	98599.	82.81	83.68	0.78	4.88	12737.	13451.	-5.6	1736.
R-717-018L*	89.67	181.7	179.7	0.0883	89.36	26.17	17.0	15.2	48452.	82.73	84.26	1.49	6.17	12795.	12654.	1.1	1378.
R-717-019L*	92.47	189.7	188.0	0.0882	91.88	26.06	9.8	8.8	28436.	83.26	85.86	2.57	7.91	12664.	12654.	0.1	1065.
R-717-020L*	101.48	217.7	216.8	0.0882	100.02	25.74	3.8	3.4	11254.	83.20	89.58	6.37	15.08	12256.	12118.	1.1	540.
R-717-021L*	87.53	174.7	173.5	0.0921	87.15	27.40	34.7	31.1	97919.	82.22	83.13	0.81	4.85	13453.	13988.	-4.0	1844.
R-717-022L*	88.85	178.7	177.3	0.0935	88.46	27.77	21.0	18.8	59373.	82.15	83.52	1.31	6.01	13599.	13704.	-0.8	1503.
R-717-023L*	92.57	189.7	188.3	0.0937	91.84	27.69	9.7	8.7	27892.	82.66	85.45	2.77	8.51	13450.	13418.	0.2	1051.
R-717-024L*	94.18	194.7	193.2	0.0932	93.46	27.46	7.6	6.8	21913.	82.70	86.21	3.48	9.73	13294.	13195.	0.7	908.
R-717-025L*	97.21	204.2	202.8	0.0932	96.26	27.35	5.4	4.8	15680.	82.60	87.48	4.88	12.17	13150.	13136.	0.1	718.
R-717-026L*	102.02	220.2	218.7	0.0937	100.74	27.34	3.8	3.5	11301.	82.72	89.44	6.71	15.94	13001.	12875.	1.0	542.
R-717-027L*	87.45	174.7	173.3	0.0460	86.76	13.69	34.7	31.1	100973.	84.97	85.47	0.40	2.23	6725.	6942.	-3.2	2001.
R-717-028L*	88.17	176.7	175.3	0.0461	87.43	13.72	21.0	18.8	61250.	85.07	85.76	0.63	2.76	6726.	6600.	1.9	1623.
R-717-029L*	89.58	180.7	179.4	0.0463	88.50	13.73	9.8	8.8	28775.	84.86	86.24	1.35	4.03	6715.	6654.	0.9	1108.
R-717-030L*	90.60	183.7	182.4	0.0458	89.46	13.57	7.5	6.7	22017.	85.07	86.84	1.74	4.65	6620.	6529.	1.4	947.
R-717-031L*	91.99	188.2	186.6	0.0454	90.65	13.43	5.4	4.8	15875.	85.01	87.41	2.38	5.78	6534.	6407.	1.9	751.
R-717-032L*	93.80	193.2	192.1	0.0459	91.73	13.56	3.9	3.5	11626.	84.70	87.92	3.21	7.49	6571.	6314.	3.9	584.
R-717-033L*	87.86	175.2	174.4	0.0583	86.97	17.36	34.7	31.1	100708.	84.69	85.31	0.53	2.86	8517.	9123.	-7.1	1977.
R-717-034L*	89.48	179.7	179.1	0.0581	88.34	17.25	21.0	18.8	61602.	85.57	86.48	0.86	3.45	8436.	8975.	-6.4	1625.
R-717-035L*	90.75	184.2	182.9	0.0580	89.60	17.19	9.8	8.8	28679.	84.84	86.54	1.68	5.06	8384.	8199.	2.2	1102.
R-717-036L*	91.79	186.7	186.0	0.0578	90.50	17.12	7.6	6.8	22306.	84.84	87.03	2.17	5.85	8329.	8213.	1.4	946.
R-717-037L*	94.08	194.2	192.9	0.0573	92.41	16.93	5.3	4.7	15505.	85.04	88.15	3.10	7.48	8196.	8099.	1.2	728.
R-717-038L*	96.91	202.7	201.8	0.0570	95.01	16.78	3.9	3.5	11612.	85.21	89.36	4.14	9.62	8072.	8038.	0.4	558.
R-717-039L*	84.89	166.7	166.1	0.0805	83.92	24.05	34.7	31.1	95541.	80.27	81.08	0.70	4.21	11877.	12187.	-2.6	1875.
R-717-040L*	87.14	173.2	172.4	0.0806	85.92	24.03	21.0	18.8	58751.	81.38	82.57	1.14	5.16	11808.	11902.	-0.8	1520.
R-717-041L*	89.20	179.2	178.3	0.0814	87.94	24.18	9.8	8.8	27501.	80.60	83.01	2.38	7.39	11833.	11691.	1.2	1065.
R-717-042L*	90.83	184.2	183.1	0.0805	89.43	23.88	7.6	6.8	21423.	80.85	83.90	3.02	8.46	11643.	11496.	1.3	915.
R-717-043L*	93.85	193.2	192.2	0.0809	92.17	23.89	5.4	4.8	15328.	81.04	85.28	4.22	10.69	11572.	11374.	1.7	720.
R-717-044L*	97.99	206.7	205.3	0.0817	95.97	23.99	3.9	3.5	11245.	81.12	86.94	5.81	13.96	11516.	11357.	1.4	548.

Table D.11 (continued)

Run No.	T_v (°F)	P (psia)	P_{sat} (psia)	F_c (gpm)	T_c (°F)	m_c (lb_m/h)	F_w (gpm)	v (ft/s)	Re	$T_{w,in}$ (°F)	$T_{w,out}$ (°F)	ΔT_w (°F)	$\overline{\Delta T}$ (°F)	Q_c (Btu/h)	Q_w (Btu/h)	Δ (%)	U (Btu/h·ft^2·°F)
R-717-045L*	83.30	162.7	161.8	0.0502	82.14	15.03	34.7	31.1	95729.	80.56	81.11	0.44	2.46	7448.	7565.	-1.6	2010.
R-717-046L*	84.17	164.7	164.1	0.0501	82.83	15.01	21.0	18.8	58124.	80.73	81.47	0.69	3.07	7423.	7187.	3.2	1608.
R-717-047L*	86.00	170.2	169.2	0.0503	84.43	15.02	9.8	8.8	27277.	80.81	82.30	1.46	4.44	7401.	7148.	3.4	1107.
R-717-048L*	86.93	172.7	171.8	0.0504	85.30	15.03	7.6	6.8	21267.	80.82	82.73	1.88	5.15	7389.	7136.	3.4	954.
R-717-049L*	88.99	178.7	177.7	0.0501	87.25	14.90	5.4	4.8	15199.	81.14	83.79	2.63	6.52	7292.	7085.	2.8	743.
R-717-050L*	91.28	185.7	184.4	0.0503	89.26	14.92	3.9	3.5	11059.	80.87	84.45	3.55	8.62	7266.	6952.	4.3	561.

Table D.12. Experimental data for ammonia condensing on Tube L* (vertical, no rod on water side)

Run No.	T_v (°F)	P (psia)	P_{sat} (psia)	F_c (gpm)	T_c (°F)	m_c (lb_m/h)	F_w (gpm)	v (ft/s)	Re	$T_{w,in}$ (°F)	$T_{w,out}$ (°F)	ΔT_w (°F)	$\overline{\Delta T}$ (°F)	Q_c (Btu/h)	Q_w (Btu/h)	Δ (%)	U (Btu/h·ft²·°F)
R-717-051L*N	86.03	169.7	169.3	0.0983	84.48	29.36	41.2	23.9	179434.	79.62	80.40	0.72	6.02	14460.	14779.	-2.2	1598.
R-717-052L*N	88.17	176.2	175.3	0.0986	86.48	29.37	21.0	12.2	91556.	79.41	80.79	1.36	8.07	14400.	14301.	0.7	1186.
R-717-053L*N	94.04	193.7	192.8	0.1007	91.89	29.75	9.8	5.6	43262.	80.03	83.00	2.95	12.53	14403.	14359.	0.3	764.
R-717-054L*N	96.64	201.7	201.0	0.1008	94.35	29.69	7.6	4.4	33794.	79.82	83.56	3.74	14.96	14294.	14169.	0.9	635.
R-717-055L*N	102.26	220.2	219.5	0.1003	99.53	29.31	5.4	3.1	24226.	79.80	85.02	5.20	19.84	13934.	14017.	-0.6	467.
R-717-056L*N	107.82	239.7	239.0	0.1017	104.63	29.48	4.1	2.4	18762.	79.75	86.34	6.58	24.77	13832.	13621.	1.5	371.
R-717-057L*N	77.75	147.7	147.3	0.0341	76.18	10.29	41.2	23.9	170017.	75.59	75.92	0.26	2.00	5156.	5365.	-4.0	1714.
R-717-058L*N	78.67	150.2	149.6	0.0336	76.97	10.13	21.0	12.2	86870.	75.68	76.20	0.50	2.73	5068.	5259.	-3.8	1234.
R-717-059L*N	80.70	155.2	154.9	0.0333	78.55	10.03	9.8	5.7	40771.	75.86	76.91	1.03	4.32	4996.	5060.	-1.3	769.
R-717-060L*N	81.73	158.7	157.6	0.0331	79.59	9.96	7.6	4.4	31510.	75.76	77.10	1.31	5.30	4951.	4959.	-0.2	621.
R-717-061L*N	83.92	164.7	163.4	0.0330	81.45	9.91	5.4	3.1	22583.	75.87	77.71	1.82	7.13	4902.	4914.	-0.3	457.
R-717-062L*N	87.09	173.2	172.2	0.0331	84.29	9.88	3.8	2.2	16206.	76.03	78.58	2.53	9.79	4854.	4859.	-0.1	330.
R-717-063L*N	82.84	161.2	160.5	0.0735	81.55	22.03	41.2	23.9	175871.	78.11	78.71	0.53	4.43	10924.	10956.	-0.3	1640.
R-717-064L*N	84.85	166.7	166.0	0.0737	83.57	22.05	21.0	12.2	90100.	78.28	79.35	1.05	6.03	10888.	10980.	-0.8	1200.
R-717-065L*N	87.67	174.7	173.9	0.0742	86.24	22.11	9.8	5.6	41481.	77.03	79.26	2.22	9.52	10355.	10808.	0.4	758.
R-717-066L*N	89.85	181.2	180.2	0.0738	88.27	21.93	7.5	4.4	32209.	76.93	79.78	2.83	11.49	10714.	10645.	0.7	620.
R-717-067L*N	94.27	194.7	193.5	0.0741	92.32	21.88	5.3	3.1	22853.	76.93	80.89	3.94	15.36	10588.	10460.	1.2	458.
R-717-068L*N	100.18	213.7	212.4	0.0744	97.71	21.78	3.9	2.3	16941.	77.19	82.41	5.20	20.38	10403.	10121.	2.7	339.
R-717-069L*N	83.82	164.7	163.2	0.0898	83.03	26.87	41.2	23.9	175630.	77.94	78.66	0.65	5.52	13298.	13422.	-0.9	1601.
R-717-070L*N	85.78	169.7	168.6	0.0898	84.80	26.82	21.0	12.2	89599.	77.73	79.02	1.27	7.41	13217.	13347.	-1.0	1186.
R-717-071L*N	91.11	184.7	183.9	0.0909	89.84	26.94	9.8	5.7	42495.	78.33	80.99	2.65	11.45	13129.	12956.	1.3	762.
R-717-072L*N	93.67	192.7	191.7	0.0906	92.20	26.77	7.6	4.4	33158.	78.24	81.64	3.40	13.73	12973.	12910.	0.5	628.
R-717-073L*N	98.44	208.2	206.7	0.0910	96.71	26.71	5.4	3.2	23882.	78.18	82.82	4.63	17.94	12807.	12581.	1.8	475.
R-717-074L*N	106.84	237.2	235.5	0.0918	104.59	26.61	3.7	2.2	16585.	78.36	85.01	6.64	25.15	12516.	12362.	1.2	331.
R-717-075L*N	83.05	162.7	161.1	0.0811	82.54	24.30	41.2	23.9	175177.	77.76	78.43	0.60	4.96	12046.	12374.	-2.7	1615.
R-717-076L*N	85.25	167.7	167.1	0.0810	84.54	24.18	21.0	12.2	89825.	77.98	79.16	1.17	6.68	11931.	12268.	-2.8	1188.
R-717-077L*N	89.64	180.7	179.6	0.0810	88.54	24.04	9.8	5.6	42131.	78.17	80.59	2.41	10.26	11753.	11718.	0.3	762.
R-717-078L*N	92.52	189.7	188.1	0.0819	91.38	24.22	7.6	4.4	33113.	78.48	81.60	3.11	12.48	11768.	11807.	-0.3	627.
R-717-079L*N	97.71	205.7	204.4	0.0831	96.22	24.41	5.4	3.1	23828.	78.89	83.24	4.34	16.64	11722.	11695.	0.2	468.
R-717-080L*N	104.06	227.2	225.7	0.0837	102.01	24.35	3.9	2.3	17522.	79.21	85.02	5.81	21.95	11526.	11368.	1.4	349.
R-717-081L*N	79.76	152.7	152.4	0.0444	78.73	13.35	41.2	23.9	173113.	76.96	77.37	0.34	2.60	6664.	7009.	-5.2	1704.
R-717-082L*N	81.09	156.7	155.9	0.0443	79.85	13.31	21.0	12.2	88683.	77.23	77.89	0.64	3.53	6624.	6684.	-0.9	1247.
R-717-083L*N	83.49	163.2	162.3	0.0441	81.98	13.21	9.8	5.7	41778.	77.24	78.56	1.31	5.59	6541.	6442.	1.5	778.
R-717-084L*N	85.02	167.2	166.4	0.0443	83.41	13.26	7.6	4.4	32447.	77.36	79.07	1.68	6.81	6548.	6398.	2.3	640.
R-717-085L*N	87.74	174.7	174.1	0.0443	85.73	13.21	5.5	3.2	23558.	77.50	79.86	2.35	9.06	6482.	6440.	0.6	476.
R-717-086L*N	91.24	185.2	184.3	0.0438	88.80	13.00	3.9	2.3	16755.	77.31	80.53	3.21	12.32	6335.	6238.	1.5	342.
R-717-087L*N	80.06	154.2	153.2	0.0567	79.18	17.05	41.2	23.9	172238.	76.53	77.00	0.41	3.30	8503.	8386.	1.4	1713.
R-717-088L*N	81.47	157.7	156.9	0.0563	80.45	16.91	21.0	12.2	88101.	76.63	77.45	0.79	4.43	8409.	8329.	0.9	1263.
R-717-089L*N	84.52	165.7	165.1	0.0563	83.09	16.84	9.8	5.7	41458.	76.70	78.37	1.66	6.99	8323.	8113.	2.5	792.
R-717-090L*N	86.42	171.2	170.4	0.0562	84.87	16.77	7.6	4.4	32243.	76.86	78.98	2.09	8.50	8253.	7924.	4.0	645.
R-717-091L*N	89.45	179.7	179.0	0.0559	87.55	16.62	5.4	3.2	23206.	76.76	79.66	2.89	11.24	8130.	7850.	3.4	481.
R-717-092L*N	94.26	194.2	193.5	0.0561	91.76	16.59	3.8	2.2	16495.	76.68	80.72	4.03	15.56	8031.	7741.	3.6	343.
R-717-093L*N	81.15	157.2	156.0	0.0637	80.46	19.15	41.2	23.9	173425.	77.03	77.58	0.48	3.85	9527.	9948.	-4.4	1645.
R-717-094L*N	82.73	161.2	160.2	0.0637	81.91	19.11	21.0	12.2	88631.	77.04	77.98	0.92	5.22	9476.	9660.	-1.9	1208.
R-717-095L*N	86.53	171.7	170.7	0.0638	85.22	19.03	9.8	5.7	41832.	77.44	79.37	1.92	8.12	9365.	9392.	-0.3	767.
R-717-096L*N	88.43	176.7	176.1	0.0641	87.03	19.07	7.6	4.4	32720.	77.33	79.80	2.44	9.87	9349.	9309.	0.4	630.
R-717-097L*N	92.20	188.7	187.2	0.0635	90.48	18.81	5.3	3.1	23009.	77.30	80.71	3.40	13.19	9143.	9067.	0.8	461.
R-717-098L*N	97.29	204.2	203.0	0.0639	95.09	18.78	3.9	2.3	16881.	77.19	81.84	4.63	17.77	9031.	9012.	0.2	338.

Table D.13. Experimental data for ammonia condensing on Tube T (vertical)

Run No.	T_v (°F)	P (psia)	P_{sat} (psia)	F_c (gpm)	T_c (°F)	m_c (lb_m/h)	F_w (gpm)	v (ft/s)	Re	$T_{w,in}$ (°F)	$T_{w,out}$ (°F)	ΔT_w (°F)	$\overline{\Delta T}$ (°F)	Q_c (Btu/h)	Q_w (Btu/h)	Δ (%)	U (Btu/h·ft²·°F)
R-717-001T	79.98	153.7	153.0	0.1092	79.59	32.83	34.0	27.4	80508.	70.05	71.12	0.98	9.39	16376.	16633.	-1.6	1086.
R-717-002T	82.30	159.7	159.1	0.1096	81.69	32.87	21.2	17.1	50750.	70.61	72.19	1.54	10.90	16317.	16282.	0.2	933.
R-717-003T	87.60	174.7	173.7	0.1111	86.72	33.08	9.8	7.9	23828.	70.67	73.95	3.26	15.29	16240.	16015.	1.4	662.
R-717-004T	90.17	181.7	181.1	0.1118	89.15	33.16	7.6	6.1	18479.	70.60	74.79	4.17	17.47	16193.	15815.	2.3	578.
R-717-005T	94.83	196.2	195.2	0.1130	93.52	33.31	5.4	4.4	13219.	70.20	76.21	6.00	21.62	16100.	16164.	-0.4	464.
R-717-006T	100.18	214.2	212.4	0.1135	98.49	33.22	3.9	3.1	9650.	69.98	78.08	8.09	26.15	15866.	15746.	0.8	378.
R-717-007T	80.25	154.7	153.7	0.0610	80.23	18.34	34.0	27.4	85536.	74.99	75.62	0.54	4.95	9143.	9160.	-0.2	1152.
R-717-008T	81.25	156.7	156.3	0.0608	81.13	18.25	21.0	16.9	52928.	74.99	75.91	0.85	5.80	9079.	8958.	1.3	976.
R-717-009T	84.17	164.7	164.1	0.0608	83.70	18.17	9.8	7.9	25019.	75.14	76.97	1.81	8.12	8986.	8875.	1.2	690.
R-717-010T	85.50	168.7	167.8	0.0607	85.02	18.11	7.6	6.1	19338.	75.01	77.37	2.34	9.31	8931.	8865.	0.7	597.
R-717-011T	88.14	175.7	175.2	0.0611	87.35	18.17	5.4	4.3	13739.	74.96	78.27	3.31	11.52	8911.	8873.	0.4	482.
R-717-012T	91.33	185.2	184.6	0.0609	90.15	18.03	3.9	3.1	9970.	74.89	79.42	4.53	14.17	8782.	8744.	0.4	386.
R-717-013T	81.76	158.7	157.6	0.0291	80.56	8.75	34.0	27.4	90275.	79.37	79.73	0.27	2.20	4347.	4665.	-7.3	1229.
R-717-014T	82.54	160.7	159.7	0.0289	81.09	8.67	21.0	16.9	56033.	79.72	80.17	0.39	2.59	4304.	4086.	5.1	1034.
R-717-015T	84.20	164.7	164.2	0.0289	82.48	8.64	9.8	7.9	26463.	80.06	80.94	0.87	3.70	4273.	4265.	0.2	720.
R-717-016T	84.83	166.7	165.9	0.0289	83.16	8.65	7.6	6.1	20425.	79.96	81.09	1.13	4.31	4269.	4303.	-0.8	618.
R-717-017T	85.87	169.7	168.8	0.0286	84.01	8.56	5.4	4.4	14662.	79.82	81.39	1.57	5.26	4216.	4274.	-1.4	499.
R-717-018T	87.36	174.2	173.0	0.0286	85.21	8.53	3.9	3.2	10581.	79.80	81.94	2.13	6.49	4188.	4175.	0.3	402.
R-717-019T	83.01	162.2	161.0	0.0968	82.18	29.01	34.0	27.4	85112.	74.45	75.40	0.86	8.09	14378.	14537.	-1.1	1107.
R-717-020T	84.52	165.7	165.1	0.0971	83.49	29.05	21.0	16.9	52662.	74.36	75.76	1.34	9.46	14353.	14018.	2.3	945.
R-717-021T	88.91	178.7	177.5	0.0976	87.64	29.02	9.8	7.9	24927.	74.32	77.21	2.87	13.15	14209.	14113.	0.7	673.
R-717-022T	91.06	184.7	183.8	0.0974	89.55	28.87	7.6	6.1	19332.	74.33	78.00	3.65	14.90	14072.	13858.	1.5	588.
R-717-023T	95.12	197.2	196.1	0.0978	93.37	28.85	5.4	4.4	14048.	74.68	79.72	5.04	17.91	13935.	13701.	1.7	485.
R-717-024T	100.11	213.2	212.2	0.0989	97.87	28.97	3.9	3.1	10151.	74.47	81.47	7.00	22.14	13838.	13616.	1.6	389.
R-717-025T	82.53	160.2	159.7	0.0850	82.31	25.46	34.0	27.4	85761.	75.09	75.93	0.75	7.02	12631.	12654.	-0.2	1122.
R-717-026T	83.99	164.7	163.6	0.0847	83.55	25.35	21.0	16.9	53193.	75.22	76.46	1.18	8.15	12538.	12384.	1.2	958.
R-717-027T	87.57	174.2	173.6	0.0856	86.97	25.49	9.8	7.9	25033.	74.83	77.37	2.52	11.48	12515.	12374.	1.1	679.
R-717-028T	89.67	180.7	179.7	0.0852	88.93	25.27	7.6	6.1	19461.	75.08	78.29	3.19	12.99	12352.	12095.	2.1	593.
R-717-029T	93.38	191.7	190.8	0.0860	92.27	25.41	5.4	4.4	13980.	75.31	79.78	4.48	15.83	12323.	12061.	2.1	485.
R-717-030T	97.90	205.7	205.0	0.0871	96.46	25.57	3.9	3.2	10255.	75.27	81.47	6.20	19.53	12277.	12119.	1.3	392.
R-717-031T	82.19	159.7	158.8	0.0722	81.52	21.64	34.0	27.4	86657.	75.95	76.69	0.65	5.87	10745.	10958.	-2.0	1140.
R-717-032T	83.66	164.2	162.7	0.0717	82.78	21.47	21.2	17.1	54404.	76.33	77.38	0.99	6.80	10627.	10471.	1.5	973.
R-717-033T	86.73	171.7	171.2	0.0722	85.53	21.52	9.8	7.9	25366.	76.05	78.20	2.12	9.61	10584.	10433.	1.4	686.
R-717-034T	88.54	177.2	176.4	0.0726	87.17	21.60	7.6	6.1	19669.	76.13	78.91	2.76	11.02	10584.	10457.	1.2	598.
R-717-035T	91.54	186.2	185.2	0.0729	90.02	21.60	5.4	4.4	14212.	76.20	80.04	3.83	13.42	10518.	10414.	1.0	488.
R-717-036T	94.99	196.7	195.7	0.0731	93.12	21.56	3.9	3.2	10277.	75.92	81.16	5.24	16.45	10418.	10248.	1.6	395.
R-717-037T	79.93	153.7	152.8	0.0458	78.47	13.79	34.0	27.4	86708.	76.11	76.62	0.42	3.56	6880.	7056.	-2.6	1204.
R-717-038T	80.75	155.7	155.0	0.0455	79.14	13.69	21.0	16.9	53702.	76.23	76.93	0.65	4.17	6819.	6778.	0.6	1018.
R-717-039T	83.04	161.7	161.1	0.0453	81.17	13.61	9.8	7.9	25365.	76.45	77.81	1.34	5.91	6745.	6570.	2.6	710.
R-717-040T	84.11	164.7	164.0	0.0457	82.22	13.69	7.5	6.1	19386.	76.33	78.09	1.75	6.90	6769.	6562.	3.1	611.
R-717-041T	85.88	169.7	168.8	0.0454	83.66	13.58	5.4	4.4	13973.	76.28	78.72	2.44	8.38	6690.	6563.	1.9	498.
R-717-042T	88.23	176.2	175.5	0.0453	85.71	13.51	3.9	3.2	10202.	76.31	79.61	3.30	10.27	6623.	6456.	2.5	402.
R-717-043T	79.55	152.7	151.9	0.0358	78.01	10.79	34.0	27.4	87165.	76.56	76.99	0.34	2.77	5387.	5750.	-6.7	1210.
R-717-044T	80.57	155.2	154.5	0.0358	78.95	10.76	21.0	16.9	54188.	77.00	77.57	0.50	3.29	5362.	5291.	1.3	1016.
R-717-045T	82.10	159.7	158.5	0.0354	80.35	10.62	9.8	7.9	25471.	76.91	78.00	1.06	4.65	5275.	5224.	1.0	707.
R-717-046T	83.03	161.7	161.0	0.0353	81.13	10.60	7.6	6.1	19708.	76.98	78.37	1.38	5.35	5252.	5217.	0.7	611.
R-717-047T	84.28	166.2	164.4	0.0354	82.34	10.62	5.4	4.4	14020.	76.79	78.75	1.95	6.51	5249.	5256.	-0.1	502.
R-717-048T	86.36	171.2	170.2	0.0354	84.00	10.59	3.9	3.2	10231.	76.86	79.51	2.64	8.18	5213.	5171.	0.8	397.

Table D.13 (continued)

Run No.	T_v (°F)	P (psia)	P_{sat} (psia)	F_c (gpm)	T_c (°F)	m_c (lb_m/h)	F_w (gpm)	v (ft/s)	Re	$T_{w,in}$ (°F)	$T_{w,out}$ (°F)	ΔT_w (°F)	$\overline{\Delta T}$ (°F)	Q_c (Btu/h)	Q_w (Btu/h)	Δ (%)	U (Btu/h·ft²·°F)
R-717-049T	80.70	155.7	154.9	0.0708	80.12	21.26	34.0	27.4	85117.	74.56	75.30	0.65	5.77	10590.	10958.	-3.5	1143.
R-717-050T	82.33	159.7	159.2	0.0707	81.57	21.19	21.0	16.9	53009.	75.05	76.09	0.98	6.76	10520.	10288.	2.2	970.
R-717-051T	85.56	169.2	168.0	0.0705	84.40	21.06	9.8	7.9	24868.	75.08	77.19	2.08	9.43	10382.	10173.	2.0	686.
R-717-052T	87.85	175.2	174.4	0.0712	86.72	21.19	7.6	6.1	19536.	75.63	78.33	2.69	10.86	10396.	10188.	2.0	596.
R-717-053T	90.52	183.2	182.2	0.0714	89.15	21.19	5.4	4.4	13930.	75.36	79.16	3.80	13.26	10340.	10235.	1.0	486.
R-717-054T	94.34	194.7	193.7	0.0721	92.69	21.28	3.9	3.2	10209.	75.41	80.62	5.21	16.33	10298.	10189.	1.1	393.

Table D.14. Experimental data for ammonia condensing on Tube V (vertical)

Run No.	T_v (°F)	P (psia)	P_{sat} (psia)	F_c (gpm)	T_c (°F)	m_c (lb_m/h)	F_w (gpm)	v (ft/s)	Re	$T_{w,in}$ (°F)	$T_{w,out}$ (°F)	ΔT_w (°F)	$\overline{\Delta T}$ (°F)	Q_c (Btu/h)	Q_w (Btu/h)	Δ (%)	U (Btu/h·ft²·°F)
R-717-001V	88.49	176.7	176.3	0.0715	87.47	21.26	34.3	32.3	82349.	68.87	69.60	0.63	19.26	10417.	10746.	-3.2	276.
R-717-002V	90.05	181.2	180.8	0.0717	88.84	21.29	21.0	19.8	50458.	68.77	69.81	0.99	20.76	10401.	10441.	-0.4	255.
R-717-003V	94.52	195.2	194.3	0.0720	92.91	21.25	9.8	9.3	23900.	68.97	71.06	2.07	24.51	10278.	10213.	0.6	214.
R-717-004V	96.70	201.7	201.1	0.0719	94.89	21.15	7.5	7.1	18394.	68.96	71.68	2.72	26.38	10179.	10247.	-0.7	197.
R-717-005V	100.18	213.7	212.4	0.0718	97.92	21.02	5.3	5.0	13156.	69.15	72.88	3.73	29.16	10041.	9969.	0.7	176.
R-717-006V	104.13	226.7	225.9	0.0716	101.37	20.85	3.9	3.7	9636.	68.82	73.91	5.07	32.76	9867.	9888.	-0.2	154.
R-717-007V	82.46	160.2	159.5	0.0265	80.91	7.94	34.3	32.3	89459.	75.45	75.78	0.24	6.84	3942.	4056.	-2.9	294.
R-717-008V	83.25	162.2	161.6	0.0262	81.37	7.86	21.2	20.0	55385.	75.54	75.95	0.38	7.50	3894.	3966.	-1.9	265.
R-717-009V	84.82	166.7	165.9	0.0265	82.78	7.95	9.8	9.3	25706.	75.25	76.08	0.82	9.15	3924.	4054.	-3.3	219.
R-717-010V	85.38	168.2	167.4	0.0265	83.29	7.91	7.5	7.1	19642.	74.88	75.96	1.07	9.95	3904.	4023.	-3.1	200.
R-717-011V	86.67	171.7	171.1	0.0261	84.12	7.81	5.4	5.1	14221.	74.95	76.36	1.40	11.02	3843.	3812.	0.8	178.
R-717-012V	88.62	177.2	176.6	0.0263	85.75	7.83	3.9	3.7	10210.	74.91	76.91	1.99	12.71	3836.	3876.	-1.0	154.
R-717-013V	87.73	175.2	174.0	0.0501	86.64	14.92	34.3	32.3	88511.	74.53	75.06	0.44	12.93	7323.	7564.	-3.3	289.
R-717-014V	89.05	179.2	177.9	0.0503	87.77	14.95	21.0	19.8	54415.	74.75	75.48	0.69	13.94	7318.	7271.	0.6	268.
R-717-015V	91.91	187.7	186.3	0.0505	90.31	14.96	9.8	9.3	25591.	74.58	76.05	1.47	16.59	7279.	7224.	0.8	224.
R-717-016V	93.52	192.2	191.2	0.0505	91.77	14.93	7.6	7.2	19820.	74.67	76.55	1.86	17.91	7236.	7068.	2.3	206.
R-717-017V	96.08	200.2	199.2	0.0505	94.11	14.86	5.4	5.1	14172.	74.79	77.41	2.61	19.98	7163.	7023.	2.0	183.
R-717-018V	99.15	210.2	209.1	0.0503	96.70	14.76	3.9	3.7	10368.	74.95	78.47	3.52	22.44	7066.	6878.	2.7	161.
R-717-019V	87.65	175.2	173.8	0.0582	86.83	17.33	34.3	32.3	85797.	72.12	72.71	0.49	15.23	8509.	8436.	0.9	285.
R-717-020V	88.77	178.2	177.1	0.0580	87.91	17.24	21.3	20.1	53276.	72.00	72.83	0.79	16.36	8442.	8406.	0.4	263.
R-717-021V	92.08	187.7	186.8	0.0575	90.77	17.01	9.8	9.3	24790.	72.03	73.73	1.69	19.20	8274.	8285.	-0.1	220.
R-717-022V	93.78	193.2	192.0	0.0572	92.27	16.91	7.6	7.2	19181.	72.02	74.17	2.14	20.69	8191.	8118.	0.9	202.
R-717-023V	96.48	201.7	200.4	0.0568	94.47	16.71	5.4	5.1	13849.	72.15	75.07	2.92	22.86	8048.	7937.	1.4	180.
R-717-024V	100.50	214.7	213.5	0.0570	98.15	16.68	3.9	3.6	9894.	72.01	76.16	4.14	26.42	7963.	7993.	-0.4	154.
R-717-025V	86.51	171.7	170.6	0.0641	85.72	19.12	34.3	32.3	82322.	68.88	69.54	0.56	17.30	9411.	9581.	-1.8	277.
R-717-026V	87.97	175.7	174.7	0.0641	87.01	19.08	21.0	19.8	50491.	68.87	69.81	0.90	18.63	9358.	9444.	-0.9	256.
R-717-027V	91.83	187.2	186.1	0.0642	90.31	19.01	9.8	9.2	23738.	68.78	70.69	1.88	22.09	9250.	9250.	0.0	214.
R-717-028V	93.60	192.7	191.5	0.0643	92.09	18.99	7.6	7.2	18400.	68.63	71.07	2.43	23.75	9203.	9232.	-0.3	198.
R-717-029V	96.79	202.2	201.4	0.0636	94.73	18.73	5.4	5.1	13319.	68.88	72.22	3.34	26.24	9014.	9091.	-0.9	175.
R-717-030V	100.79	215.2	214.5	0.0637	98.36	18.65	3.9	3.7	9665.	68.92	73.50	4.57	29.58	8897.	8948.	-0.6	153.
R-717-031V	84.49	165.7	165.0	0.0335	82.94	10.03	34.3	32.3	89538.	75.49	75.88	0.30	8.81	4955.	5219.	-5.3	287.
R-717-032V	85.50	168.7	167.8	0.0335	83.66	10.02	21.0	19.8	54988.	75.67	76.18	0.48	9.58	4939.	5018.	-1.6	263.
R-717-033V	87.48	174.7	173.4	0.0336	85.31	10.03	9.8	9.3	25821.	75.50	76.53	1.03	11.47	4925.	5042.	-2.4	219.
R-717-034V	88.66	177.7	176.7	0.0338	86.45	10.06	7.6	7.2	19975.	75.55	76.87	1.31	12.45	4930.	4952.	-0.4	202.
R-717-035V	90.10	181.7	180.9	0.0333	87.41	9.89	5.4	5.1	14341.	75.42	77.20	1.77	13.79	4831.	4810.	0.4	179.
R-717-036V	92.42	189.2	187.8	0.0333	89.59	9.88	3.9	3.7	10359.	75.40	77.88	2.48	15.78	4803.	4848.	-0.9	155.
R-717-037V	86.07	170.2	169.4	0.0401	83.97	11.98	34.3	32.3	89400.	75.34	75.79	0.36	10.51	5901.	6177.	-4.7	286.
R-717-038V	87.17	173.2	172.5	0.0406	85.02	12.11	21.0	19.8	54803.	75.35	75.97	0.59	11.50	5949.	6171.	-3.7	264.
R-717-039V	89.80	180.7	180.0	0.0403	87.27	12.00	9.8	9.3	25874.	75.57	76.78	1.21	13.63	5866.	5961.	-1.6	220.
R-717-040V	91.08	184.7	183.8	0.0405	88.34	12.02	7.6	7.2	20002.	75.53	77.11	1.56	14.76	5856.	5922.	-1.1	202.
R-717-041V	93.08	190.7	189.9	0.0404	89.96	11.97	5.4	5.1	14400.	75.57	77.69	2.11	16.46	5806.	5729.	1.3	180.
R-717-042V	95.96	199.7	198.8	0.0403	92.48	11.89	3.9	3.7	10381.	75.72	78.70	2.97	18.74	5732.	5783.	-0.9	156.

Appendix E

SI CONVERSION FACTORS

An attempt has been made to present all key tables and figures in dual units (ACU and SI). The following conversion factors may be used to convert from ACU to SI units:

To convert from	To	Multiply by
Btu/h	W	0.2929
$Btu/h \cdot ft^2$	W/m^2	3.152
$Btu/h \cdot ft \cdot {}^oF$	$W/m \cdot K$	1.730
$Btu/h \cdot ft^2 \cdot {}^oF$	$W/m^2 \cdot K$	5.675
Btu/lb_m	J/kg	2.324×10^3
$Btu/lb_m \cdot {}^oF$	$J/kg \cdot K$	4.184×10^3
ft	m	0.3048
ft^2	m^2	0.0929
ft/h^2	m/s^2	2.35×10^{-8}
ft/s	m/s	0.3048
gpm	m^3/s	6.309×10^{-5}
in.	cm	2.54
lb_f/ft	N/m	14.59
lb_m/ft^3	kg/m^3	16.02
$lb_m/h \cdot ft$	$Pa \cdot s$	4.134×10^{-4}
$lb_m/h \cdot ft^2$	$Pa \cdot s/m$	1.356×10^{-3}
psia	Pa	6.895×10^3
$\Delta({}^oF)$	$\Delta(K)$ or $\Delta({}^oC)$	0.5556

Temperature conversion: $T(K) = 5/9 \times [T({}^oF) - 32] + 273.15$

$T({}^oC) = 5/9 \times [T({}^oF) - 32]$

ORNL-5826
Dist. Category UC-93

Internal Distribution

1. H. G. Arnold
2. F. C. Chen
3. S. K. Combs
4-39. N. Domingo
40. R. D. Ellison
41. W. Fulkerson
42. A. Golshani
43. R. E. Goodson (Consultant)
44. T. J. Hanratty (Consultant)
45. C. V. Hardin
46. H. W. Hoffman
47. T. R. LaPorte (Consultant)
48. R. L. Linkous
49. R. N. Lyon (Consultant)
50. J. W. Michel
51. L. I. Moss (Consultant)
52. R. W. Murphy
53. R. C. Robertson
54. T. W. Robinson, Jr.
55. H. E. Trammell
56. ORNL Patent Office
57. Central Research Library
58. Document Reference Section
59-60. Laboratory Records Department
61. Laboratory Records (RC)

External Distribution

62. J. Hilbert Anderson, Sea Solar Power, Inc., 2422 South Queen St., York, PA 17402
63. David Aronson, David Aronson Associates, 9 Riverview West, Upper Montclair, NH 07043
64. Professor Kenneth J. Bell, School of Chemical Engineering, Oklahoma State University, Stillwater, OK 74074
65. Professor A. E. Bergles, Department of Mechanical Engineering, Iowa State University, Ames, IA 50010
66. Eugene S. Burcher, Research and Technology Development Branch, Division of Ocean Energy Systems, Department of Energy, 600 E. Street, NW, Room 408, Washington, DC 20585
67. Dr. Gordon L. Dugger, Applied Physics Laboratory, John Hopkins University, John Hopkins Road, Silver Spring, MD 20810
68. Sigmond Gronich, Division of Solar Energy, Department of Energy, 600 E. Street, NM, Washington, DC 20545
69. Dr. R. Phillip Hammond, R&D Associates, 4640 Admiralty Way, P.O. Box 9695, Marina del Rey, CA 90291
70. Frank Herbaty, U.S. Department of Energy, Chicago Operations Office, 9800 South Cass Ave., Argonne, IL 60439
71. Donald Hornburg, DSS Engineers, Inc., 7483 Northwest 4th St., Fort Lauderdale, FL 33317
72. Dr. Matthew Kelleher, Naval Postgraduate School, Department of Mechanical Engineering, Monterey, CA 93940
73. Eugene H. Kinelski, Ocean Systems Branch, Division of Central Solar Energy, Department of Energy, Washington, DC 20545
74. Professor James G. Knudsen, Engineering Experimental Station, Oregon State University, Covell Hall 219, Corvallis, OR 97331
75. Dr. Abrahim Lavi, Department of Engineering, Carnegie-Mellon University, Schenley Park, Pittsburgh, PA 15213

76. Dr. A. L. London, 4020 Amaranta Ave., Palo Alto, CA 94306
77. Dr. Paul Marto, Naval Postgraduate School, Department of Mechanical Engineering, Monterey, CA 93940
78. Bernard Messigner, 4162 Sunridge Road, Pebble Beach, CA 93953
79. W. C. Moore, York Division, Borg Warner Corp., York, PA 17403
80. Frank Notaro, Union Carbide Corp., Linde Division, P.O. Box 44, Tonawanda, NY 14150
81. Dr. W. L. Owen, Lockheed Missiles and Space Company, Inc., P.O. Box 504, Sunnyvale, CA 95088
82. Terry Penny, Solar Energy Research Institute, 1536 Cole Blvd., Golden, CO 80401
83. Robert W. Perkins, Spiral Tubing Corp., 533 John Downey Drive, New Britain, CT 06051
84. Dr. H. F. Poppendiek, Geoscience, Ltd., 410 South Cedros Ave., Solona Beach, CA 92075
85. Dr. Thomas Rabas, Steam-Turbine Generator Technical Operations Division, Westinghouse Electric Corporation, Lester Branch, P.O. Box 9175 N2, Philadelphia, PA 19113
86. Kenneth F. Read, 448 Ferry Point Road, Annapolis, MD 21403
87. William Richards, Ocean Systems Branch, Division of Central Solar Technology, Department of Energy, 600 E. Street, NW, Washington, DC 20545
88. Dr. Warren M. Rohsenow, Director, Heat Transfer Laboratory, Massachusetts Institute of Technology, Cambridge, MA 02139
89. Dr. R. R. Rothfus, Chemical Engineering Department, Carnegie-Mellon University, Schenley Park, Pittsburgh, PA 15213
90. Norman F. Sather, Argonne National Laboratory, 9700 South Cass Ave., Argonne, IL 60439
91. Ben Shelpuk, Solar Energy Research Institute, 1536 Cole Blvd., Golden, CO 80401
92. J. E. Snyder, III, TRW Systems and Energy Inc., One Space Park, Redondo Beach, CA 90278
93. Professor Kenneth E. Starling, School of Chemical Engineering and Materials Science, Room 23, University of Oklahoma, 202 West Boyd, Norman, OK 73069
94. Jerry Taborek, Heat Transfer Research, Inc., 1000 S. Fremont, Alhambra, CA 91803
95. Dr. W. H. Thielbahr, Chief, Energy Conservation Branch, Department of Energy, Idaho Operations Office, 550 Second Street, Idaho Falls, ID 83401
96. Lloyd C. Trimble, Lockheed Missiles and Space Company, Inc., P.O. Box 504, Sunnyvale, CA 94088
97. Professor Ralph Webb, Department of Mechanical Engineering, Penn State University, University Park, PA 16802
98. Jack Yampolsky, General Atomic Company, 10955 John Jay Hopkins Drive, San Diego, CA 92121
99. Office of Assistant Manager for Energy Research and Development, DOE, ORO, Oak Ridge, TN 37830

100-264. Given distribution as shown in DOE/TIC-4500 under category UC-93, Energy Conversion